

# EXHIBIT H

# Tumour necrosis factor is a compact trimer

Paul Wingfield, Roger H. Pain<sup>+</sup> and Stewart Craig<sup>+</sup>

Biogen S.A. 3 route de Troinex, F-1227 Carouge, Geneva, Switzerland and <sup>+</sup>Department of Biochemistry, University of Newcastle, Newcastle upon Tyne, NE1 7RU, England

Received 20 October 1986

Recombinant produced human tumour necrosis factor (TNF) has been studied to characterise the subunit structure of the protein. TNF is shown to be a trimer  $M_r$  52000 in which the subunits are associated in a compact, triangular form. In secondary structure it belongs to the  $\alpha$ - $\beta$  class of proteins. It has high thermodynamic stability and the unfolded subunits can fold and associate spontaneously to form native, biologically active TNF.

Tumour necrosis factor; Molecular mass; Subunit structure; Secondary structure; Thermodynamic stability

## 1. INTRODUCTION

Tumour necrosis factor can be produced in serum by treatment with lipopolysaccharide of an animal previously primed with materials such as BCG or zymosan [1]. Its ability to bring about regression of tumours in mice makes this protein a focus of attention. Human TNF has been expressed in *E. coli* from genetic material derived from cell lines [2,3] and this has opened the door to characterisation of structure-function relationships. We have clarified the uncertainty in the literature concerning the polymeric nature of the smallest form of TNF present at concentrations as low as 50 ng·ml<sup>-1</sup> and investigated its conformation and assembly.

Correspondence address: R.H. Pain, Dept of Biochemistry, University of Newcastle, Newcastle upon Tyne, NE1 7RU, England

**Abbreviations:** TNF, tumour necrosis factor; Gdn·HCl, guanidine HCl; SDS-PAGE, polyacrylamide gel electrophoresis in the presence of SDS;  $\Delta G^\circ_{H_2O}$ , apparent free energy of stabilization in the absence of denaturant; CD, circular dichroism; UV, ultraviolet

## 2. MATERIALS AND METHODS

Chemicals were analar grade (BDH, Poole, England). Tris was from Sigma and Ultrapure Gdn·HCl from BRL. The buffer used in the experiments was 0.01 M Tris, 0.09 M NaCl, 1 mM disodium EDTA, adjusted to pH 8.5 with HCl unless otherwise described in the text.

Recombinant TNF was supplied by Biogen Res. Corp. (Cambridge, USA). It was assayed as described [3].

### 2.1. Circular dichroism

Circular dichroism spectra were measured using a Jobin-Yvon dichrograph IV linked to a BBC microcomputer for recording data. Spectra are averages of 4-10 scans with the baseline subtracted. Protein concentrations were estimated using a calculated value of  $A_{278}^{1\%} = 12.7$  at 278 nm. All solutions were filtered (0.22  $\mu$ m, Millipore GVWP filters) before use.

Additions of Gdn·HCl were made from a concentrated stock solution. The equilibrium unfolding data were analysed using the linear extrapolation method [4]. A plot of  $\ln K_{eq}$  versus [Gdn·HCl] was extrapolated to [Gdn·HCl] = 0 to obtain a value of the apparent free energy change

for the transition at zero concentration of denaturant,  $\Delta G_{H_2O}$ .  $\ln K'_{eq}$  was plotted against  $\ln[Gdn \cdot HCl]$  to obtain  $C_m$ , the midpoint of the transition where  $\ln K'_{eq} = 0$  and the slope,  $n$ , which is a measure of the cooperativity of the transition.

Unfolding and refolding kinetics were measured as described in the legends.

## 2.2. Absorbance

Absorbance spectra and protein concentrations were measured using a Cary 210 spectrophotometer with thermostatted cell holders.

## 2.3. Fluorescence

Fluorescence measurements were made using a Perkin Elmer MPF3 spectrofluorimeter with thermostatted cell holder. All solutions were filtered (0.22  $\mu$ m, Millipore) before use.

## 2.4. Analytical ultracentrifugation

Sedimentation equilibrium and sedimentation velocity measurements were made as described [5].

## 2.5. Urea-gradient polyacrylamide gel electrophoresis

Urea-gradient polyacrylamide gel electrophoresis was carried out in a BRL model V-16-2 vertical gel electrophoresis apparatus using 19.5  $\times$  16.0 cm gel plates with 1.5 mm thick spacers. The electrophoresis buffer was 50 mM Tris-glycine, pH 9.2. Preparation of the urea gradient (0–8 M) and acrylamide gradient (15–11%) and conditions of polymerization were carried out according to Goldenberg and Creighton [6].

# 3. RESULTS AND DISCUSSION

## 3.1. Molecular structure of TNF

The relative molecular mass of human TNF as measured by SDS-PAGE in the absence or presence of reducing agent was shown to be 17 kDa in keeping with the DNA-derived sequence value of 17356 Da [3]. Molecular masses measured by sedimentation equilibrium at starting protein concentrations of 0.125 mg·ml<sup>-1</sup> and 0.48 mg·ml<sup>-1</sup> were 49.6 and 50.4 kDa, respectively. The linearity of the plots of protein distribution (fig.1) over a total range of 0.02–0.8 mg·ml<sup>-1</sup> show that there is no dissociation or further association of TNF over this range of concentration. The

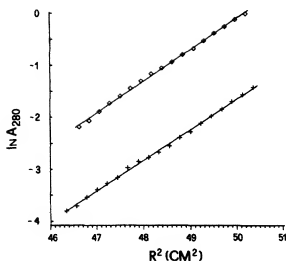


Fig.1. Sedimentation equilibrium of recombinant human TNF. The logarithm of absorbance at 280 nm ( $\ln A_{280}$ ) is plotted as a function of the square of the distance in cm from the axis of rotation ( $r^2$ ). The slopes were evaluated from the least squares fit of the data. Plots were derived from TNF in 50 mM Tris-HCl, pH 7.5, 1% (w/v) KCl at starting concentrations of 0.125 (x) and 0.48 (o) mg·ml<sup>-1</sup>, respectively. Sedimentation equilibrium was established by centrifugation at 14000 rpm for 18 h at 20°C.

molecular mass of the murine TNF was similarly shown to be 50 kDa. These results show that TNF is a trimer held together by non-covalent interactions.

The mode of association of the subunits will determine the flow properties of the trimer in solution, the two extreme configurations being a linear and a planar, triangular association, respectively. Experimental values of the geometric factor for subunit arrangement were calculated from the hydrodynamic properties of TNF (table 1) by the method of Teller et al. [7] and compared with predicted values. These results lead to the proposal that TNF is associated with two inter subunit contacts for each subunit.

The near UV CD spectrum of TNF (fig.2a) exhibits an intense positive ellipticity with a double peak at 280.5 and 285.5 nm and a minor peak at 292.5 nm. These reflect the asymmetric environment of one or both of the two tryptophan residues together with a contribution from tyrosine residues. The CD spectrum in the range

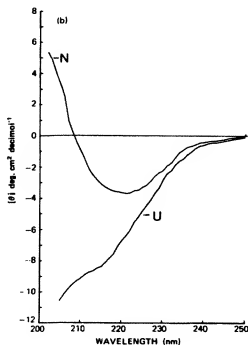
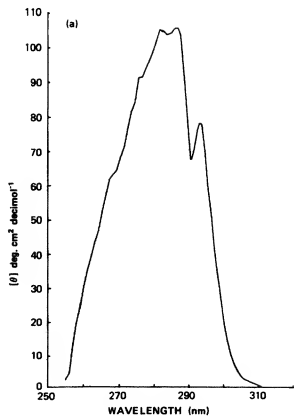


Table 1

Hydrodynamic properties of recombinant human TNF

Parameter	Value
$\nu$ (ml · g <sup>-1</sup> )	0.729
$s^0$	4.13 S
$r_s$ cm × 10 <sup>4</sup> (a)	3.01
$r_s$ cm × 10 <sup>4</sup> (b)	2.70
$r_s$ cm × 10 <sup>4</sup> (c)	2.47 (2.81)
$f/f_0$ (d)	1.22 (1.07)
$F_n$ (e)	0.967 (0.956, 0.864)

(a) Stokes' radius estimated from  $M_r$  of 52000,  $s_{20,w}$  of 4.13 S and  $\nu$  of 0.729 ml · g<sup>-1</sup> according to the Svedberg equation [18]. (b) Stokes' radius estimated from gel permeation chromatography on LKB Ultragel AcA54. (c) Stokes' radius predicted for an anhydrous sphere or a hydrated sphere (value in parentheses) of  $M_r$  of 52000 and  $\nu = 0.729$  ml · g<sup>-1</sup>. A hydration value of 0.350 g H<sub>2</sub>O/g protein was calculated from the amino acid composition [19]. (d) Frictional coefficient calculated using  $f_0$  values calculated for an anhydrous sphere or a hydrated sphere (value in parentheses). (e) Geometric factor for subunit arrangement calculated according to the method of Teller et al. [7]. The values in parentheses are the predicted values for a planar triangular trimer and a linear trimer, respectively.

200–250 nm (fig.2b) is of relatively low intensity with a trough centred at 221 nm. Analysis of the spectrum in terms of secondary structure [8] gives 3% helix and 45%  $\beta$ -structure placing TNF, like interleukin 1 [9], in the all- $\beta$  class of proteins [10].

Human TNF contains two cysteine residues which form a disulphide bond as shown by reaction with 2-nitro-5-thiobenzoic acid [11]. This bond can readily be cleaved under non-denaturing conditions and the resultant sulphhydryl groups alkylated with iodoacetamide. The product has  $M_r = 50000$ ,  $s_{20,w} = 4.0$  S and biological activity similar to that of native TNF. The disulphide does

Fig.2. Circular dichroism spectra of TNF. The spectra are an average of 4 (near UV) and 8 (far UV) scans with the baseline subtracted. Protein concentration 0.87 mg/ml in 0.01 M Tris, 0.09 M NaCl, 1 mM disodium EDTA, pH 8.5. Spectra were recorded at 20°C using 1 cm and 0.01 cm pathlength cells at 1 nm and 2 nm bandwidths for near and far UV regions, respectively. The far UV spectrum is shown for native TNF (N) and for TNF unfolded (U) in 4 M Gdm · HCl.

not therefore appear to play an important role in stability of subunit association or activity.

### 3.2. Subunit interactions

On urea-gradient electrophoresis, TNF shows a single transition between 0 and 8 M urea which occurs at  $\sim 3.8$  M urea at pH 9 and  $8^\circ\text{C}$ . The transition is continuous and independent of whether TNF is applied in zero or 8 M urea (fig.3). Under these conditions therefore TNF unfolds reversibly and rapidly relative to the time of electrophoresis. The thermodynamic stability was estimated [12] under these conditions as being  $26 \text{ kJ} \cdot \text{mol}^{-1}$ .

Initial attempts to study the unfolding equilibria in free solution showed that at  $25^\circ\text{C}$  unfolded TNF in 5 M Gdn·HCl aggregates significantly so that refolding after 60 s in that solvent results in only 50–60% yield of native protein. Yields of 80–90% can be obtained however when TNF is unfolded in high concentrations of Gdn·HCl at  $6^\circ\text{C}$  over the pH range 5.9–9.5. Samples which refolded at pH 8.5 were active on bioassay. The reversible unfolding transitions at pH 8.5 (fig.4) measured by near and far UV ellipticity at  $11^\circ\text{C}$  are superimposable. This fact and the high cooperativity ( $n = \text{dln } K'/\text{dln[Gdn·HCl]} = 17.6$ ) support the

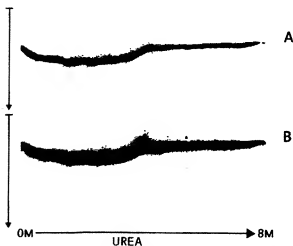


Fig.3. Urea-gradient electrophoresis of recombinant human TNF. The buffer for electrophoresis and sample application was 50 mM Tris-glycine, pH 9.2. Electrophoresis was towards the anode at  $6.5 \text{ V} \cdot \text{cm}^{-1}$  for 15 h at  $8^\circ\text{C}$ . (A) Native TNF ( $150 \mu\text{g}$ ) and (B) native TNF ( $150 \mu\text{g}$ ) migrated into the gel before application of unfolded TNF ( $150 \mu\text{g}$ ) dissolved in 8 M urea.

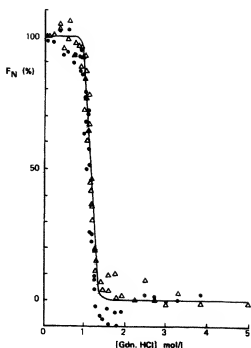


Fig.4. Reversible unfolding transition for TNF. The unfolding and refolding were monitored by ellipticity at 285.5 nm ( $\bullet$ ), 292.5 nm ( $\Delta$ ) and 208 nm (solid line). Protein solutions in 0.01 M Tris, 0.09 M NaCl, 1 mM disodium EDTA, pH 8.5, were titrated with small weighed additions of a concentrated stock solution of Gdn·HCl made up in the same buffer to give final protein concentrations of 0.34–0.82 mg/ml.

assumption of a 2-state transition and strong interaction of the subunits. The thermodynamic stability of the native protein relative to the fully unfolded state is  $40.6 \pm 3.6 \text{ kJ} \cdot \text{mol}^{-1}$  based on results from both near and far UV CD. The midpoint of the transition under these conditions occurs at  $C_m = 1.14 \text{ M Gdn·HCl}$ .

This transition was further characterised by sedimentation experiments carried out under the same conditions. At zero and 0.5 M Gdn·HCl sedimentation coefficients were 4.0 S and 3.8 S, respectively, and at 4 M Gdn·HCl,  $s_{20,w} = 1.0 \text{ S}$ . At intermediate concentrations within the transition high  $s$  values were obtained indicating aggregation. Similar experiments carried out in urea solutions showed similar phenomena, with a transition occurring between 4 and 5 M urea. Sedimentation equilibrium in 6 M urea led to a convex plot of  $\ln c$  vs  $r^2$  indicating non-ideality. The estimated

value of  $M_r = 16000$  was obtained using a partial specific volume  $v = 0.712 \text{ ml} \cdot \text{g}^{-1}$  [13].

These results show that the single denaturation transition is between folded trimer and unfolded monomer with no intermediate species other than artifactual aggregates. The trimer is stable over a wide pH range, there being no change in sedimentation coefficient between pH 4.8 and 10.5. Measurements of fluorescence show that TNF is denatured on lowering the pH with a  $pK$  of approx. 4.3 leading to a product shown by sedimentation experiments to be moderately aggregated. This is consistent with the irreversible loss of TNF found on dialysis for 24 h at pH values below 5.5 [14].

The strength of the interaction between the monomers is supported by a gel filtration experiment in which TNF was radiolabelled during biosynthesis. At an initial concentration of  $200 \text{ ng} \cdot \text{ml}^{-1}$  this eluted at a volume identical to that for unlabelled TNF at higher concentrations ( $7 \text{ mg} \cdot \text{ml}^{-1}$ ) showing that no dissociation of the trimer could be detected at the lower concentration.

### 3.3. Conclusions

There is a species variation in the extent of TNF glycosylation, for example, murine TNF appears in nature to be a glycoprotein [14] whereas there is no evidence for the glycosylation of human TNF. Both human and murine recombinant TNF have been shown to be trimers so that glycosylation does not appear to affect the degree of polymerisation. The recombinant protein studied here has identical chemical composition to authentic human TNF and therefore reflects properties of the authentic molecules. Existing uncertainties concerning the subunit structure, e.g. [15], have been resolved by the determination of an absolute molecular mass using equilibrium sedimentation which shows beyond doubt that TNF is a trimer of 17 kDa polypeptides. The significance of higher molecular mass species with TNF activity, e.g. [16], has yet to be clarified. The subunits are associated strongly in a compact form, showing no sign of dissociation at low concentrations. The bioassay however is carried out in the picogram concentration range, probably similar to levels in serum, so it has yet to be established conclusively whether the monomer or the trimer is active. However, the local concen-

tration of the protein at the region of the cell surface receptor *in vivo* may be significantly higher than the normal serum levels. The demonstrated strong tendency to associate would be important if the TNF receptor is activated by being cross linked by the ligand, as proposed for the IgE stimulation of mast cells [17] and for stimulation of the primary immune response [18].

The protein, which is of the  $\alpha\beta$  type, can be dissociated into fully unfolded subunits and will then refold spontaneously into the active, native conformation. The 17 kDa polypeptide thus contains the information required for folding to the species which associates specifically to give biologically active TNF. This shows that the unusually long 76 residue presequence is not required for folding as in proinsulin [19] or pepsinogen [20] but is conformationally independent and presumably therefore has a separate biochemical function in secretion or targeting.

### ACKNOWLEDGEMENTS

We wish to thank Dr D.R. Thatcher (Biogen Res. Corp.) for supplying the human TNF and Dr S.-M. Liang for the murine TNF. We also thank Dr M. Hirchi (Biogen SA) for performing the bioassays and Dr R. Movva (Biogen SA) for preparing the biosynthetically  $^{35}\text{S}$ -labelled TNF.

### REFERENCES

- [1] Old, L.J. (1985) *Science* 230, 630-632.
- [2] Pennica, D., Nedwin, G.E., Hayflick, J.S., Seeburg, P.H., Derynck, R., Palladino, M.A., Kohr, W.J., Aggarwal, B.B. and Goeddel, D.V. (1984) *Nature* 312, 724-729.
- [3] Marnenout, A., Fransen, L., Tavernier, J., Van der Heyden, J., Tizard, R., Kawashima, E., Shaw, A., Johnson, M.-J., Seman, D., Mueller, R., Ruyschaert, M.-R., Van Vliet, A. and Fiers, W. (1985) *Eur. J. Biochem.* 152, 515-522.
- [4] Pace, N.C. (1975) *CRC Crit. Rev. Biochem.* 3, 1-43.
- [5] Wingfield, P., Payton, M., Tavernier, J., Barnes, M., Shaw, A., Rose, K., Simona, M.G., Demczuk, S., Williamson, K. and Dayer, J.-M. (1986) *Eur. J. Biochem.*, in press.
- [6] Goldenberg, D.P. and Creighton, T.E. (1984) *Anal. Biochem.* 138, 1-18.

- [7] Teller, D.C., Swanson, E. and De Haen, C. (1979) *Methods Enzymol.* 61, 103-124.
- [8] Provencher, S.W. (1982) *Comput. Phys. Commun.* 27, 229-242.
- [9] Craig, S., Schmeissner, U., Wingfield, P. and Pain, R.H., submitted.
- [10] Levitt, M. and Chothia, C. (1976) *Nature* 261, 552-558.
- [11] Thannhauser, T.W., Konishi, Y. and Scheraga, H.A. (1984) *Anal. Biochem.* 138, 181-188.
- [12] Hollecker, M. and Creighton, T.E. (1982) *Biochim. Biophys. Acta* 701, 395-404.
- [13] Prakash, V. and Timasheff, S.N. (1981) *Anal. Biochem.* 117, 330-335.
- [14] Haranaka, K., Carswell, E.A., Williamson, B.D., Prendergast, J.S., Satomi, N. and Old, L. (1986) *Proc. Natl. Acad. Sci. USA* 83, 3949-3953.
- [15] Aggarwal, B.B., Kohr, W.J., Hass, P.E., Moffat, B., Spencer, S.A., Henzel, W.J., Bringman, T.S., Nedwin, G.E., Goeddel, D.V. and Harkins, R.N. (1985) *J. Biol. Chem.* 260, 2345-2354.
- [16] Kull, F.C. and Cuatrecasas, P. (1981) *J. Immunol.* 126, 1279-1283.
- [17] Maeyama, K., Hohman, R.J., Metzger, H. and Beaven, M.A. (1986) *J. Biol. Chem.* 261, 2583-2592.
- [18] Vogelstein, B., Dintzis, R.Z. and Dintzis, H.M. (1982) *Proc. Natl. Acad. Sci. USA* 79, 395-399.
- [19] Anfinsen, C.B. (1966) *Harvey Lect.* 61, 95-116.
- [20] Ahmad, F. and McPhie, P. (1978) *Int. J. Pept. Protein Res.* 12, 155-163.
- [21] Van Holde, K.E. (1975) *The Proteins* (3rd Edn) 1, 226-287.
- [22] Kuntz, I.D. (1971) *J. Am. Chem. Soc.* 93, 514-516.

# EXHIBIT I



## The Active Form of Tumor Necrosis Factor Is a Trimer\*

(Received for publication, December 1, 1986)

Richard A. Smith† and Corrado Baglioni

From the Department of Biological Sciences, State University of New York at Albany, Albany, New York 12222

Natural human and recombinant human and murine tumor necrosis factors (TNF) were fractionated by gel filtration chromatography on Sephadex G-75. The active form of TNF was identified by its inhibitory activity in receptor binding assays with HeLa cells and was eluted as a protein of  $M_r \sim 55,000$ . Radioiodinated human and murine TNF were fractionated by gel filtration into a major peak of  $M_r \sim 55,000$ , corresponding to a trimer, and a minor peak of  $M_r \sim 17,000$ , corresponding to a monomer. Binding assays showed that the trimer was at least 8-fold more active than the monomer. The human TNF partially dissociated into monomers upon addition of the nonionic detergent Triton X-100. Isolated monomers showed low binding affinity ( $K_D = 70$  nM) and reduced cytotoxicity, whereas trimers showed high binding affinity ( $K_D = 90$  pM) and cytotoxicity. When  $^{125}\text{I}$ -TNF was bound to cells, no release of monomer was detectable, suggesting that the trimer could directly bind to cellular receptors without dissociating into subunits. Further evidence for such binding was obtained by cross-linking  $^{125}\text{I}$ -TNF trimers with bis[2-(succinimidooxycarbonyl)ethyl]sulfone. These trimers were bound to HeLa cells, could be dissociated from cellular receptors, and elicited a cytotoxic response. These results show that trimers, whether native or cross-linked, bind to receptors and are the biologically active form of TNF.

Recombinant or natural human tumor necrosis factor (hTNF) purified from tissue culture supernatants or serum in under denaturing conditions a polypeptide of  $M_r$  17,000 (1) or 17,500 (2), respectively. However, the biological activity of TNF has been recovered under nondenaturing conditions in proteins thought to consist of dimers or higher oligomers with  $M_r$  values of 45,000 (1, 3) and 70,000 (4) for human TNF; 35,000 (5), >70,000 (6), 150,000 (7), 70,000 (8), and 55,000 (8, 9) for murine TNF; and 39,000 (10) or 55,000 (11) for rabbit TNF.

Numerous reports demonstrate that TNF interacts with

\* This work was supported in part by United States Public Health Service Grant CA-29805 of the National Institutes of Health. The costs of publication of this article were defrayed in part by the payment of page charges. This article must therefore be hereby marked "advertisement" in accordance with 18 U.S.C. Section 1734 solely to indicate this fact.

† Supported by a postdoctoral fellowship of the Cancer Research Institute, New York.

The abbreviations used are: hTNF, human tumor necrosis factor; mTNF, murine TNF; BSA, bovine serum albumin; PBS, phosphate-buffered saline; GdnHCl, guanidine hydrochloride; BSOCOS, bis[2-(succinimidooxycarbonyl)ethyl]sulfone; HEPES, 4-(2-hydroxyethyl)-1-piperazineethanesulfonic acid.

cellular receptors (2, 12-14) and elicits cytotoxic (15, 16) or growth regulatory responses (17, 18). It is not known, however, which form of TNF interacts with receptors. The goal of the present work was to examine whether hTNF and mTNF are under physiological conditions oligomers of defined size and to establish whether such oligomers directly bind to receptors. We report in this communication that TNF trimers bind to cellular receptors and elicit a cytotoxic response.

### MATERIALS AND METHODS

**Cytotoxicity Assay.**—HeLa S2 cells were grown in monolayer culture in Dulbecco's medium supplemented with 10% heat-inactivated horse serum. For each assay,  $4 \times 10^5$  cells were resuspended in 0.2 ml of culture medium containing 5  $\mu\text{g}/\text{ml}$  cycloheximide and the indicated concentrations of hTNF. After 18 h, the medium containing dead cells was removed and adherent cells were stained with 0.2% crystal violet in 2% ethanol (19). The dye was solubilized with 33% acetic acid, and the  $A_{540}$  was measured with a Titertek Multiscan (Flow Laboratories). Cytotoxicity was expressed as a percentage of the  $A_{540}$  of control cells that received cycloheximide alone.

**Iodination and Cross-linking.**—Recombinant hTNF and mTNF were radioiodinated using a solid-phase lactoperoxidase procedure (20) to a specific activity of 10–58 Ci/g.  $^{125}\text{I}$ -hTNF was cross-linked with the bifunctional reagent BSOCOS (Pierce Chemical Co.); 209 ng of  $^{125}\text{I}$ -hTNF in 0.1 ml of 75 mM sodium phosphate buffer, pH 7.5, containing 0.05% BSA were reacted with 1 mM BSOCOS. After 10 min at 4°C, 0.01 ml of 1 M glycine in 0.1 M sodium phosphate buffer, pH 7.5, was added. 0.1 ml samples were applied to a Sephadex G-75 column (0.7  $\times$  24 cm) equilibrated with 10 mM PBS, 0.1% BSA, and 0.15–0.20 M fractions were collected.

**Binding Assays.**—In competitive binding experiments, 0.3–0.5 ng of radioligand were incubated 5 h at 4°C with  $1 \times 10^6$  cells in 0.15 ml of medium containing 5 mM MgCl<sub>2</sub> and 40 mM HEPES, pH 7.5, as previously described (20). In experiments designed to recover cell-bound radioligand, the binding assays were proportionately increased 10-fold to 1.5 ml. Following binding, the cells were centrifuged at 4°C and washed twice with 1 ml of PBS. To dissociate TNF-receptor complexes, 5  $\mu\text{l}$  of 6 M GdnHCl, 0.1 M sodium phosphate, pH 7.5, were added to  $10^7$  pelleted cells for 10 min at 4°C. Lysed cells were diluted with 0.1 ml of 10 mM PBS, 0.1% BSA and centrifuged for 10 min at 15,500  $\times$  g. The supernatants were chromatographed on Sephadex G-75 columns. Bindability was determined by incubating radioligands with graded amounts of excess cellular receptors, and the results were expressed as the maximum percentage of counts added that were specifically bound to HeLa S2 cells at 4°C.

**Zonal Centrifugation Studies.**—0.3 ng of  $^{125}\text{I}$ -hTNF and 0.5 mg of reference protein in 0.1 ml of PBS were layered on 5–20% linear sucrose gradients. The gradients were centrifuged for 24 h at 44,000 rpm in an SW 50 rotor at 5°C, and fractions containing 4 drops were collected. Ovalbumin ( $M_r = 45,000$ ) and BSA ( $M_r = 66,000$ ) were used as reference proteins.

### RESULTS

Gel filtration on Sephadex G-75 was used to determine the  $M_r$  value of native TNF and to establish whether iodination altered its size. Accordingly, the elution profiles of native hTNF and mTNF were compared with those of  $^{125}\text{I}$ -hTNF and  $^{125}\text{I}$ -mTNF (Fig. 1). Since small amounts of TNF were chromatographed in the presence of carrier protein, the TNF was localized by its inhibitory activity in receptor binding assays. Both recombinant TNF eluted as a single major peak (Fig. 1A). The elution profile of natural hTNF (a gift of Dr. Walter Fiers, University of Ghent) was indistinguishable from that of recombinant hTNF (data not shown). Radioiodinated hTNF and mTNF eluted as a major peak (#1) in corresponding fractions, followed by a minor peak (#2) and free  $^{125}\text{I}$  (Fig.

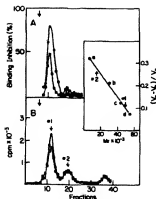


Fig. 1. Gel filtration on Sephadex G-75 of native hTNF and mTNF. A, 100 ng of hTNF (●) or mTNF (■) in 0.1 ml were chromatographed as described under "Materials and Methods." Aliquots of each fraction were assayed for inhibition of  $^{125}$ I-hTNF binding to HeLa cells. B, 0.1-ml samples containing 15,000 cpm of  $^{125}$ I-hTNF (●) or  $^{125}$ I-mTNF (■) were chromatographed on the same column and the fractions were counted in a gamma counter. The void volume is indicated by an arrow. The inset shows the elution positions of proteins of known molecular size: a, cytochrome c; b, carbonic anhydrase; c, ovalbumin; and d, bovine serum albumin.

1B). Comparison of the elution volumes of peaks 1 and 2 with those of proteins of known size (Fig. 1, inset) gave  $M_r$  ~ 55,000 and 17,000, respectively, corresponding to a trimer and a monomer. This interpretation was confirmed by zonal sedimentation studies using  $^{125}$ I-hTNF in isokinetic 5–20% sucrose gradients (21). The major peak sedimented as a globular protein of  $M_r = 54,650 \pm 2,340$  in three independent analyses.

The TNF in the monomer peak appeared to compete poorly in the receptor binding assay, since it was not detected in the chromatogram shown in Fig. 1A. To confirm this finding,  $^{125}$ I-hTNF trimer and small amounts of monomer were isolated by gel filtration. 10,000 cpm of each fraction were tested for binding to HeLa cells; 1,180  $\pm$  90 cpm of trimer were bound in a standard assay, whereas only 140  $\pm$  20 cpm of monomer were specifically bound. In subsequent experiments, the biological activity of trimer and monomer was compared in cytotoxicity assays. Since monomer was recovered in relatively small amounts in physiological solutions, different procedures were tried to obtain sufficient quantities of this species. It was thus found by gel filtration analysis that  $^{125}$ I-hTNF trimer partially dissociated upon addition of low concentrations of the nonionic detergent Triton X-100. This dissociation was dependent on hTNF concentration, since the monomer/trimer ratio increased at low hTNF concentration (Fig. 2). Monomers were separated from trimers by gel filtration in a Sephadex G-75 column (0.7  $\times$  24 cm) pre-equilibrated with either PBS, 0.1% BSA for binding assays or culture medium for cytotoxicity assays. Triton X-100 was not detected (22) in the trimer or monomer peak, but was eluted at a greater column volume than hTNF monomer. In separate experiments (data not presented), it was shown by gel filtration analysis that hTNF monomers (~1 ng/ml) prepared in this manner quantitatively reassociated to trimers when the concentration of hTNF was increased 500-fold by adding unlabeled hTNF. Therefore, hTNF trimers can be dissociated by the addition of Triton X-100 into monomers, which are relatively stable in dilute solutions but readily reassociate to trimers when the hTNF concentration is raised.

Pooled fractions of hTNF trimer and monomer were subsequently compared in competitive binding and cytotoxicity assays on an equal counts/min basis. The monomer fraction

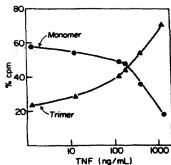


Fig. 2. Concentration dependence of the dissociation of  $^{125}$ I-hTNF by 0.1% Triton X-100. Increasing quantities of  $^{125}$ I-hTNF were incubated for 10 min at 22°C in a total volume of 0.1 ml containing 0.1% Triton X-100, 0.1% BSA, 20 mM PBS, pH 7.5, and were applied to a Sephadex G-75 column (0.7  $\times$  24 cm) equilibrated at 4°C with PBS, 0.1% BSA. 0.15-ml fractions were collected. The trimer and monomer recovered are expressed as a ratio of the counts/min in the respective peaks.

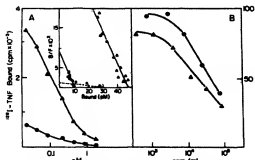


Fig. 3. Competitive binding and cytotoxicity assays comparing  $^{125}$ I-hTNF monomer and trimer fractions. Trimer (A) and monomer (B) fractions were isolated by gel filtration as described in the legend to Fig. 2. A, 30,000 cpm of each fraction were incubated for 5 h at 4°C with  $10^6$  HeLa cells and various concentrations of unlabeled hTNF in a total volume of 0.15 ml (see "Materials and Methods"). B,  $8 \times 10^4$  HeLa S2 cells were grown in monolayers in 96-well plates with 5  $\mu$ g/ml cycloheximide and the indicated cpm/ml of TNF monomer (●) or trimer (○). After 18 h the culture medium containing dead cells was removed, and the adherent cells were stained as described under "Materials and Methods." Results are expressed as a percentage of the control cells incubated with cycloheximide alone. Inset, binding data are shown as Scatchard plots with nonspecific binding subtracted; 51,300 was used as the molecular weight for TNF.

showed low binding activity and cytotoxicity compared to the trimer fraction. Binding of monomer was about 5.5-fold lower than that of trimer, as determined in competition binding assays (Fig. 3A). Scatchard plots of these data showed that the trimer was bound with a  $K_D = 90$  pM, whereas only a small component of the monomer fraction was bound with such high affinity (Fig. 3A, inset). Most of the monomer was bound with low affinity ( $K_D = 70$  nM). It seems unlikely that this binding has biological relevance, since 50% cytotoxicity of HeLa cells is observed with 2 pM hTNF (20). In parallel cytotoxicity assays, a monomer concentration 6–7-fold greater than that of trimer was needed to elicit the same biological response when tested at low concentrations (Fig. 3B). However, at the highest concentrations tested, the cytotoxicity of monomer was nearly equivalent to that of trimer. Rechromatography of the monomer fraction at the end of the incubation period showed the presence of about 10% trimer (data not shown), which could account for both the small component binding with high affinity and for the cytotoxicity at the

highest concentrations tested. These results indicated that hTNF trimer binds with higher affinity to receptors and has greater cytotoxic activity than hTNF monomer.

In the following experiment, we examined whether hTNF dissociates into monomers upon binding to receptors. A binding assay was carried out at 4 °C with low  $^{125}$ I-hTNF concentration, and the supernatant obtained after spinning out the cells was analyzed by gel filtration. The trimer peak was reduced in proportion to the  $^{125}$ I-hTNF bound to the cells, but no increase in the monomer peak could be detected (Fig. 4A). This result suggested that hTNF trimers could directly bind to receptors, but it could not be excluded that monomers

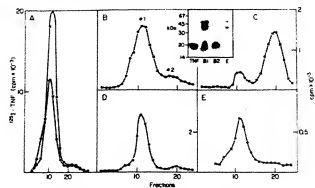


FIG. 4. Gel filtration of native and cross-linked  $^{125}$ I-hTNF on Sephadex G-75. A, 0.2-ml aliquots of pre-binding (■) and post-binding (●) cell-free supernatants containing 91,460 and 63,960 cpm, respectively, were compared by gel filtration in a Sephadex G-75 column (0.7 × 25 cm). 10,000 cpm of  $^{125}$ I-hTNF were incubated per  $10^6$  HeLa cells for 4 h at 4 °C. The cells were centrifuged at 15,500 × *g* for 30 s, and the supernatant was immediately applied to the column. The difference in peak areas represents TNF bound to cells. B–E, gel filtration in a different Sephadex G-75 column (0.7 × 24 cm). B and C, 20,000 cpm of BSOCES- $^{125}$ I-hTNF (B) or  $^{125}$ I-hTNF (C) in 5  $\mu$ l were mixed with an equal volume of 6 M GdnHCl. After 10 min, 85  $\mu$ l of column buffer and 5  $\mu$ l of glycerol were added, and the sample was applied to the column. D, 40  $\mu$ l of  $^{125}$ I-hTNF in PBS, 0.1% BSA were mixed with 40  $\mu$ l of 6 M GdnHCl and after 10 min at room temperature was dialyzed for 24 h at 4 °C against PBS, 0.1% BSA and 20  $\mu$ M 2-mercaptoethanol before chromatography. E,  $4 \times 10^6$  HeLa cells with bound BSOCES- $^{125}$ I-hTNF (6,750 cpm) were washed with PBS and then treated with 10  $\mu$ l of 3 M GdnHCl to dissociate bound TNF. After 10-min centrifugation at 15,500 × *g* to remove cellular debris, 0.1 ml of supernatant containing 2,800 cpm and 5% glycerol was applied to the column. The inset shows an electrophoretic analysis of  $^{125}$ I-hTNF (monomer) and of peak fractions recovered from the chromatograms in B and E containing cross-linked trimers and dimers. M, markers are indicated on the left.

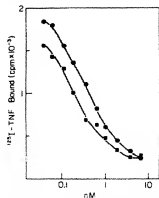


FIG. 5. Competitive binding assays comparing cross-linked and native hTNF. 18,000 cpm of  $^{125}$ I-hTNF (●) or BSOCES- $^{125}$ I-hTNF (■) were incubated with  $10^6$  HeLa cells and unlabeled hTNF as described under "Materials and Methods."

or dimers were binding and that the subunits released were reassociating into trimers. Therefore, to demonstrate that trimers can bind to cells and have biological activity, the hTNF was cross-linked to prevent its dissociation.

The  $^{125}$ I-hTNF was reacted with the cross-linking reagent BSOCES and compared to control  $^{125}$ I-hTNF by gel filtration chromatography, binding to HeLa cell receptors, and cytotoxicity assays. The cross-linked  $^{125}$ I-hTNF eluted with  $M_r \sim 55,000$  even after treatment with 3 M GdnHCl (Fig. 4B). This demonstrated that cross-linking stabilized hTNF against dissociation. In contrast, 85% of the control  $^{125}$ I-hTNF treated with 3 M GdnHCl eluted with an  $M_r = 17,000$  (Fig. 4C). This dissociation was in large part reversible, since after dialysis  $^{125}$ I-hTNF eluted as a trimer (Fig. 4D). These experiments showed that hTNF cross-linked with BSOCES is a trimer resistant to dissociation by relatively strong denaturing reagents, such as GdnHCl. However, drastic denaturing treatment of the cross-linked trimer, such as boiling in 1% sodium dodecyl sulfate under reducing conditions, resulted in partial dissociation into dimers and monomers, as judged by gel electrophoresis (Fig. 4, inset).

A binding assay carried out with cross-linked hTNF showed that it could bind to TNF receptors of HeLa cells. These cells were treated with 3 M GdnHCl to release bound BSOCES- $^{125}$ I-hTNF, and the supernatant was analyzed by gel filtration. A single peak of radioactivity was present (Fig. 4E), demonstrating that the bound hTNF could be eluted from HeLa cell receptors as a trimer. In order to determine whether cross-linking or acylation of amino groups had altered its binding to cell receptors, BSOCES- $^{125}$ I-hTNF was compared with  $^{125}$ I-hTNF in competitive binding assays (Fig. 5). Since BSOCES- $^{125}$ I-hTNF had lower bindability (39% compared to 45% for  $^{125}$ I-hTNF), equivalent amounts of bindable radioligands were added. The binding of both ligands was inhibited in a parallel manner by unlabeled hTNF, but only half as much unlabeled hTNF was required for 50% competition of BSOCES- $^{125}$ I-hTNF. This indicated that chemical changes introduced by the cross-linking reagent resulted in partial loss of binding activity. However, binding was 90% specific for both ligands. In agreement with the loss of binding activity, the cytotoxicity of BSOCES- $^{125}$ I-hTNF for HeLa cells was on average 4.5-fold less than that of control  $^{125}$ I-hTNF. A similar 5–10-fold decrease in cytotoxicity of BSOCES- $^{125}$ I-hTNF was observed in experiments with SK-MEL-109 melanoma cells (data not shown). These results with cross-linked TNF confirmed the findings with native TNF by showing that stable TNF trimers bind to cellular receptors and elicit a biological response.

## DISCUSSION

Natural human TNF, recombinant hTNF and mTNF, and cross-linked  $^{125}$ I-hTNF coelute in gel filtration under non-denaturing conditions as a major peak with an apparent  $M_r \sim 55,000$  (Figs. 1 and 4). The formation of homotrimers from 17,100 monomers (1) gives a predicted  $M_r = 51,300$ , which is in fairly good agreement with the  $M_r$  value obtained from gel filtration or zonal sedimentation. Furthermore, after cross-linking  $^{125}$ I-hTNF with BSOCES, radioactive bands corresponding to trimers, dimers, and monomers are observed by gel electrophoresis. Cross-linking data for other oligomeric proteins similarly show that incompletely cross-linked homotrimers may be dissociated into monomers and dimers (23). Therefore, three lines of evidence indicate that natural and recombinant TNF exist predominantly as a trimer under physiological conditions.

Gel filtration analyses show that monomers are present as

a small component of radioiodinated TNF (Fig. 1). The isolated monomers are only 12% as active as trimers in binding assays. Furthermore,  $^{125}$ I-hTNF can be dissociated into monomers by several treatments, such as a short incubation at pH 3.0.<sup>2</sup> Several reports have indicated that the biological activity of TNF is pH-sensitive (6, 9, 11, 24). Treatment with 3 M GdnHCl also dissociates  $^{125}$ I-hTNF (Fig. 4C). Of particular interest is the finding that low concentrations of the nonionic detergent Triton X-100 partially dissociate hTNF into monomers (Fig. 2), suggesting that weak hydrophobic interactions may be responsible for stabilizing the trimers (25). Dissociation by Triton X-100 can be used in combination with gel filtration chromatography to obtain monomer and trimer fractions for competitive binding and cytotoxicity assays.

These  $^{125}$ I-hTNF monomers show low receptor binding activity when compared to trimers. Monomer binding is characterized by high and low affinity components. The high affinity component is the same as that observed for the trimer, but rechromatography of monomer fractions shows the presence of some trimers. Therefore, small amounts of contaminating trimers may account for the high affinity binding component. In contrast, the trimer exhibits a single high affinity binding and greater cytotoxicity than monomer. At low concentrations, the cytotoxicity of the monomer fraction is 6–7-fold less than that of the trimer, but at higher concentrations monomer cytotoxicity becomes equivalent to that of trimer. This finding may be explained by the reassociation of monomers into active trimers. Other reports suggest that TNF monomers and oligomers are all active (1, 4, 12, 26).

The most direct evidence that hTNF trimer is biologically active comes from experiments wherein  $^{125}$ I-hTNF is cross-linked with BSOCOES. The cross-linked hTNF binds to receptors (Fig. 5) and is cytotoxic. Moreover, cross-linked hTNF trimers are recovered after binding to cells (Fig. 4E). In view of the remarkably low concentrations of hTNF that are biologically active in cytotoxicity assays (27), we are lead to speculate that these trimers may interact simultaneously or sequentially with more than one receptor. A possible result of such multiple interactions may be a heightened effective concentration at the cell surface (28). Furthermore, simultaneous binding to neighboring receptors might favor the interaction of the cytoplasmic domain of receptors (29) and either trigger or amplify the as-yet unknown signaling mechanism of the TNF receptor. In addition, dissociation of TNF into monomers at low concentrations may have some physiological relevance in the action of this factor. Since the monomer appears to be less active than the trimer, this dissociation may limit some of the deleterious effects of TNF (30) at sites remote from those where it is produced in high amounts by macrophages (31).

#### REFERENCES

- Aggarwal, B. B., Kohr, W. J., Haas, P. E., Moffat, B., Spencer, S. A., Henzel, W. J., Brimacombe, T. S., Newlin, G. E., Goeddel, D. V., and Harkins, R. N. (1985) *J. Biol. Chem.* **260**, 2345–2354
- Baglioni, C., McCandless, S., Tavernier, J., and Fiers, W. (1985) *J. Biol. Chem.* **260**, 13395–13397
- Shindl, T., Yamaguchi, H., Ito, H., Todd, C. W., and Wallace, B. (1985) *Nature* **313**, 803–806
- Williamson, B. D., Carswell, E. A., Rubin, B. Y., Prendergast, Y. S., and Old, L. J. (1983) *Proc. Natl. Acad. Sci. U. S. A.* **80**, 5397–5401
- Marmenout, A., Fransen, L., Tavernier, J., Van der Heyden, J., Tizard, R., Kewashima, E., Shaw, A., Johnson, M.-J., Semon, D., Müller, R., Ruyschaert, M.-R., Van Vliet, A., and Fiers, W. (1985) *Eur. J. Biochem.* **152**, 515–522
- Beutler, B., Mahoney, J., Le Trang, N., Pekala, P., and Cerami, A. (1985) *J. Exp. Med.* **161**, 984–995
- Green, S., Dobryjansky, A., Carswell, E. A., Kassel, R. L., Old, L. J., Fiore, N., and Schwartz, M. K. (1976) *Proc. Natl. Acad. Sci. U. S. A.* **73**, 381–385
- Kull, F. C., Jr., and Cuatrecasas, P. (1984) *Proc. Natl. Acad. Sci. U. S. A.* **81**, 7932–7936
- Takeda, Y., Shimada, S., Sugimoto, M., Woo, H. J., Higuchi, M., and Osawa, T. (1985) *Cell. Immunol.* **96**, 277–289
- Hernandez, K., Satomi, N., Sakurai, A., and Nariuchi, H. (1985) *Int. J. Cancer* **36**, 395–400
- Ruff, M., and Gifford, G. E. (1980) *J. Immunol.* **125**, 1671–1677
- Kull, F. C., Jacobs, S., and Cuatrecasas, P. (1985) *Proc. Natl. Acad. Sci. U. S. A.* **82**, 5756–5760
- Rubin, B. Y., Anderson, S. L., Sullivan, S. A., Williamson, B. D., Carswell, E. A., and Old, L. J. (1985) *J. Exp. Med.* **162**, 1099–1104
- Tsujiimoto, M., Yip, Y. K., and Vilček, J. (1985) *Proc. Natl. Acad. Sci. U. S. A.* **82**, 7626–7630
- Carswell, E. A., Old, L. J., Kassel, R. L., Green, S., Fiore, N., and Williamson, B. (1975) *Proc. Natl. Acad. Sci. U. S. A.* **72**, 3666–3670
- Williamson, B. D., Carswell, E. A., Rubin, B. Y., Prendergast, J. S., and Old, L. J. (1983) *Proc. Natl. Acad. Sci. U. S. A.* **80**, 5397–5401
- Sugarmann, B. J., Aggarwal, B. B., Haas, P. E., Figari, I. S., Palladino, M. A., and Shepard, H. M. (1985) *Science* **230**, 943–945
- Vilček, J., Palombella, V. J., Henryksen-DeStefano, D., Swenson, C., Feinman, R., Hirai, M., and Tsujiimoto, M. (1986) *J. Exp. Med.* **163**, 632–643
- Zacharchuk, C. M., Drysdale, B.-E., Mayer, M. M., and Shin, H. S. (1983) *Proc. Natl. Acad. Sci. U. S. A.* **80**, 6341–6345
- Smith, R. A., Kirstein, M., Fiers, W., and Baglioni, C. (1986) *J. Biol. Chem.* **261**, 14871–14874
- Martin, R. G., and Ames, B. N. (1961) *J. Biol. Chem.* **236**, 1372–1379
- Yoshida, K., Ishihara, K., Ohara, S., Asanuma, Y., and Hotta, K. (1980) *Anal. Biochem.* **108**, 162–165
- Daves, G. E., and Stark, G. R. (1970) *Proc. Natl. Acad. Sci. U. S. A.* **66**, 651–656
- Wang, A. M., Crasney, A. A., Ladner, M. B., Lin, L. S., Strickler, J., Van Arndell, J. N., Yamamoto, R., and Mark, D. F. (1985) *Science* **228**, 149–154
- Helenius, A., McCaslin, D. R., Fries, E., and Tanford, C. (1979) *Methods Enzymol.* **56**, 734–749
- Hahn, T., Tokier, L., Budilovskiy, S., Aderka, D., Eshhar, Z., and Wallach, D. (1985) *Proc. Natl. Acad. Sci. U. S. A.* **82**, 3814–3818
- Ruff, M. R., and Gifford, G. E. (1981) *Infect. Immun.* **31**, 380–385
- Goldstein, L. (1976) *Methods Enzymol.* **44**, 397–443
- Heffetz, D., and Zick, Y. (1986) *J. Biol. Chem.* **261**, 889–894
- Tracey, K. J., Beutler, B., Lowry, S. F., Merryweather, J., Wolpe, S., Milsark, I. W., Hariri, R. J., Fahey, T. J., Zentella, A., Albert, J. D., Shires, G. T., and Cerami, A. (1986) *Science* **234**, 470–474
- Beutler, B., and Cerami, A. (1986) *Nature* **320**, 584–588

<sup>2</sup> R. A. Smith and C. Baglioni, unpublished observations.

## EXHIBIT J

## AFFINITY PRECIPITATION OF ENZYMES

Per-Olof LARSSON and Klaus MOSBACH

Biochemical Division, Chemical Center, University of Lund, P.O. Box 740, S-220 07 Lund 7, Sweden

Received 21 December 1978

## 1. Introduction

Bifunctional nucleotide derivatives, i.e., nucleotides connected by a spacer, such as AMP-AMP or the heterofunctional compound AMP-ATP [1], have earlier been prepared with the objective of using them primarily as affinity chromatography ligands. It occurred to us that compounds of this type might function as precipitating agents for enzymes. In particular, dimeric NAD-derivatives should be useful since NAD has affinity for a large number of enzymes. Further, these derivatives would allow utilization of the principles of ternary complex formation, which increases the interaction and ensures a high degree of specificity [2]. Such affinity precipitation of enzymes should not only provide a new tool in the analysis and purification of enzymes (dehydrogenases), but also be useful in morphologic and topographic studies of dehydrogenases in analogy to studies using bis-biotinyl diamines and avidin [3].

This paper describes the preparation of a bifunctional NAD compound,  $N_1, N_2'$ -adipodihydrazido-bis-( $N^6$ -carbonylmethyl-NAD) (Bis-NAD), and its properties as a complexing/precipitating agent for the tetrameric enzyme lactate dehydrogenase (LDH).

## 2. Materials and methods

## 2.1. Materials

LDH (beef heart, type III, in  $(\text{NH}_4)_2\text{SO}_4$ , 550 U/mg), adipic acid dihydrazide and 1-ethyl-3-(3-dimethylaminopropyl) carbodiimide were

obtained from Sigma, St. Louis, MO. Before use the enzyme was dialyzed overnight against 0.05 M sodium phosphate buffer (pH 7.5) and freed from insoluble matter by centrifugation.  $N^6$ -Carboxymethyl-NAD was prepared as in [4]. All other reagents were of analytical grade and obtained from commercial sources.

2.2. Synthesis of  $N_1, N_2'$ -adipodihydrazido-bis-( $N^6$ -carbonylmethyl-NAD) (Bis-NAD)

Adipic acid dihydrazide dihydrochloride (105 mg, 0.60 mmol) and  $N^6$ -carboxymethyl-NAD (900 mg, 1 mmol) were dissolved in 10 ml water (15°C) and pH adjusted to 4.0 with 1 M HCl. The condensing agent, 1-ethyl-3-(3-dimethylaminopropyl)-carbodiimide, was added as a 1 M aqueous solution (0°C) in 0.1 ml portions. After 30 min by which time 15 portions (1.5 mmol) had been added, thin-layer chromatography indicated that most of the  $N^6$ -carboxymethyl-NAD had been converted and the reaction was terminated. The reaction mixture was diluted to 1.0 l and adjusted to pH 8.0 with  $\text{NH}_4\text{OH}$ . The solution was applied to a column with cellulose anion exchanger (Whatman DE-52, 2.5 × 80 cm), successively equilibrated with 1 M  $\text{NH}_4\text{HCO}_3$  (pH 8.0) and water. The column was washed with water and the nucleotide was then eluted with a 4 l ammonium bicarbonate gradient from 0–0.25 M.

The desired product, Bis-NAD, was eluted between 1.2 l and 1.6 l. Lyophilization gave 400 mg of a white product which was homogeneous as judged from thin-layer chromatography.  $R_F$  values on silica gel (Merck, Darmstadt) developed in 0.5 M ammonium acetate : ethanol = 2.5 were:  $N^6$ -carboxymethyl-NAD = 0.22; Bis-NAD = 0.05; and the monosubstituted derivative

$N_2$ -adipodihydrazido- $N^6$ -carboxymethyl-NAD = 0.19. Based on ultraviolet spectra and phosphate analysis the  $\epsilon$ -value at 266 nm in neutral aqueous solution for Bis-NAD was  $21\,400\text{ M}^{-1}\text{ cm}^{-1}$ . The yield based on  $N^6$ -carboxymethyl-NAD was calculated as 44%.

### 2.3. Affinity precipitation of LDH (standard procedure)

The precipitation procedure was carried out at  $0-6^\circ\text{C}$  in the following way: To 1.5 ml dialyzed LDH (1.1 mg/ml) in 0.05 M sodium phosphate buffer (pH 7.5) was added 0.25 ml 0.12 mM Bis-NAD (water) followed by 0.25 ml 0.8 M sodium pyruvate (water). After gentle mixing in a test tube the solution was allowed to stand. Within 30 min, a heavy precipitate began to form and after 16 h (overnight) the precipitate was isolated by centrifugation.

The amount of LDH in the precipitate and the supernatant fluid was determined by the Lowry procedure [5] and from activity measurements. LDH activity was determined by following the oxidation of NADH at 340 nm. The assay medium consisted of 1 mM sodium pyruvate and 0.30 mM NADH in 0.05 M phosphate buffer (pH 7.5). The assay was initiated by adding a suitably diluted enzyme solution (to give  $\Delta A_{340} < 0.1/\text{min}$ ). Some enzyme inhibition due to ternary complex formation with Bis-NAD and pyruvate was sometimes observed, but was corrected for by references.

### 2.4. Affinity precipitation in agarose gels

Agarose gels (0.8%) were cast on microscope glass slides and wells were punched out with a die. In double diffusion experiments [6] the agarose gel contained 0.3 M sodium pyruvate and 0.05 M sodium phosphate buffer (pH 7.5); the center well contained 15  $\mu\text{l}$  LDH solution (5–50  $\mu\text{g}$  enzyme) and the peripheral wells contained 7  $\mu\text{l}$  reagent (Bis-NAD, or NAD or buffer). After diffusion for 1.5–16 h in a moist chamber at room temperature the precipitated protein was stained with Amido black [6].

In single radial diffusion experiments [6] the agarose was cast in the presence of pyruvate and Bis-NAD when LDH was to be quantified and in the presence of pyruvate and LDH when Bis-NAD was to be quantified.

## 3. Results and discussion

### 3.1. Structural assignment

When designing the preparation of bifunctional NAD compounds, principally equivalent to the one depicted in fig. 1, i.e., compounds built by connecting two NAD entities symmetrically by a spacer, it appeared reasonable to use the available compounds  $N^6$ -carboxymethyl-NAD [4] or  $N^6$ -[ $N$ -(6-aminohexyl)-carbamoylmethyl]-NAD [4]. A direct condensation of these two NAD analogs by a carbodiimide proved unsatisfactory since the yield was very low owing to side reactions [1]. Other methods based on condensation of two  $N^6$ -[ $N$ -(6-aminohexyl)carbamoylmethyl]-NAD with reactive diimidoesters (adipimide) or with very reactive diacid dichlorides (adipic acid dichloride) were feasible, although the exact procedure when mixing reactants was critical and great care had to be exercised if a satisfactory result was to be expected. In addition, the connecting spacers in these cases were considered unnecessarily long and an alternative linking procedure based on  $N^6$ -carboxymethyl derivatives of NAD was therefore tried.  $N^6$ -Carboxymethyl-NAD was thus condensed with adipic acid dihydrazide in a carbodiimide-mediated reaction, giving a bis-nucleotide with a spacer of moderate length (fig. 1). The distance between the exocyclic nitrogen atoms of the two adenines is  $\sim 17\text{ \AA}$  (measured from an extended space-filling model), a distance that should allow easy and simultaneous interaction with active sites of two dehydrogenase molecules, provided the sites are not too deeply buried. The spacer is comparatively hydrophilic, which is preferable because it reduces the risk of non-specific hydrophobic interactions.

The condensation reaction described in section 2 proceeds very smoothly at pH 4.0, due to the favourable  $\text{pK}_a$  values of the reactants (2.5–3.0 for

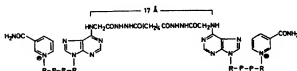


Fig. 1. Bis-NAD =  $N_2, N'_2$ '-adipodihydrazido-bis- $N^6$ -carboxymethyl-NAD).

$N^6$ -carboxymethyl-NAD and 4.9 for adipic acid dihydrazide) which also allow for sufficient buffering to make external pH-control virtually unnecessary.

The structure assigned to Bis-NAD is based on several facts. The method of synthesis, a carbodiimide mediated condensation of  $N^6$ -carboxymethyl-NAD and adipic acid dihydrazide, should yield only two new compounds (besides breakdown products), namely adipic acid dihydrazide mono- and disubstituted with NAD. In agreement herewith, an ion-exchange chromatography of the crude reaction product gave three major peaks, the last of which to emerge was unreacted  $N^6$ -carboxymethyl-NAD. The other two peaks were assigned to be the mono-substituted compound,  $N_2$ -adipodihydrazido- $N^6$ -carbonylmethyl-NAD (the first peak; yield ~10%) and Bis-NAD (the second peak; yield ~40%). In a separate verifying experiment the condensation was carried out with a 20-fold excess of adipic acid dihydrazide and as, expected, only one product was formed, namely the monosubstituted compound. The monosubstituted compound gave positive reaction with trinitrobenzene sulfonic acid reagent [7], whereas Bis-NAD did not, proving that the latter compound lacked the free hydrazide group.

Comparison of 100 MHz proton NMR spectra of  $N^6$ -carboxymethyl-NAD,  $N_2$ -adipodihydrazido- $N^6$ -carbonylmethyl-NAD and Bis-NAD also confirmed the structures assumed. The two latter compounds thus gave two new signals corresponding to the protons of the four adjacent methylene groups of the spacer. Besides physicochemical tests, the Bis-NAD was shown to act as a coenzyme with LDH.

### 3.2. Affinity precipitation, basic properties

Initial experiments showed that LDH could be precipitated from a solution containing equivalent amounts of Bis-NAD (i.e., 1 NAD/enzyme subunit). The explanation to the precipitation event is believed to be rather straightforward. Molecules of LDH, Bis-NAD and pyruvate form strong dead-end ternary complexes and since Bis-NAD can interact with two LDH molecules and since LDH is a tetrameric enzyme it can easily be understood that large aggregates will form. When these aggregates have grown sufficiently large, they turn insoluble and precipitate out.

In order to obtain an optimal 'yield' of precipitation several parameters were varied. The pH value

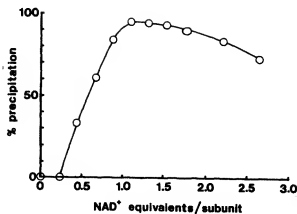


Fig.2. The efficiency of the affinity precipitation as function of the NAD-equiv./subunit ratio. LDH (20  $\mu$ N) dissolved in 0.05 M phosphate buffer (pH 7.5) 0.1 M with respect to pyruvate was treated with varying amounts of Bis-NAD in small test tubes. Total volume was 0.4 ml. The mixture was kept at 4°C overnight and the precipitated LDH centrifuged down. The amount of precipitated LDH was measured directly by the Lowry method or calculated from the LDH activity of the supernatant.

did not appreciably affect the precipitation in the region pH 6.5–8.0 (phosphate buffer). The concentration of pyruvate was not critical if well above the mM range. Therefore 0.1 M pyruvate was routinely employed.

The correct stoichiometry of reactants (Bis-NAD/enzyme) in the affinity precipitation process is obviously important. Figure 2 gives the degree of precipitation as a function of the ratio between NAD-equivalents and enzyme subunits. It is evident that maximum precipitation occurs near equinormality of enzyme subunits and NAD. When the ratio between coenzyme equivalents and enzyme subunits is lower than unity, the precipitation yield is low, e.g., a ratio of 0.3 gives hardly any precipitation. On the other hand, if the ratio is above unity, the precipitation yield is not so markedly affected, a ratio of 2.5, for example, still giving a precipitation efficiency of 75%.

To confirm these results an additional experiment was carried out in which the composition of the precipitate was determined. For this purpose a precipitate prepared by the standard procedure was centrifuged and treated with urea to obtain a clear



solution. The solution was analyzed in ultraviolet light (266 nm and 290 nm) and the content of nucleotide and enzyme calculated. It turned out that the composition of the precipitate corresponded well to the ratio at which the precipitation was best, i.e., 1.1 NAD equiv./LDH subunit.

To obtain macromolecular aggregates, a minimum of 2 (average) subunits/LDH molecule must be engaged in complexes, and this minimum corresponds to a ratio of 0.5; when all subunits are engaged the ratio would be 1.0, a value close to the observed value of 1.1. This reasoning is, of course, valid only with the assumption that the cofactor, pyruvate and enzyme form a firm complex. It is also assumed that Bis-NAD does not participate in intramolecular crosslinking, an unlikely situation since the 17 Å spacer (fig.1) would be too short to cover the distance between two cofactor binding sites within the same molecule [8].

### 3.3. Redissolution of affinity precipitated dehydrogenase

In some applications of affinity precipitation, e.g., purification of enzymes, it would be necessary to remove pyruvate and Bis-NAD as a final step, and in such a way as to preserve activity. Table 1 illustrates the feasibility of regenerating the free enzyme from the precipitate by gel filtration. In order to discriminate between losses of activity due

to the affinity precipitation process and losses due to the regeneration, several references were included. Gel filtration on Sephadex G-50 gave a recovery of ~85%, the 15% loss of activity being caused both by the precipitation and the gel filtration, as judged from the references. Prior to the gel filtration the precipitate had to be dissolved and to this end NADH was added to 10 mM. The precipitate dissolved within 1 min, the mechanism behind the phenomenon obviously being that NADH forms a strong complex with LDH ( $K_{dis} \sim 1 \mu M$ , NADH is present in high concentration) and thus efficiently competes for the active sites. Also, the simultaneous presence of NADH and LDH would consume the comparatively small amount of pyruvate present in the precipitate. Another competitive ligand, AMP (10 mM) was also tried, but was less efficient in solubilizing the precipitate in accordance with its higher dissociation constant,  $K_{dis} \sim 1$  mM. Summarizing, it is feasible by simple means to regenerate affinity precipitated material.

### 3.4. Affinity precipitation in gels

Affinity precipitation of enzymes resembles, at least superficially, immunoprecipitation, i.e., the aggregation of antibodies and antigens. In a set of experiments we exploited this and adopted the techniques commonly used in immunodiffusion

Table 1  
Recovery of affinity precipitated LDH

Sample reference	Additions in the precipitation step	Treatment in the recovery step	Recovery %
Sample	Pyruvate + Bis-NAD	NADH; G-50	85
Reference 1	Pyruvate + NAD	NADH; G-50	92
Reference 2	None	NADH; G-50	92
Reference 3	None	None	100

Samples and references contained 25  $\mu N$  LDH in 0.05 M phosphate buffer (pH 7.5). In the precipitation step pyruvate (0.1 M) and Bis-NAD (30  $\mu N$ ) or NAD (30  $\mu N$ ) were added as indicated. The total volume was 1.20 ml. After 16 h the precipitate (formed in the samples only) was centrifuged down and the supernatant discarded. In the recovery step the LDH in samples and references was freed from pyruvate and nucleotide by gel filtration (Sephadex G-50,  $1.5 \times 30$  cm; 1 ml/min). Before application on the G-50 column the sample and the reference were steeped in 10 mM NADH (in order to dissolve the precipitated protein in the sample). The activity of the LDH after the various treatments is given relative to that of reference 4 (100%)

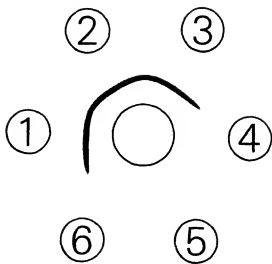


Fig.3. Diffusion-precipitation in agarose gel. The center well contained 30  $\mu$ g lactate dehydrogenase in 15  $\mu$ l buffer. The peripheral wells contained 7  $\mu$ l reagents: wells 1-3, 1.5 nmol Bis-NAD; well 5, 3.0 nmol NAD; wells 4, 6, buffer only.

experiments. Figure 3 shows the result of a double diffusion experiment (Ouchterlony test [6]) in agarose-containing pyruvate, where the center well contained enzyme, the peripheral wells Bis-NAD or NAD or buffer. A precipitation band was observed only where LDH and Bis-NAD had been allowed to diffuse towards each other. The figure shows the situation after 1.5 h diffusion. Prolonged diffusion for 16 h gave approximately the same pattern. The single radial diffusion technique (Mancini method [6]) was briefly evaluated with respect to its ability to quantify lactate dehydrogenase and/or Bis-NAD. The agarose gel in this case was cast in the presence of pyruvate and Bis-NAD (or lactate dehydrogenase) and the linearly-arranged wells were filled with different amounts of lactate dehydrogenase (or Bis-NAD). Precipitation rings were formed around the wells; the diameters being approximately proportional to the amount of lactate dehydrogenase (or Bis-NAD) present in the well.

#### 4. Conclusion

Affinity precipitation of enzymes has been

exemplified here with lactate dehydrogenase and Bis-NAD (+ pyruvate) and is likely to be applicable also to other NAD-dependent dehydrogenases although preliminary experiments with liver alcohol dehydrogenase and the Bis-NAD used in this study (+ pyrazol) indicate that at least for alcohol dehydrogenase a longer spacer is required. Affinity precipitation should be applicable also to enzymes/proteins other than dehydrogenases, provided that suitable bifunctional ligands are available. In cases in which the interaction between the bifunctional ligand and the enzyme is not sufficiently strong, formation of ternary complexes could be tried as exemplified here. Thus, besides dead-end complex formation also other ternary complexes could be utilized, for instance complexes with coenzyme and inhibitor and complexes with coenzyme-substrate adducts [9]. Alternatively, a careful addition of salts, e.g., ammonium sulphate or solvents, e.g., polyethylene glycol might enhance the precipitation without impairing the specificity.

Affinity precipitation of enzymes using binucleotides of varying spacer length may be useful in topographic studies of enzymes, e.g., in the determination of the depth of an active site/ligand binding site. Also information concerning the spatial arrangements of subunits in an oligomeric enzyme might be obtained from precipitated aggregates by using electron microscopy analogous to the study of complexes between avidin and biotinylated diamines [3]. In certain cases enzyme purification procedures may benefit from the principle, e.g., when conventional affinity chromatography is less satisfactory because of sterically-impaired interaction between the enzyme and its immobilized ligand. Further, the method of diffusion-precipitation in gels might find, for example, clinical applications. The procedure could, for instance, be used for detecting abnormal levels of enzymes and other proteins found in serum; compared with the immunodiffusion technique an obvious advantage of this method is that antibodies, which might be difficult to raise, would not be needed.

Finally, it deserves mentioning that bifunctional ligands (including those interacting with effector sites) may prove useful as agents permitting precipitation/immobilization of biomolecules in a reversible manner.

### Acknowledgement

The financial support of the Swedish Natural Science Research Council is gratefully acknowledged.

### References

- [1] Lee, C.-Y., Larsson, P.-O. and Mosbach, K. (1977) *J. Solid-Phase Biochem.* 2, 31–39.
- [2] Mosbach, K. (1978) *Adv. Enzymol.* 46, 205–278.
- [3] Green, N. M., Konieczny, L., Toms, E. J. and Valentine, R. C. (1971) *Biochem. J.* 125, 781–791.
- [4] Mosbach, K., Larsson, P.-O. and Lowe, C. (1976) *Methods Enzymol.* 44, 859–887.
- [5] Lowry, O. H., Rosebrough, N. J., Farr, A. L. and Randall, R. J. (1951) *J. Biol. Chem.* 193, 265–275.
- [6] Clausen, J. (1969) in: *Laboratory Techniques in Biochemistry and Molecular Biology* (Work, T. S. and Work, E. eds) vol. 1, pp. 397–546, North-Holland, Amsterdam.
- [7] Satake, K., Okuyama, T., Ohashi, M. and Shinoda, T. (1960) *J. Biochem.* 47, 654–660.
- [8] Boyer, P. D. ed (1975) *The Enzymes* vol. 11, pt A, Academic Press, New York.
- [9] Everse, J., Zoll, E. C., Kahan, L. and Kaplan, N. O. (1971) *Bioorg. Chem.* 1, 207–233.

## EXHIBIT K

## CHAPTER 22

### Affinity Precipitation Methods

*Jane A. Irwin and Keith F. Tipton*

#### 1. Introduction

##### 1.1. Overview

Affinity chromatography (*see* Chapter 16) is a powerful protein purification technique, that exploits the specific interaction between a biological ligand (e.g., a substrate, coenzyme, hormone, antibody, or nucleic acid) or its synthetic analog and its complementary binding site on a protein. One of the variations on this technique (*see* refs. 1–3 for reviews) was that of affinity precipitation. As in affinity chromatography, the protein binds to a specific ligand, but the latter is free in solution, rather than bound to an insoluble support. Ligand binding gives rise to the precipitation of the protein from solution, which is then followed by centrifugation. The pellet contains the protein of interest and the ligand, whereas the other components of the mixture remain in the supernatant, allowing easy separation.

There are two main approaches to affinity precipitation. The first of these is called the “bis-ligand” or “homobifunctional ligand” approach. The ligand is bifunctional, bearing two identical ligands connected by a spacer arm. If the spacer is long enough, each ligand can bind to a ligand binding site on a different protein molecule. Oligomeric proteins can bind two or more bis-ligands, with the consequent formation of crosslinked lattices. When the lattice becomes large enough, it will precipitate from solution.

The second approach to affinity precipitation differs from this in that the affinity ligand has two functions, one of which binds the target protein and a second to promote the precipitation of the aggregate. In some

From: *Methods in Molecular Biology*, Vol. 59: *Protein Purification Protocols*  
Edited by: S. Doonan Humana Press Inc., Totowa, NJ

cases, precipitation is induced by the addition of a third component, e.g., a lectin or metal ion. This technique is referred to in the literature as affinity precipitation, but in contrast to the first approach, the precipitation of the complex does not occur as a direct consequence of the affinity interaction between the protein and its ligand, but as a result of adding a third component. Table 1 gives a list of examples of both "bis-ligand" and this second form of affinity precipitation.

This chapter is confined to a discussion of the "bis-ligand" form of affinity precipitation, that can be described as "true" affinity precipitation, occurring solely as a result of the direct interaction between the ligand and the protein, and not as a result of a third component of the system.

### 1.2. Bis-Coenzymes and Their Applications

Larsson and Mosbach were the first to synthesize a bifunctional affinity precipitation reagent (4). This affinity precipitation reagent was  $N_2,N'_2$ -adipodihydrazido-bis-( $N^6$ -carbonylmethyl)NAD<sup>+</sup> (bis-NAD<sup>+</sup>). It consisted of two molecules of the NAD<sup>+</sup> derivative  $N^6$ -carboxymethyl-NAD<sup>+</sup>, linked by an adipic acid dihydrazide spacer arm (Fig. 1). This compound was used to affinity precipitate purified lactate dehydrogenase from bovine heart in up to 90% yield. Bovine liver GDH and yeast alcohol dehydrogenase were also precipitated by this technique (5-7). The latter enzyme also required high ionic strengths for precipitation to occur. Further applications of bis-NAD<sup>+</sup> are mentioned in Table 1, and some limitations on its use are described in Note 1.

An alternative synthesis of a range of bis-NAD<sup>+</sup> affinity reagents has been developed (28). It involves the carbodiimide-mediated condensation of two molecules of  $N^6$ -(2-aminoethyl)NAD<sup>+</sup> with different dicarboxylic acids (Fig. 2). The synthesis of bis-coenzyme derivatives has not been limited only to NAD<sup>+</sup>; a synthesis of a bis-ATP derivative,  $N_2,N'_2$ -adipodihydrazido-bis-( $N^6$ -carbonylmethyl)ATP (10) is described here.

### 1.3. Structural and Kinetic Requirements for Affinity Precipitation with Bis-Coenzymes

The technique of bis-ligand affinity precipitation with bis-NAD<sup>+</sup> only works under certain conditions (29), which may be summarized as follows:

1. The enzyme of interest has to contain more than one coenzyme binding site.
2. The bis-ligand has to have a strong affinity for the enzyme.

Table 1  
Published Examples of Protein Purification by Affinity Precipitation

Protein	Bis-ligand <sup>a</sup>		Refs.
	Bis-ligand	Bis-ligand	
LDH	Bis-NAD <sup>+</sup>		4-8
GDI	Bis-NAD <sup>+</sup>		5-7,9
YADH	Bis-NAD <sup>+</sup>		5,7
Acetate dehydrogenase	Bis-NAD <sup>+</sup>		10
Protein A	Bis-NAD <sup>+</sup>		10
LDH (rabbit)	Bis-Chroton Blue F1G-A		11,12
Bovine serum albumin	Bis-Chroton Blue F1G-A		11,12
LDH (rabbit)	Methoxylated <i>p</i> -sulfonated isomer of Procion Blue 11-B		13,14
GDI (recombinant)	EGTA (Zn <sup>2+</sup> )		15
Human hemoglobin, sperm whale myoglobin	Cu(II)EGTA, Cu(II) <sub>2</sub> polyethylene glycol-(iminodiacetic acid) <sub>2</sub>		16
Protein	Hetero-bifunctional ligands <sup>a</sup>		Refs.
	Ligand	Carrier	
Trypsin	<i>p</i> -Aminobenzamide	<i>N</i> -acryloyl-aminobenzoic acid	17
Trypsin	Soybean trypsin inhibitor	Chitosan	18
Wheat germ agglutinin	<i>N</i> -acetyl-D-glucosamine	Chitosan	19
Protein A	IgG	Hydroxymethyl cellulose	20
Recombinant protein A	IgG	Acetate succinate	21
IgG	Protein A	Euclagrit S100	22
LDH	Chroton Blue	Galactanmannan	23
Trypsin	Soybean trypsin inhibitor	Dextran	24
Protein A	Euclagrit	Alginic acid	25
Trypsin	<i>p</i> -Aminobenzamide	<i>N</i> -isopropylacrylamide polymer	26
		<i>N</i> -isopropylacrylamide polymer	27

<sup>a</sup>These do not require a second component to effect affinity precipitation.

<sup>b</sup>These require a ligand carrier and a third component to promote the precipitation of the ligand-protein complex.

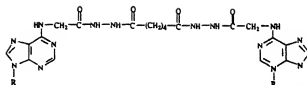


Fig. 1. Structure of bis-NAD<sup>+</sup>, first synthesized by Larsson and Mosbach (4), and used as an affinity ligand for several dehydrogenases. R represents nicotinamide mononucleotide.

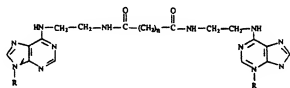


Fig. 2. General structure of bis-NAD<sup>+</sup> derivatives, based on *N*<sup>6</sup>-(2-aminoethyl)-NAD<sup>+</sup> as a starting material. These include *N,N'*-bis(*N*<sup>6</sup>-ethylene-NAD<sup>+</sup>) glutaramide ( $n = 3$ ); *N,N'*-bis(*N*<sup>6</sup>-ethylene-NAD<sup>+</sup>) adipamide ( $n = 4$ ), and *N,N'*-bis(*N*<sup>6</sup>-ethylene-NAD<sup>+</sup>) pimelamide ( $n = 5$ ). R represents nicotinamide mononucleotide phosphoribose.

3. The spacer connecting the two ligands has to be long enough to bridge the distance between two ligand binding sites on two different enzyme molecules. In the case of *N*<sub>2</sub>, *N*<sub>2</sub>'-adipodihydrazido-bis-(*N*<sup>6</sup>-carbonylmethyl)-NAD<sup>+</sup> (bis-NAD<sup>+</sup>), the spacer length was approx 1.7 nm, which permitted easy simultaneous access for a molecule of bis-NAD<sup>+</sup> to two different molecules of a dehydrogenase.

A further limitation is the ratio of coenzyme derivative to enzyme subunit. If this is low, a lattice will not form since there are not enough crosslinks; if it is too high, each dehydrogenase subunit can be occupied by a separate molecule of bis-NAD<sup>+</sup> and no crosslinks will form. Maximum crosslinking occurs at an optimum ratio of NAD<sup>+</sup> eq/enzyme subunit (assuming two NAD<sup>+</sup> Eq/bis-NAD<sup>+</sup>), which in the case of tetramers has been found to be approximately unity. This can vary; for example, the hexameric mammalian glutamate dehydrogenase (GDH) precipitated over a broad range of NAD<sup>+</sup> equivalents to active site ratios (0.3:10), with up to 70% precipitation occurring at a ratio as low as 0.16, although



this probably involves the existence of higher GDH polymers (5). The ratio of approximately unity for tetramers is similar to the behavior observed in immunoprecipitation, in which two antigen molecules/antibody give rise to the optimum precipitation of immune complexes (30).

Adding bis-NAD<sup>+</sup> alone to a crude extract containing many different dehydrogenases will not in itself cause specific affinity precipitation, since it is a "general ligand," binding to most NAD<sup>+</sup>-dependent dehydrogenases. In addition to being nonspecific, bis-NAD<sup>+</sup> forms a weak binary complex with several dehydrogenases, e.g., lactate and horse liver alcohol dehydrogenases. The addition of a substrate analog (usually a competitive inhibitor, relative to the enzyme's second substrate) strengthens the binding interaction. Since NADH binds, on average, one order of magnitude more tightly to the active sites of many dehydrogenases than NAD<sup>+</sup>, it displaces bis-NAD<sup>+</sup> and is commonly used to dissolve crosslinked aggregates.

The specificity of bis-NAD<sup>+</sup> of affinity precipitation for any given dehydrogenase is conferred by a property described by O'Carra as the "locking-on" effect (31). This was originally developed to increase the strength of enzyme binding to an immobilized ligand by adding analogs of substrates specific to the enzyme under study. In the case of lactate dehydrogenase, for example, the strength of adsorption to an immobilized NAD<sup>+</sup> derivative was increased by adding oxalate, a structural analog of lactate, to the irrigating buffer. The enzyme was eluted by simply leaving out the oxalate.

This "locking-on" property does not occur with all enzymes. It is confined to those with sequential mechanisms (see refs. 3 and 31 for more details). Most coenzyme-dependent enzymes, including the majority of dehydrogenases, have ordered sequential kinetic mechanisms, in which the coenzyme binds before the second substrate. If this is the case, the "locking-on" effect occurs. The addition of an unreactive, competitive inhibitor of the second substrate will displace the coenzyme binding equilibrium by ternary complex formation (sometimes described as an "abortive" complex) and thereby increase the strength of binding. In affinity precipitation, the bis-coenzyme is "locked" into place by the substrate analog, provided it is saturating. Some enhancement of bis-ligand binding can occur for an enzyme with a random sequential mechanism, provided that the equilibrium of the reaction under the conditions employed in affinity precipitation is such that the binding of the substrate analog then favors coenzyme binding.

The identity of the substrate analog will determine which dehydrogenase is precipitated from a crude extract. For example, adding bis-NAD<sup>+</sup> and glutarate will lead to the precipitation of GDH from a crude extract; addition of pyrazole or oxalate would favor alcohol dehydrogenase or lactate dehydrogenase precipitation, respectively. This is the key to making the technique specific for one enzyme.

In the case of the only reported bis-ATP derivative, which was used to affinity precipitate bovine heart phosphofructokinase, precipitation was not accomplished with the aid of a second substrate analog, but by the use of the allosteric inhibitor citrate. ATP is both a substrate and an allosteric inhibitor of this enzyme, and this inhibition is potentiated by citrate (10).

#### **1.4. Affinity Precipitation with Other Bifunctional Ligands**

Examples of bis-ligand affinity precipitation in the literature are few, and the technique has not gained widespread popularity since it has only been found to work with a few proteins. In order to extend its use, other ligands have been synthesized, but these have been limited so far to triazine dyes and immobilized metal ions. Triazine dyes have been widely used as pseudo-affinity ligands (see Chapter 17 for a discussion of dye-ligand chromatography). A bis-derivative of Cibacron Blue F3GA was found to precipitate bovine serum albumin and lactate dehydrogenase (11), and a monofunctional synthetic analog of Procion Blue H-B was found to precipitate rabbit muscle lactate dehydrogenase selectively (13,14). The synthesis of this analog is reported in ref. 13, and the method for large-scale LDH purification is described in ref. 14. Only two examples of metal ion affinity precipitation have been reported to date, one of which consisted of the precipitation of recombinant galactose dehydrogenase containing a pentahistidine affinity tail by a (Zn)<sub>2</sub>-EGTA chelate (15). In the second case, myoglobin and hemoglobin were precipitated by an EGTA-Cu(II) chelate or, alternatively, by a bis-ligand consisting of Cu(II) cations chelated by molecules of iminodiacetic acid immobilized on each end of a molecule of polyethylene glycol (17).

### **2. Materials**

#### **2.1. Synthesis of Coenzyme Derivatives**

##### **2.1.1. Synthesis of Bis-NAD<sup>+</sup>**

This compound is commercially obtainable, but is quite expensive (\$90.00 for 5 mg, Sigma, St. Louis, MO, 1995). The starting material is

*N*<sup>6</sup>-carboxymethyl-NAD<sup>+</sup>. This is also obtainable from Sigma, but may be readily synthesized. The following reagents are required.

2.1.1.1. *N*<sup>6</sup>-CARBOXYMETHYL-NAD<sup>+</sup>

1. NAD<sup>+</sup> (98%, free acid).
2. Iodoacetic acid.
3. 2*M* LiOH.
4. 96% (w/v) Ethanol.
5. Sodium dithionite.
6. 0.24*M* NaHCO<sub>3</sub>.
7. Yeast alcohol dehydrogenase (crystalline, Sigma or Boehringer Mannheim, Mannheim, Germany).
8. A sintered funnel (fairly large, at least 10 cm in diameter).
9. AG 1 × 2 anion-exchange resin (200–400 mesh, Cl<sup>−</sup> form, Bio-Rad, Hercules, CA).
10. CaCl<sub>2</sub>.

2.1.1.2. Bis-NAD<sup>+</sup>

1. Adipic acid dihydrazide dichloride (Sigma).
2. 2*M* NH<sub>4</sub>OH.
3. NH<sub>4</sub>HCO<sub>3</sub>.
4. DEAE-cellulose (Whatman DE52, equilibrated with 10 column volumes of 1*M* NH<sub>4</sub>HCO<sub>3</sub>, and washed with water).

2.1.2. N<sub>9</sub>N<sub>2</sub>-Adipodihydrazido-Bis-(*N*<sup>6</sup>-Carbonylmethyl-ATP)

As for *N*<sup>6</sup>-carboxymethyl-NAD<sup>+</sup>, except that NAD<sup>+</sup> is replaced by ATP and LiCl is used in place of CaCl<sub>2</sub>. Neither this ATP derivative nor *N*<sup>6</sup>-carboxymethyl-ATP is commercially available.

2.1.3. Other Bis-NAD<sup>+</sup> Derivatives

1. NAD<sup>+</sup> (Sigma, Boehringer; 98% free acid)
2. Ethyleneimine (Serva, Heidelberg, Germany). **Caution: This is toxic and carcinogenic.**
3. 70% HClO<sub>4</sub>.
4. 96% Ethanol.
5. LiCl.
6. Bio-Rex 70 cation exchange resin (100–200 mesh, Na<sup>+</sup> form, Bio-Rad).
7. 1*M* LiOH.
8. 1*M* HCl.

Bio-Rex 70 can be converted to the H<sup>+</sup> form by washing it exhaustively with 0.5–1.0*M* HCl. The absence of Na<sup>+</sup> ions can be tested by

flame photometry. The column is then washed with 1 mM HCl, pH 3.0, and equilibration is checked by pH and conductivity measurements.

For bis-NAD<sup>+</sup> synthesis: Glutaric, adipic, and pimelic acid (all available from Sigma) have been found to serve as satisfactory, water-soluble spacers. Also required: 1-ethyl-3-(3-dimethylaminopropyl)-carbodiimide hydrochloride (EDC), 5M NaOH, 1M HCl, DE52 cellulose, equilibrated with 0.5M ammonium acetate, pH 7.0, to convert it to the acetate form; this is then equilibrated for chromatography by washing it with 10 column volumes of 0.05M ammonium acetate, pH 7.0.

In addition to this, a rotary evaporator and chromatographic columns (dimensions variable) are needed for all described syntheses. Three different TLC solvent systems have been used for monitoring the products of these syntheses:

System A: (NH<sub>4</sub>)<sub>2</sub>SO<sub>4</sub>: 0.1M potassium phosphate, pH 6.8: 1-propanol (60:100:2 [w/v/v]).

System B: isobutyric acid: 1M aqueous NH<sub>3</sub> (5:3 [v/v]), saturated with Na<sub>2</sub>EDTA.

System C: isobutyric acid: water: 25% aqueous NH<sub>3</sub> (66:33:1 [v/v/v]).

Plates: aluminum-backed, silica gel 60, fluorescent indicator F<sub>254</sub>, layer thickness 0.2 mm (Merck). A source of fluorescent light (wavelength 254 nm) can be used to visualize the spots, which appear purple on a green background.

HPLC system: reverse-phase,  $\mu$ Bondapak C-18 column (Waters; 3.9  $\times$  300 mm), equilibrated with 0.1M potassium dihydrogen phosphate, pH 6.0, containing 10% (v/v) methanol for separating monosubstituted NAD<sup>+</sup> derivatives and 20% methanol for separation of bis-NAD<sup>+</sup> derivatives. All solutions used in HPLC must be degassed using a vacuum pump and filtered with a 0.22- $\mu$ m filter to exclude particulate matter and avoid air bubbles. In addition, all samples must be centrifuged for 2 min in a minifuge to pellet particles before application to the column. The absorbance should be monitored at 254 nm.

## 2.2. Pilot Affinity Precipitation Studies

1. A source of the protein of interest, e.g., a crude tissue extract supernatant, or a commercially available preparation of the protein to ensure the reagent is effective.
2. The bis-ligand.
3. Stock solutions of a substrate analog, e.g., 560 mM oxalate for lactate dehydrogenase, 560 mM pyrazole for alcohol dehydrogenase, and 700 mM glutarate for GDH.

4. 0.4M Potassium phosphate buffer (62.4 g/L  $\text{NaH}_2\text{PO}_4$ , titrated to pH 7.4 with 5M KOH), for some applications.
5. 1.5-mL Polypropylene minifuge tubes.
6. Assay reagents for enzymes (see, e.g., ref. 32).

### 2.3. Enzyme Purification

Apart from the reagents and apparatus mentioned in Section 2.2., reagents and apparatus for electrophoresis, e.g., PAGE/SDS-PAGE are needed to check the purity of the affinity-precipitated protein (33). In addition, reagents for a protein assay (e.g., by the Lowry or Bradford method) are required to determine the protein concentration.

For the separation of LDH isoenzymes (see Section 3.3.3.), materials for starch gel electrophoresis are appropriate. These include hydrolyzed potato starch (Sigma), electrophoresis-grade Trizma base to buffer the gel, and grade III  $\text{NAD}^+$  (Sigma). The activity stain for LDH contains 1.21 g Tris, 7.72 mL 70% Na DL-lactate (8 g), 50 mg nitroblue tetrazolium, 50 mg grade III  $\text{NAD}^+$ , and 4 mg phenazine methosulfate. (Caution: Nitroblue tetrazolium and phenazine methosulfate are toxic and the latter is light sensitive). Make the volume up to 200 mL with water, and adjust the pH to 7.1 with 6M HCl.

## 3. Methods

### 3.1. Synthesis of Coenzyme Derivatives

#### 3.1.1. Bis- $\text{NAD}^+$

The synthesis of  $N^6$ -carboxymethyl- $\text{NAD}^+$  is described in ref. 34, but some modifications are given here. The synthesis of bis- $\text{NAD}^+$  is a modified and more detailed version of that described in ref. 4.

1. Dissolve 9 g of fresh iodoacetic acid in approx 1 mL of water, neutralize the solution with 2M LiOH, and add 3 g of  $\text{NAD}^+$ . Adjust the pH to 6.5 with 2M HCl (the total volume should be about 30 mL), and leave the solution in darkness for 7 d at room temperature (approx 20°C) or, alternatively, at 37°C for 2 d. The pH should be checked daily (or every 4–6 h at the higher temperature), and readjusted to 6.5 with 2M HCl as required. The progress of the reaction should also be followed by TLC and/or HPLC.
2. When the reaction is complete, adjust the pH to 3.0 with 6M HCl, and add 2 vol of 96% (v/v) ethanol. This gives a milky, pink-tinged suspension, which precipitates on the addition of a further 10 vol of cold 96% ethanol. (The water/ethanol ratio is important; using a wet vessel can give rise to the formation of a brown, sticky substance that is water-soluble. This also applies to the corresponding ATP derivative.) Filter the crude  $N(1)$ -carboxymethyl- $\text{NAD}^+$

- on a sintered funnel, wash with ethanol and diethyl ether, and dry under vacuum (average yield 2.9 g). Store the product at  $-20^{\circ}\text{C}$  under vacuum.
3. Dissolve the crude  $N(1)$ -carboxymethyl-NAD $^{+}$  in 0.24M NaHCO $_3$  (90 mL), which gives a pale orange solution, and adjust the pH to 8.5 with 1M NaOH. Deoxygenate the solution by bubbling N $_2$  gas through it for 2 min, add 1.5 g of sodium dithionite, and leave the solution in the dark until maximum reduction is achieved. This depends on the dithionite—monitor the reaction by taking samples, diluting them 1:50 or 1:100, and measuring the increase in  $A_{340}$ .
  4. Terminate the reaction by stirring vigorously for 10 min to oxygenate the solution, and then bubble N $_2$  gas through for 2 min. Adjust the pH to 11.5 with 1M NaOH, and leave in a water bath at  $75^{\circ}\text{C}$  to allow the Dimroth rearrangement from the  $N(1)$  to the  $N^6$ -substituted derivative to occur. (See ref. 35 for a reaction mechanism.) Monitor the rearrangement by HPLC or TLC. Cool the reaction mixture to room temperature, and add 6 mL of 2M Tris and 1.5 mL of redistilled acetaldehyde. Adjust the pH to 7.5 with 1M HCl, and add 8–24 mg of yeast alcohol dehydrogenase (2500–7500 U). Monitor the reaction at 340 nm as in step 3. When a minimum  $A_{340}$  is reached, add 1 vol of 96% ethanol, and pour the milky flocculant precipitate into 10 vol of vigorously stirred 96% ethanol. Leave for 30 min (or overnight, if desired), and collect the precipitate by filtration. The crude  $N^6$ -carboxymethyl-NAD $^{+}$  can be stored at  $-20^{\circ}\text{C}$  under vacuum for up to a month (yield approx 2.6 g).
  5. The product from step 4 can be purified by dissolving the crude powder (2.6 g) in 30 mL water, adjusting the pH to 8.0 with 1M LiOH, and applying this solution to a column of Dowex AG 1X2 (200–400 mesh, Cl $^{-}$  form,  $4 \times 10$  cm). Wash the column beforehand with 1 L of 3M HCl, followed by exhaustive washing with at least 20 L of water until neutral pH is reached. After applying the coenzyme solution, wash the column with 0.5 L of water, followed by 1 L of 5 mM CaCl $_2$ , until the pH of the effluent is 2.8. Apply a linear gradient ( $2 \times 1$  L) from 5 mM CaCl $_2$ , pH 2.7, to 50 mM CaCl $_2$ , pH 2.0. Collect 10–20 mL fractions, and monitor the absorbance at 260 nm. The composition of the fractions can be monitored by TLC.  $R_f$  values: system A, NAD $^{+}$ , 0.41,  $N(1)$ -carboxymethyl-NAD $^{+}$ , 0.31,  $N^6$ -carboxymethyl NAD $^{+}$ , 0.22; system B, NAD $^{+}$ , 0.44,  $N(1)$ -carboxymethyl-NAD $^{+}$ , 0.27,  $N^6$ -carboxymethyl NAD $^{+}$ , 0.22. The values can vary slightly with changes in the solvent composition over time (see Note 2). Pool the fractions containing the  $N^6$  derivative, adjust the pH to 7.0 with 2M Ca(OH) $_2$ , and concentrate to 5–10 mL by rotary evaporation at  $40^{\circ}\text{C}$ . Precipitate with 96% ethanol as in step (4), and dry under vacuum. This gives a pale yellow compound (yield 0.82 g, 25%).  $\epsilon = 19,300/M$  cm at 266 nm.

6. To synthesize bis-NAD<sup>+</sup>, dissolve 0.82 g of purified N<sup>6</sup>-carboxymethyl-NAD<sup>+</sup> and 105 mg of adipic acid dihydrazide dihydrochloride in 20 mL water to give a brownish solution. Adjust the pH to 4.6 with 1M HCl, and then add 0.5M EDC at 0°C in 15 100- $\mu$ L aliquots over a period of 35 min. Monitor the pH, and readjust it to 4.6 before each addition. Add water (2 L) to dilute the solution 100-fold, adjust the pH to 8.0 with 2M NH<sub>4</sub>HCO<sub>3</sub>, apply the solution to a DE52 column (2.5  $\times$  30 cm) equilibrated with 1M NH<sub>4</sub>HCO<sub>3</sub>, pH 8.0, and then wash with water. Wash the column with water until the  $A_{260}$  is < 0.1, and apply a linear gradient (2  $\times$  1 L) from 0–0.25M NH<sub>4</sub>HCO<sub>3</sub>, pH 8.0. Monitor the  $R_f$  values of the fractions by TLC ( $R_f$  of bis-NAD<sup>+</sup>: system A, 0.09; system B, 0.05; see Note 2). The yield from pure N<sup>6</sup>-carboxymethyl-NAD<sup>+</sup> is approx 14%.  $\epsilon$  = 42,800/M/cm at 266 nm.

### 3.1.2. Bis-ATP (36,37)

1. Dissolve 3.4 g of fresh iodoacetic acid in 1 mL of water, and adjust the pH to 7.0 with 2M LiOH. Dissolve 1.16 g of ATP in the solution, and leave it at pH 6.5 in the dark for 4 d at 30°C, adjusting the pH to 6.5 every day. Monitor the reaction by HPLC and/or TLC, or follow the decrease in absorbance at 640 nm. When the reaction is complete, as judged by TLC, HPLC, or absorbance change, add 1 vol of cold 96% ethanol to give a milky suspension, and add this to 6–8 vol of stirring absolute ethanol at 0°C. Filter, and wash as for the corresponding NAD<sup>+</sup> derivative. (Typical yield 82–87%, about 1.4 g.)
2. Dissolve 1.4 g of product in 30 mL of water to give a reddish solution. Adjust the pH to 8.5 with 1M LiOH and incubate at 90°C for 100 min, with pH adjustment every 20 min. Monitor the reaction over this time by TLC or HPLC. The solution can be cooled on ice and stored overnight at 4°C, if required. HPLC retention times: ATP, 4.5 min, N(1)-carboxymethyl-ATP 3.1 min, N<sup>6</sup>-carboxymethyl-ATP, 4.1 min.
3. Adjust the pH of the solution at 20°C to 2.75 with 6M HCl, and apply it to an AG 1  $\times$  2 column (200–400 mesh, Cl<sup>−</sup> form, 4  $\times$  9 cm), equilibrated with water. Wash the column with 1 L of 0.3M LiCl, pH 2.75, until the  $A_{260}$  is < 1.0, and then apply a 2  $\times$  1 L linear gradient, 0.3M LiCl, pH 2.75–0.5M LiCl, pH 2.0. Monitor the  $R_f$  values of the fractions by TLC as previously. ( $R_f$  values: system A, ATP, 0.54, N(1)-carboxymethyl-ATP, 0.73, N<sup>6</sup>-carboxymethyl-ATP, 0.54, system B, ATP, 0.35, N(1)-carboxymethyl-ATP, 0.27, N<sup>6</sup>-carboxymethyl-ATP, 0.21; see Note 2.) Pool the fractions containing the N<sup>6</sup> derivative, and adjust the pH with 2M LiOH. Yield: 32–38% from ATP.  $\epsilon$  = 17,300/M/cm at 266 nm. This procedure should be carried out as quickly as possible, preferably within 1 d, since ATP is unstable under acidic conditions.

4. Bis-ATP: Dissolve 105 mg of adipic acid dihydrazide dihydrochloride in a solution containing 0.42 g of  $N^6$ -carboxymethyl-ATP in 100 mL. Adjust the pH to 4.0 with 1M HCl, and add 3 1-mL aliquots of 1M EDC over a period of 45 min, while stirring continuously, and monitoring the pH. Dilute to 2 L with water to stop the reaction, and adjust the pH to 8.0 with 2M  $\text{NH}_4\text{OH}$ . This solution can be stored at  $-20^\circ\text{C}$  for about a week.
5. The compound can be purified by applying the dilute solution to a DE-52 column ( $2.5 \times 25$  cm), equilibrated with 2–4 L 1M  $\text{NH}_4\text{HCO}_3$ , and then washed with 8 L water. Elute the bis-ATP with a 0–0.4M  $\text{NH}_4\text{HCO}_3$  gradient, pH 8.0 ( $2 \times 1$  L). Collect 10–20 mL fractions and pool and freeze-dry the fractions containing bis-ATP, as judged by HPLC or by affinity precipitation of phosphofructokinase (see Section 3.3.4.) Ensure that the compound is completely dry before storage at  $-20^\circ\text{C}$ , as it is very hygroscopic. Yield: 0.06 g from 0.42 g  $N^6$ -carboxymethyl-ATP (yield approx 2% from ATP).  $\epsilon = 39,600\text{ M}^{-1}\text{cm}^{-1}$  at 266 nm (see Note 3).

### 3.1.3. Other Bis- $\text{NAD}^+$ Derivatives

1. The synthesis of  $N^6$ -(2-aminoethyl)- $\text{NAD}^+$  is carried out essentially as described in ref. 38. However,  $N(1)$ -(2-aminoethyl) $\text{NAD}^+$  can be rearranged to the  $N^6$ -substituted derivative without removal of the unreacted  $\text{NAD}^+$  by ion-exchange chromatography (39), and the following procedure is a modification of this. Dissolve crude  $N(1)$ -(2-aminoethyl)- $\text{NAD}^+$  (contains approx 70%  $N(1)$ -(2-aminoethyl) $\text{NAD}^+$ ; 3.05 g, 4.3 mmol) in 850 mL of water. Adjust the pH to 6.5 with 1M LiOH. Place the solution in a water bath at  $50^\circ\text{C}$ , and allow the rearrangement to proceed for 6–7 h. Monitor the reaction by HPLC/TLC/change in absorbance maximum over this time. The wavelength of maximum absorbance should change from 260 nm to at least 264 nm, since the  $\lambda_{\text{max}}$  for  $N^6$ -(2-aminoethyl) $\text{NAD}^+$  is 266 nm. Terminate the reaction by cooling the solution to room temperature, and adjust the pH to 5.5 with 1M HCl. Concentrate the solution by rotary evaporation at  $35^\circ\text{C}$  to approx 20 mL. The compound is stable in concentrated solution for at least 1 wk at  $4^\circ\text{C}$ .
2. Apply the concentrated reaction mixture to a Bio-Rex 70 cation-exchange column ( $\text{H}^+$  form,  $2.7 \times 73$  cm), pre-equilibrated with 1 mM HCl, pH 3.0. Wash the column with this solution, and collect fractions of 10–20 mL, in a total volume of approx 4 L. Monitor the  $A_{260}$  as an indicator of coenzyme concentration. The last peak to elute contains the  $N^6$ -(2-aminoethyl) $\text{NAD}^+$ . Some overlap may occur with the previous peak, containing the tricyclic  $\text{NAD}^+$  derivative 1,  $N^6$ -ethanoadenine- $\text{NAD}^+$ . Pool and rotary evaporate the fractions containing the desired compound to approx 5 mL. Lyophilization gives a fluffy pale yellow compound, stable for at least 12 mo at  $-20^\circ\text{C}$  in an air-tight container.  $\epsilon = 21,600\text{ M}^{-1}\text{cm}^{-1}$  at 266 nm. HPLC retention times:



NAD<sup>+</sup>, 6.3 min; *N*(1)-(2-aminoethyl)NAD<sup>+</sup>, 4.4 min; *N*<sup>6</sup>-(2-aminoethyl)NAD<sup>+</sup>, 5.7 min; 1, *N*<sup>6</sup>-ethanoadenine-NAD<sup>+</sup>, 4.7 min. TLC *R<sub>f</sub>* values: system C, NAD<sup>+</sup> 0.28, *N*(1)-(2-aminoethyl)NAD<sup>+</sup>, 0.10, *N*<sup>6</sup>-(2-aminoethyl)-NAD<sup>+</sup>, 0.16, 1, *N*<sup>6</sup>-ethanoadenine-NAD<sup>+</sup>, 0.08 (28).

3. Dissolve the spacer (glutaric, adipic, or pimelic acid) in water to give a 50-mM solution. Adjust the pH to 7.0 with 5*M* NaOH, and add 700  $\mu$ L of this solution to 50 mg (67  $\mu$ mol) of *N*<sup>6</sup>-(2-aminoethyl)NAD<sup>+</sup> to give a 2:1 molar ratio of coenzyme to spacer arm. Adjust the pH from approx 3.0–5.4 with 5*M* NaOH. Add solid EDC (34 mg, 335  $\mu$ mol) to the solution in six to seven portions over 20 min, while monitoring the reaction by TLC/HPLC. The pH tends to rise; readjust it to 5.5–6.0 when it reaches a value of 6.9–7.0. Stop the reaction after 40 min by freezing the reaction mixture at –20°C. TLC indicates that at least four side products are formed in addition to bis-NAD<sup>+</sup>.
4. To purify the bis-NAD<sup>+</sup>, dilute the sample twofold with 50 mM ammonium acetate, pH 7.0, and apply it to a Whatman DE-52 anion-exchange column (2.3  $\times$  16 cm), equilibrated as described in Section 2.1.3. Wash the column with this buffer. The last major peak contains the bis-NAD<sup>+</sup> derivative. This can be checked by TLC, HPLC, or by the ability of the fractions to cause affinity precipitation of GDH. Pool and rotary evaporate the fractions containing bis-NAD<sup>+</sup> to 3–5 mL, and freeze-dry these (stable for at least 4 mo at 4°C or –20°C). The compound can also be stored for approx 1 mo in solution at 4°C, although bacterial contamination can result. TLC *R<sub>f</sub>* values (system C) for bis-NAD<sup>+</sup> derivatives: *N,N'*-bis(*N*<sup>6</sup>-ethylene-NAD<sup>+</sup>)glutaramide, 0.09, *N,N'*-bis(*N*<sup>6</sup>-ethylene-NAD<sup>+</sup>) adipamide, 0.12, *N,N'*-bis(*N*<sup>6</sup>-ethylene-NAD<sup>+</sup>)pimelamide, 0.15.  $\epsilon = 44,200 \pm 1400$ /M/cm. HPLC retention times (in 0.1*M* potassium phosphate buffer, pH 6.0, containing 20% methanol) are 7.8, 11.2, and 13 min for the compounds, respectively.

### 3.2. Pilot Precipitation Study

1. Take a source of the enzyme of interest (e.g., a crude supernatant), and assay it for enzyme activity (see ref. 32 for a wide range of assays) to determine the specific activity.
2. Calculate the approximate concentration of enzyme based on the specific activity.
3. Add 100–200  $\mu$ L of the enzyme solution to a series of minifuge tubes. If the study is to be carried out with purified enzyme, dilute a stock solution of 400 mM potassium phosphate buffer, pH 7.4, to give a final concentration of 20 mM. Set up all samples in duplicate, including two control tubes to which water has been added in place of the coenzyme derivative. Set up duplicate controls in addition to these, which contain no bis-ligand or substrate analog. This enables the percent inhibition owing to the presence of the substrate analog to be calculated.

4. Calculate the concentration of a stock solution of bis-coenzyme spectrophotometrically, using the extinction coefficients given in Section 3.1.
5. Add bis-NAD<sup>+</sup> (or bis-ATP) to give a range of coenzyme Eq/enzyme subunit from approx 0.1–20, calculating the concentration from the extinction coefficient.
6. Add the appropriate substrate analog, and leave at 4°C for at least 30 min (or overnight, if required).
7. Centrifuge in a minifuge for 5 min, and assay the supernatant. Calculate the precipitation as a percentage of the activity remaining in the control sample. The tube giving the minimal residual activity shows the maximum affinity precipitation. This indicates the appropriate concentration of bis-coenzyme to be added to obtain maximum affinity precipitation.

### 3.3. Enzyme Purification Protocols

The following are a selection of protocols for purifying enzymes with bis-ligands.

#### 3.3.1. Purification of Yeast Alcohol Dehydrogenase (YADH; EC 1.1.1.1)

1. The yeast lysis is carried out according to a modification of the procedure in ref. 40. Crumble 40 g of fresh baker's yeast into 21 mL of toluene, preheated to 45°C in a water bath. (Caution: Keep the vessel covered, or incubate in a fume cupboard.) Allow the mixture to liquefy over a period of 90 min with occasional stirring. (see Note 4).
2. Leave the mixture at room temperature for 3 h, and add 42 mL of 1 mM Na<sub>2</sub>EDTA as a protease inhibitor. Stir for 2 h at 4°C, and leave the mixture at that temperature overnight.
3. Centrifuge the lysate at 47,800g for 10 min, remove the top fatty layer by aspiration, and retain the supernatant. Add solid (NH<sub>4</sub>)<sub>2</sub>SO<sub>4</sub> slowly, until 60% saturation is reached (7.22 g to 20 mL), and centrifuge for 10 min at 47,800g. The ammonium precipitation step removes some proteins that would otherwise precipitate on addition of bis-NAD<sup>+</sup> and gives a purification of approx three- to fourfold. Dissolve the pellet in approx 3 mL of 20 mM potassium phosphate buffer, pH 7.4, containing 1 mM Na<sub>2</sub>EDTA and dialyze against two changes of 2 L of this buffer to remove the salt (alternatively, gel filter on a column of Sephadex G-25, at least 1 × 50-cm long).
4. Carry out a pilot precipitation of this supernatant. This can be performed before or after removing the (NH<sub>4</sub>)<sub>2</sub>SO<sub>4</sub>. However, if the (NH<sub>4</sub>)<sub>2</sub>SO<sub>4</sub> has been removed, it must be added back to a concentration of at least 0.5M, since it is required to promote precipitation. Dilute the supernatant 1:4 with buffer, and add pyrazole to a final concentration of 28 mM. A suitable range of concentrations of NAD<sup>+</sup> equivalents is 0–20 μM. Allow precipitation to occur for at least 3 h (preferably overnight).

5. Assay the supernatants as described in ref. 32, diluting the enzyme solution if necessary, and determine which concentration of bis-NAD<sup>+</sup> gives maximum precipitation. Add the appropriate concentration of bis-NAD<sup>+</sup> to whatever vol of supernatant is required, along with (NH<sub>4</sub>)<sub>2</sub>SO<sub>4</sub> and pyrazole. Allow precipitation to occur as described above, and centrifuge the precipitate for 10 min at 12,000g to pellet the crosslinked enzyme aggregate.
6. Resolubilize the pellet by adding 0.6 mM NADH in 20 mM potassium phosphate buffer, pH 7.4 (the volume can be varied, depending on what final enzyme concentration is required). Allow resolubilization to proceed for at least 3 h, preferably 12 h, at 4°C on a rocking tray or with occasional stirring (see Note 4). The enzyme should be essentially homogeneous, as shown by SDS-PAGE on a 12.5% gel.

### 3.3.2. Purification of GDH (EC 1.4.1.3) from Beef and Rat Liver (9)

1. If beef liver is used, transport this from the abattoir on ice.
2. Homogenize the tissue, and carry out ammonium sulfate precipitation and DEAE-cellulose chromatography as described in ref. 41.
3. Pool the fractions from the DE-52 column that contain GDH activity (32), and concentrate them to a volume of approx 10 mL by ultrafiltration through an Amicon XM-50 membrane. Dialyze the solution overnight at 4°C against 200 mL of sodium or potassium phosphate buffer, pH 7.4, with at least one change of buffer.
4. Carry out a pilot precipitation as described in Section 3.2. Incubate 100-μL samples of the dialyzed solution in the presence of 12.7 μL of 0.7M glutarate, pH 7.0, and bis-NAD<sup>+</sup> for 15 min. Assume a subunit *M<sub>r</sub>* for GDH of 56,700. The optimum ratio of NAD<sup>+</sup> Eq/enzyme subunit may vary with the preparation used; for example, with a preparation of beef liver enzyme that had a specific activity of 2.7 U/mg, about half the activity was precipitated at a ratio of 2 NAD<sup>+</sup> Eq/GDH subunit. However, a preparation with the lower specific activity of 0.8 U/mg required approx 8 NAD<sup>+</sup> Eq/GDH subunit to precipitate half the enzyme activity. The precipitation yield also depends on the protein concentration.
5. Take the dialyzed solution, and add glutarate to a final concentration of 79 mM. Add the appropriate amount of bis-NAD<sup>+</sup> to achieve maximum precipitation. Keep the mixture on ice overnight, and centrifuge at 10,000g for 15 min. Redissolve the pellet by stirring for 6 h in 1 mL of 20 mM sodium or potassium phosphate buffer, pH 7.4, containing 0.6 mM NADH. Dialyze the redissolved pellet against 200 mL of the same buffer as in step 3. A purification summary is given in Table 2. This method appears to avoid some of the proteolysis encountered in more conventional methods of purifying this enzyme. Although affinity precipitation was obtained with

Table 2  
Purification of Beef and Rat Liver GDH\*

Step	Volume, mL		Total protein, mg		Total activity, U		Specific activity, U/mg		Purification factor		Yield, %	
	Beef	Rat	Beef	Rat	Beef	Rat	Beef	Rat	Beef	Rat	Beef	Rat
Homogenate	370	90	8580	2720	1920	760	0.2	0.3	--	--	100	100
Resuspended (NH <sub>4</sub> ) <sub>2</sub> SO <sub>4</sub> precipitate	75	35	2010	980	1640	505	0.3	0.5	4	2	86	67
DEAE-cellulose chromatography	8.4	9.8	139	130	408	195	2.9	1.5	13	5	21	26
Affinity precipitation	1.2	1.0	9.4	5.1	376	190	40	37	180	140	20	25

\*Reproduced from Grialam et al. (9). The first three steps were carried out according to the method of Mc Carthy et al. (41). The purification of the enzyme from beef liver used 46 g and that from rat used 10 g liver.

preparations that had not been subjected to chromatography on DEAE-cellulose, the yield was much lower and the precipitated material was not completely pure.

### 3.3.3. Separation of Lactate Dehydrogenase (LDH; EC 1.1.1.27) Isoenzymes

This technique is based on the principle that both M and H isoenzyme subunits of LDH form abortive complexes with NAD<sup>+</sup> and oxalate, whereas the H form gives rise to abortive ternary complexes with NAD<sup>+</sup> and oxamate. In a mixture of H and M subunits, ternary complexes and, thus, crosslinks will form only with the H subunits, and tetramers with predominantly M subunits will tend not to be precipitated.

1. Select a source of LDH isoenzymes (e.g., a crude supernatant or Sigma Type X bovine muscle LDH, which contains varying proportions of all five isoenzymes). Determine the specific activity, and hence, estimate the concentration of the enzyme (32).
2. Carry out a pilot precipitation as described in Section 3.2. The precipitation solution should contain 20 mM potassium phosphate buffer, pH 7.4, and potassium oxamate to a final concentration of 20 mM. Optimum affinity precipitation should be obtained with a ratio of approx 1 NAD<sup>+</sup> Eq/LDH subunit. Allow precipitation to occur overnight at 4°C. Centrifuge for 10 min and retain the supernatant for further analysis.
3. Resolubilize the precipitated enzyme by adding 50  $\mu$ L of 0.6 mM NADH in the above buffer and incubate overnight. Centrifuge the samples for 10 min at 12,000g to pellet any remaining crosslinked enzyme.
4. The isoenzymic composition of the pellet and supernatant can be analyzed by starch gel electrophoresis. This is carried out by the method described in ref. 42. Make an 11% starch gel. Apply 10- $\mu$ L samples of the enzyme solution to the gel on small squares of filter paper (about 0.5  $\times$  0.5 cm), and carefully insert these, using a forceps, in wells cut across the middle of the gel. Place a piece of polyethylene wrap over the gel, and put a cooling plate on top. Run the gel for 4 h at 550 V and 60 mA in a cold room at 4°C. After electrophoresis, stain the gel with an activity stain for LDH (see Section 2.3.) until the bands appear. Wash the gel exhaustively with water, otherwise overstaining can easily occur, and treat the gel gently, since starch gels are fragile. Figure 3 shows a starch gel on which the separation pattern can be seen.

### 3.3.4. Purification of Beef Heart Phosphofructokinase (PFK; EC 2.7.1.11)

1. Obtain a fresh portion of beef heart from a freshly slaughtered animal, and keep it on ice. Remove the ventricular muscles and adipose tissue, dice the

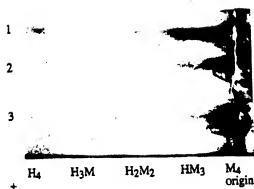


Fig. 3. Starch gel electrophoresis of LDH isoenzymes. The gel was stained with an activity stain for LDH, as described in the text. Lane 1 consists of Sigma Type X bovine muscle LDH (1.4 U) containing all isoenzymes of LDH with M and H subunits. Lane 2 contains the supernatant after affinity precipitation in the presence of bis-NAD<sup>+</sup> (1 NAD<sup>+</sup> Eq/LDH subunit) and 20 mM oxamate. Lane 3 contains the resolubilized pellet from the same sample as lane 2. The pellet was resolubilized in 20 mM potassium phosphate, pH 7.4, containing 0.6 mM NADH. Affinity precipitation and resolubilization were carried out in a final vol of 100  $\mu$ L.

remaining tissue, and wash it in distilled water. Homogenize it in a pre-cooled blender for 10 s, take 500 g of mince, and add 10 mM Tris-HCl buffer containing 2mM EDTA, pH 8.2, to a total vol of 1.25 L. Homogenize this for 90 s at high speed, and then centrifuge the homogenate at 2,600g for 10 min. Discard the supernatant.

2. Resuspend the pellet in 10 mM Tris-HCl containing 0.5 mM ATP, 50 mM MgSO<sub>4</sub>, and 5 mM 2-mercaptoethanol, pH 8.0, to a total vol of 1 L. Pre-warm the buffer to 37°C. Stir the suspension at 37°C for 30 min. This extraction procedure gives rise to a decrease in pH of 0.6–0.8 pH units. Remove solid material by centrifugation for 15 min at 8000g, followed by a further centrifugation at 12,000g. The supernatant contains about 90% of the PFK activity.
3. Set up a pilot precipitation (see Section 3.2.) to determine the concentration of bis-ATP giving optimum precipitation. The following volumes are appropriate: 100  $\mu$ L enzyme solution, 30  $\mu$ L of 30 mM citrate, pH 7.0, 60  $\mu$ L 0.16M MgSO<sub>4</sub>. Add bis-ATP to give a range of ATP Eq/PFK subunit ratios (0–8 is suitable, at an enzyme concentration of 0.38 mg/mL PFK). Make the volume up to 500  $\mu$ L with extraction buffer. A ratio of 4–6 is usually found

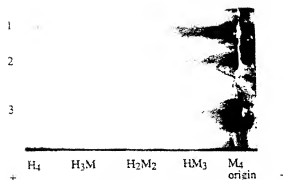


Fig. 3. Starch gel electrophoresis of LDH isoenzymes. The gel was stained with an activity stain for LDH, as described in the text. Lane 1 consists of Sigma type X bovine muscle LDH (1.4 U) containing all isoenzymes of LDH with M

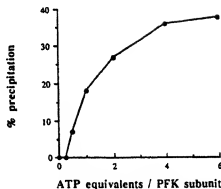


Fig. 4. Affinity precipitation of PFK. A pilot precipitation was set up as described in the text. The precipitation mixture contained 0.1 mL enzyme supernatant, 20  $\mu$ L 0.5M citrate, pH 7.0, bis-ATP (0.25–6 ATP Eq/ATP subunit), and 20  $\mu$ L 0.5M  $\text{MgSO}_4$ . The tubes were left overnight at 0°C, and centrifuged for 10 min to pellet the enzyme.

Table 3  
Purification of PFK from Bovine Heart (200 g Tissue) (36)<sup>a</sup>

Step	Volume, mL	Total protein, mg	Total activity, U	Specific activity, U/mg	Purification, factor	Yield, %
Crude extract						
Resuspended						
Precipitate	490	3675	970	0.26	1	100
Supernatant						
After extraction	548	376	883	3.2	12.3	91
Affinity precipitation	3	7.1	214	30.1	115.7	22

<sup>a</sup>The method used is that given in Section 3.3.4.

to be optimum for precipitation (see Fig. 4). A similar pilot experiment varying the enzyme concentration can also be set up at a fixed concentration of bis-coenzyme. A sample purification table is given (Table 3).

- The volume for precipitation can be scaled up as required. The enzyme can be recovered by dialysis, which causes resolubilization of the pellet.

#### 4. Notes

- Bis-NAD<sup>+</sup> has been used as a ligand with several NAD<sup>+</sup>-linked dehydrogenases, but only for three enzymes (YADH, LDH, GDH) has it successfully



been applied for purification purposes. A partial purification of isocitrate dehydrogenase giving rise to a yield of 18% has been described (7). Horse liver alcohol dehydrogenase has also been observed to form aggregates with bis-NAD<sup>+</sup> and pyrazole (5,8), but it does not affinity precipitate, despite the fact that it may form larger polymers. Other enzymes that do not successfully affinity precipitate include malate, alanine, and glyceraldehyde-3-phosphate dehydrogenases (28). Malate dehydrogenase is a dimer, and the other two enzymes, although tetrameric, may fail to form crosslinked ternary complexes, possibly owing to steric or kinetic factors.

2. The  $R_f$  values given for TLC of coenzyme derivatives are not exact. They can vary by up to  $\pm 0.05$ . This may be owing to slight changes in the solvent composition over time, possibly because of evaporation.
3. To date, bis-ATP has only been used in the purification of PFK. The yields obtained for this compound are low, and it is unstable, possibly owing to hydrolysis of the spacer arm, catalyzed intramolecularly by a phosphate group. It should be used within 4 d of synthesis. Because of this, the reagent must be regarded as being of limited practical use, and further studies on the synthesis of a more stable bis-ATP derivative are necessary.
4. YADH has essential thiol groups, and if these are oxidized, the enzyme loses activity. They should be kept reduced by the addition of 1 mM dithiothreitol or 1 mM 2-mercaptoethanol. The breaking of the yeast cells may also be carried out using glass beads.

### Acknowledgments

Support from Trinity College, Dublin and EOLAS (Forbairt; The Irish Science and Technology Agency) is gratefully acknowledged.

### References

1. Chen, J.-P. (1990) Novel affinity based processes for protein purification. *J. Ferment. Bioeng.* 70, 199–209.
2. Luong, J. H. T. and Nguyen, A.-L. (1992) Novel separations based on affinity interactions. *Adv. Biochem. Eng. Biotechnol.* 47, 138–158.
3. Irwin, J. A. and Tipton, K. F. (1995) Affinity precipitation: a novel approach to protein purification. *Essays Biochem.* 29, 137–156.
4. Larsson, P.-O. and Mosbach, K. (1979) Affinity precipitation of enzymes. *FEBS Lett.* 98, 333–338.
5. Flygare, S., Griffin, T., Larsson, P.-O., and Mosbach, K. (1983) Affinity precipitation of dehydrogenases. *Anal. Biochem.* 133, 409–416.
6. Larsson, P.-O., Flygare, S., and Mosbach, K. (1984) Affinity precipitation of dehydrogenases. *Methods Enzymol.* 104, 364–369.
7. Beattie, R. E., Graham, L. D., Griffin, T. O., and Tipton, K. F. (1985) Purification of NAD<sup>+</sup>-dependent dehydrogenases by affinity precipitation with adipo-N<sub>2</sub>N<sub>2</sub>-dihydrazido bis-(N<sup>6</sup>-carboxymethyl-NAD<sup>+</sup>) (bis-NAD<sup>+</sup>). *Biochem. Soc. Trans.* 12, 433.

8. Buchanan, M., O'Dea, C. D., Griffin, T. O., and Tipton, K. F. (1989) Reversible cross-linking of alcohol and lactate dehydrogenases with the bifunctional reagent  $N_3$ ,  $N_2'$ -adipodihydrazido-bis-( $N^6$ -carboxymethyl-NAD $^+$ ). *Biochem. Soc. Trans.* 17, 422.
9. Graham, L. D., Griffin, T. O., Beatty, R. E., Mc Carthy, A. D., and Tipton, K. F. (1985) Purification of liver GDH by affinity precipitation and studies on its denaturation. *Biochim. Biophys. Acta* 828, 266-269.
10. Beattie, R. E., Buchanan, M., and Tipton, K. F. (1987) The synthesis of  $N_3$ ,  $N_2'$ -adipodihydrazido-bis-( $N^6$ -carboxymethyl-ATP) and its use in the purification of phosphofructokinase. *Biochem. Soc. Trans.* 15, 1043,1044.
11. Hayet, M. and Vijayalakshmi, M. A. (1986) Affinity precipitation of proteins using bis-dyes. *J. Chromatogr.* 376, 157-161.
12. Lowe, C. R. and Pearson, J. C. (1983) Bio-mimetic dyes, in *Affinity Chromatography and Biological Recognition* (Chaiken, I. M., Wilchek, M., and Parikh, I., eds.), Academic, London, pp. 421-432.
13. Pearson, J. C., Burton, S. J., and Lowe, C. R. (1986) Affinity precipitation of lactate dehydrogenase with a triazine dye derivative: selective precipitation of rabbit muscle lactate dehydrogenase with a Procion Blue H-B analog. *Anal. Biochem.* 158, 382-389.
14. Pearson, J. C., Clonis, Y. D., and Lowe, C. R. (1989) Preparative affinity preparation of L-lactate dehydrogenase. *J. Biotechnol.* 11, 267-274.
15. Lilius, G., Persson, M., Bülow, L., and Mosbach, K. (1991) Metal affinity precipitation of proteins carrying genetically attached polyhistidine affinity tails. *Eur. J. Biochem.* 198, 499-504.
16. Van Dam, M. E., Wuenschell, G. E., and Arnold, F. H. (1989) Metal affinity precipitation of proteins. *Biotechnol. Appl. Biochem.* 11, 492-502.
17. Schneider, M., Guillot, C., and Lamy, B. (1981) The affinity precipitation technique. Application to the isolation and purification of trypsin from bovine pancreas. *Ann. N.Y. Acad. Sci.* 369, 257-263.
18. Senstad, C. and Mattiasson, B. (1989) Affinity-precipitation using chitosan as ligand carrier. *Biotechnol. Bioeng.* 33, 216-220.
19. Senstad, C. and Mattiasson, B. (1989) Purification of wheat germ agglutinin using affinity flocculation with chitosan and a subsequent centrifugation or flotation step. *Biotechnol. Bioeng.* 34, 387-393.
20. Taniguchi, M., Kobayashi, M., Natsui, K., and Fujii, M. (1989) Purification of staphylococcal protein A by affinity precipitation using a reversibly soluble-insoluble polymer with human IgG as a ligand. *J. Ferment. Bioeng.* 68, 32-36.
21. Kamihiro, M., Kaul, R., and Mattiasson, B. (1992) Purification of recombinant protein A by aqueous two-phase extraction integrated with affinity precipitation. *Biotechnol. Bioeng.* 40, 1381-1387.
22. Bradshaw, A. P. and Sturgeon, R. J. (1990) The synthesis of soluble polymer-ligand complexes for affinity precipitation studies. *Biotechnol. Techniques* 4, 67-71.
23. Senstad, C. and Mattiasson, B. (1989) Preparation of soluble affinity complexes by a second affinity interaction: a model study. *Biotechnol. Appl. Biochem.* 11, 41-48.
24. Linné, E., Garg, N., Kaul, R., and Mattiasson, B. (1992) Evaluation of alginate as a ligand carrier in affinity precipitation. *Biotechnol. Appl. Biochem.* 16, 48-56.

25. Gupta, M. N., Dong, G. Q., and Matiasson, B. (1993) Purification of endopolygalacturonase by affinity precipitation using alginate. *Biotechnol. Appl. Biochem.* **18**, 321–328.
26. Chen, J. P. and Hoffman, A. S. (1990) Polymer–protein conjugates. II. Affinity precipitation separation of human immunoglobulin by a poly (*N*-isopropylacrylamide)-protein A conjugate. *Biomaterials* **11**, 631–634.
27. Nguyen, A. L. and Luong, J. H. T. (1989) Syntheses and applications of water-soluble reactive polymers for purification and immobilization of biomolecules. *Biotechnol. Bioeng.* **34**, 1186–1190.
28. Irwin, J. A. and Tipton, K. F. (1995) Resolution of lactate dehydrogenase isoforms by affinity precipitation. *Biochem. Soc. Trans.* **23**, 3655.
29. Larsson, P.-O. and Mosbach, K. (1981) Novel affinity techniques. *Biochem. Soc. Trans.* **9**, 285–287.
30. Feinstein, A. and Rowe, A. J. (1965) Molecular mechanism of formation of an antigen–antibody complex. *Nature* **205**, 147–149.
31. O'Carra, P. (1978) Theory and practice of affinity chromatography, in *Chromatography of Synthetic and Biological Polymers*, 2nd ed. (Epton, R., ed.), Ellis Horwood for the Chemical Society, London, Chapter 11, pp. 131–158.
32. Bergmeyer, H. U., Grassl, M., and Walter, H.-E. (1983) Reagents for enzymatic analysis, in *Methods of Enzymatic Analysis*, vol. 2, 3rd ed. (Bergmeyer, H. U., Bergmeyer, J., and Grassl, M., eds.), Verlag Chemie, Weinheim, pp. 126–328.
33. Laemmli, U. K. (1970) Cleavage of structural proteins during the assembly of the head of bacteriophage T4. *Nature* **227**, 680–685.
34. Mosbach, K., Larsson, P.-O., and Lowe, C. (1976) Immobilised coenzymes. *Methods Enzymol.* **44**, 859–887.
35. Engel, J. D. (1975) Mechanism of the Dimroth rearrangement in adenine. *Biochem. Biophys. Res. Comm.* **64**, 581–585.
36. Buchanan, M. (1988) The synthesis of  $N_2N'_2$ -Adipodihydrazido-Bis-( $N^6$ -Carboxymethyl-NAD) and  $N_2N'_2$ -Adipodihydrazido-Bis-( $N^6$ -Carboxymethyl-ATP) and Subsequent Affinity Precipitation of Enzymes. MSc Thesis, University of Dublin.
37. Beattie, R. E. (1984) The Synthesis of  $N_2N'_2$ -Adipodihydrazido-Bis-( $N^6$ -Carboxymethyl-NAD<sup>+</sup>) and its use in the Purification of Dehydrogenases. MSc Thesis, University of Dublin.
38. Bückmann, A. F. (1987) A new synthesis of coenzymically active water-soluble macromolecular NAD and NADP derivatives. *Biocatalysis* **1**, 173–186.
39. Bückmann, A. F. and Wray, V. (1992) A simplified procedure for the synthesis and purification of  $N^6$ -(2-aminoethyl)-NAD and tricyclic 1,  $N^6$ -ethanoadenine NAD. *Biotechnol. Appl. Biochem.* **15**, 303–310.
40. Butler, P. J. G. and Thelwall Jones, G. M. (1970) The preparation of alcohol dehydrogenase and glyceraldehyde-3-phosphate dehydrogenase from baker's yeast. *Biochem. J.* **118**, 375–378.
41. Mc Carthy, A. D., Walker, J. M., and Tipton, K. F. (1980) Purification of glutamate dehydrogenase from ox brain and liver. *Biochem. J.* **191**, 605–611.
42. Phelps, C. (1984) in *Techniques in the Life Sciences*: vol. B1/1, suppl. BS 104, *Protein and Enzyme Biochemistry* (Tipton, K. F., ed.), Elsevier, Shannon Industrial Estate, Ireland, pp. 1–16.

# EXHIBIT L

# Adalimumab and Infliximab Bind to Fc $\gamma$ -receptor and C1q and Generate Immuno-precipitation: A Different Mechanism From Etanercept

Isabelle Kahan, Leif Ting, Tim Kessler, B. Jack Smith, G. Blumberg, Dennis S. Lofgren, and Thomas W. J. van der Vliet

## INTRODUCTION

1. Tumor necrosis factor (TNF) antagonists have been shown to be effective in the treatment of rheumatoid arthritis (RA) and Crohn's disease (CD). The mechanism of action of these drugs is not fully understood. It is generally accepted that TNF antagonists inhibit the interaction of TNF with its receptors, thereby preventing the downstream signaling cascade that leads to the production of pro-inflammatory cytokines and the activation of T cells.

2. Etanercept, a soluble TNF receptor, is a dimeric protein that binds to TNF and prevents it from interacting with its receptors. It is thought that this mechanism of action is responsible for its therapeutic effects. However, recent studies have shown that Etanercept may also bind to Fc $\gamma$ -receptors and C1q, which could lead to the formation of immune complexes and the activation of the complement system.

## HYPOTHESIS

3. We hypothesize that the therapeutic effects of TNF antagonists are mediated by their ability to bind to TNF and prevent it from interacting with its receptors. Additionally, we hypothesize that the formation of immune complexes and the activation of the complement system may also contribute to the therapeutic effects of these drugs.

4. This hypothesis is supported by the following evidence:

- Etanercept has been shown to bind to Fc $\gamma$ -receptors and C1q.
- The formation of immune complexes and the activation of the complement system have been observed in patients treated with Etanercept.

5. Therefore, we propose that the therapeutic effects of TNF antagonists are mediated by their ability to bind to TNF and prevent it from interacting with its receptors, as well as by the formation of immune complexes and the activation of the complement system.

## METHODS

6. The following methods were used to test the hypothesis:

- **Flow cytometry:** Cells were stained with fluorescently labeled antibodies and analyzed by flow cytometry.
- **Immunoprecipitation:** Cell lysates were immunoprecipitated with anti-TNF antibodies and analyzed by Western blotting.
- **Complement activation:** Cell lysates were incubated with complement and analyzed for the presence of C3a and C5a.

7. The results of these experiments are shown in the following figures:

- **Figure 1:** Flow cytometry analysis of TNF binding to cells.
- **Figure 2:** Western blot analysis of TNF immunoprecipitation.
- **Figure 3:** Complement activation assay.

8. The data demonstrate that TNF antagonists bind to TNF and prevent it from interacting with its receptors. Additionally, the formation of immune complexes and the activation of the complement system were observed in cells treated with TNF antagonists.

9. These findings support the hypothesis that the therapeutic effects of TNF antagonists are mediated by their ability to bind to TNF and prevent it from interacting with its receptors, as well as by the formation of immune complexes and the activation of the complement system.

10. Therefore, we propose that the therapeutic effects of TNF antagonists are mediated by their ability to bind to TNF and prevent it from interacting with its receptors, as well as by the formation of immune complexes and the activation of the complement system.

## RESULTS

11. The following results were obtained from the experiments:

- **Flow cytometry:** TNF binding to cells was significantly increased in the presence of TNF antagonists.
- **Immunoprecipitation:** TNF was co-precipitated with TNF antagonists.
- **Complement activation:** C3a and C5a were released in the presence of TNF antagonists.

12. These findings indicate that TNF antagonists bind to TNF and prevent it from interacting with its receptors. Additionally, the formation of immune complexes and the activation of the complement system were observed in cells treated with TNF antagonists.

13. The data demonstrate that TNF antagonists bind to TNF and prevent it from interacting with its receptors. Additionally, the formation of immune complexes and the activation of the complement system were observed in cells treated with TNF antagonists.

14. These findings support the hypothesis that the therapeutic effects of TNF antagonists are mediated by their ability to bind to TNF and prevent it from interacting with its receptors, as well as by the formation of immune complexes and the activation of the complement system.

15. Therefore, we propose that the therapeutic effects of TNF antagonists are mediated by their ability to bind to TNF and prevent it from interacting with its receptors, as well as by the formation of immune complexes and the activation of the complement system.

Figure 1. Flow cytometry analysis of TNF binding to cells.



Figure 2. Western blot analysis of TNF immunoprecipitation.



Figure 3. Complement activation assay.



Figure 4. Flow cytometry analysis of TNF binding to cells.



Figure 5. Flow cytometry analysis of TNF binding to cells.



Figure 6. Flow cytometry analysis of TNF binding to cells.



Figure 7. Flow cytometry analysis of TNF binding to cells.



Figure 8. Flow cytometry analysis of TNF binding to cells.



## DISCUSSION

16. The results of these experiments support the hypothesis that TNF antagonists bind to TNF and prevent it from interacting with its receptors. Additionally, the formation of immune complexes and the activation of the complement system were observed in cells treated with TNF antagonists.

17. These findings indicate that TNF antagonists bind to TNF and prevent it from interacting with its receptors. Additionally, the formation of immune complexes and the activation of the complement system were observed in cells treated with TNF antagonists.

## CONCLUSIONS

18. The data demonstrate that TNF antagonists bind to TNF and prevent it from interacting with its receptors. Additionally, the formation of immune complexes and the activation of the complement system were observed in cells treated with TNF antagonists.

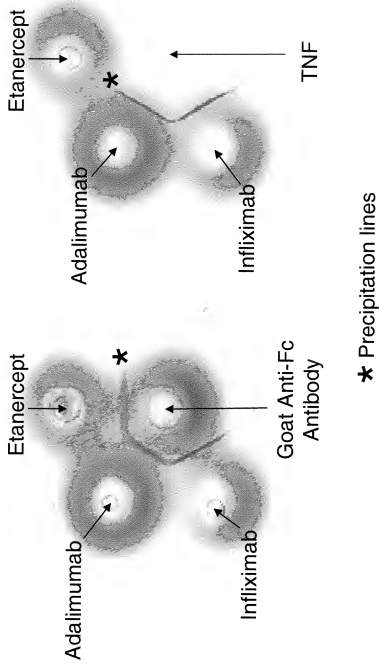
19. These findings support the hypothesis that the therapeutic effects of TNF antagonists are mediated by their ability to bind to TNF and prevent it from interacting with its receptors, as well as by the formation of immune complexes and the activation of the complement system.

## REFERENCES

1. Kahan I, Ting L, Kessler T, Smith BJ, Blumberg G, van der Vliet TWJ. Adalimumab and infliximab bind to Fc $\gamma$ -receptor and C1q and generate immuno-precipitation: a different mechanism from etanercept. *Arthritis Rheum* 2004;46:1495-1505.
2. Kahan I, Ting L, Kessler T, Smith BJ, Blumberg G, van der Vliet TWJ. Adalimumab and infliximab bind to Fc $\gamma$ -receptor and C1q and generate immuno-precipitation: a different mechanism from etanercept. *Arthritis Rheum* 2004;46:1495-1505.

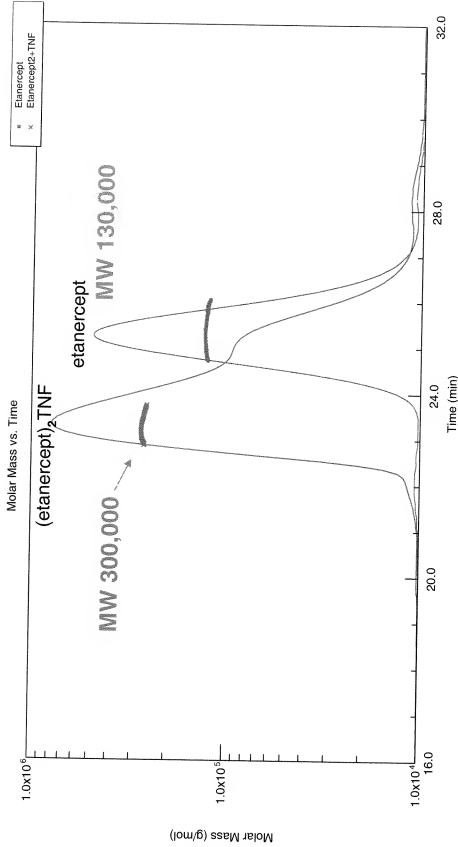
Figure 6

**A. Control experiment**      **B. Test experiment**



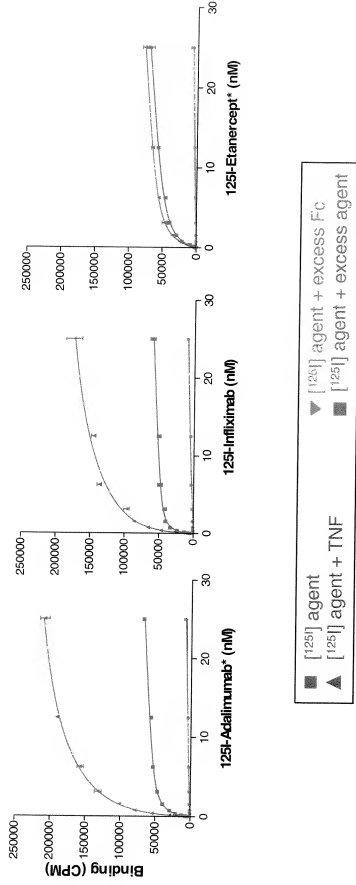
**Ouchterlony (double diffusion) analysis of  
TNF antagonists**

Figure 5



## SEC-LS analysis of etanercept-TNF complexes

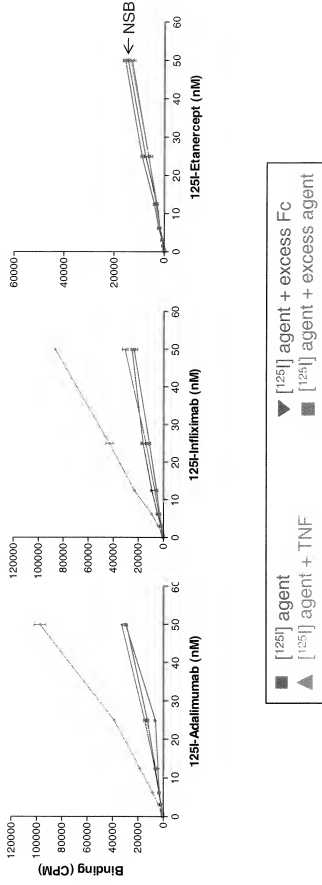
Figure 8



## Fc $\gamma$ R Binding Analysis of TNF Antagonists



Figure 9



## C1q Binding Analysis of TNF Antagonists

# EXHIBIT M

---

# Immunology

**JAN KLEIN**

*Max-Planck-Institut für Biologie*

*Tübingen*

*Federal Republic of Germany*

BLACKWELL SCIENTIFIC PUBLICATIONS

BOSTON OXFORD

LONDON EDINBURGH MELBOURNE

© 1990 by  
Blackwell Scientific Publications, Inc.  
Editorial offices:  
3 Cambridge Center, Suite 208  
Cambridge, Massachusetts 02142, USA  
Osney Mead, Oxford OX2 0EL, England  
25 John Street, London WC1N 2BL, England  
23 Ainslie Place, Edinburgh EH3 6AJ,  
Scotland  
107 Barry Street, Carlton  
Victoria 3053, Australia

All rights reserved. No part of this  
book may be reproduced in any form  
or by any electronic or mechanical  
means, including information storage  
and retrieval systems, without  
permission in writing from the  
publisher, except by a reviewer who  
may quote brief passages in a review.

First published 1990

Set by Setrite Typesetters, Hong Kong  
Printed in Great Britain at The Alden Press

90 91 92 93 5 4 3 2 1

#### DISTRIBUTORS

USA  
Blackwell Scientific Publications, Inc.  
Publishers' Business Services  
PO Box 447  
Brookline Village  
Massachusetts 02147  
(Orders: Tel: 617 524-7678)

Canada  
Oxford University Press  
70 Wynford Drive  
Don Mills  
Ontario M3C 1J9  
(Orders: Tel: 416 441-2941)

Australia  
Blackwell Scientific Publications  
(Australia) Pty Ltd  
107 Barry Street  
Carlton, Victoria 3053  
(Orders: Tel: 03 347-0300)

Outside North America and Australia  
Marston Book Services Ltd  
PO Box 87  
Oxford OX2 0DT  
(Orders: Tel: 0865 791155  
Fax: 0865 791927  
Telex: 837515)

Library of Congress  
Cataloguing-in-Publication Data

Klein, Jan, 1936-  
Immunology / Jan Klein.

p.  
Includes bibliographical references.  
ISBN 0-86542-116-1

1. Immunology. I. Title.  
[DNLM: 1. Immune System - physiology. 2. Immunity.  
QW 504 K641a]  
QR181 .J52 1990  
574.2'9 - dc20  
DNLM/DLC

British Library  
Cataloguing-in-Publication Data

Klein, Jan, 1936-  
Immunology.  
1. Immunology  
I. Title  
574.2'9  
ISBN 0-86542-116-1

and generalized swelling. Some of the affected fetuses may be aborted, others may be delivered stillborn, and others still may be born alive but with severe defects, particularly in the central nervous system, where considerable damage is caused by the deposit of bilirubin in ganglia. Haemolytic disease of the newborn does not always develop in an Rh<sup>-</sup> mother carrying an Rh<sup>+</sup> fetus. Usually the first pregnancy is not affected, but in later pregnancies, as the titre of Rh antibodies increases, the chances of haemolytic disease of the newborn also increase. The disease can be prevented by giving the mother anti-RhD IgG fraction intramuscularly at the time of delivery (within 60 h). These passively administered antibodies prevent sensitization of the mother's lymphoid system and thus the production of RhD antibodies. The passively administered antibodies are then eliminated by natural decay. This treatment reduces the risk of an anamnestic response during subsequent pregnancies by 95%.

### Type III hypersensitivities induced by immune complexes

#### Principle

The interaction of antigens with their corresponding circulating antibodies leads to the formation of antigen-antibody (immune) complexes. Normally, immune complexes are removed from the circulation through the mononuclear phagocyte (reticuloendothelial) system, particularly in the liver (by Kupffer cells), spleen, and lungs, but if they are formed in large quantities, they are deposited in various tissues. The deposited immune complexes bind and activate complement and the C3a and C5a fragments so generated bind to basophils in the blood and cause their degranulation. Immune complexes may also interact directly with basophils and platelets (the immunoglobulin Fc regions) and cause their degranulation. Some of the released mediators, in particular histamine and 5-hydroxytryptamine, cause retraction of endothelial cells and so increase the permeability of the blood vessels and lead consequently to the deposit of more immune complexes. The activated platelets aggregate and initiate the formation of small clots on the collagen of the exposed basement membrane beneath the endothelial cells. Other mediators attract neutrophils which then attempt to phagocytose the deposited complexes. The tissue-bound complexes cannot be easily engulfed, however, and the macrophages spill their

lysosomal contents over the tissue. Normally, the released lysosomal enzymes would be inactivated quickly by substances in the serum, but since the serum is to a great extent excluded from the contact zone between the phagocytes and the tissue cells, they have enough time to attack the tissue. The resulting tissue damage leads to a form of hypersensitivity which involves IgG rather than IgE antibodies. The hypersensitivity manifests itself in a characteristic tissue response which will be described shortly.

The immune complexes are deposited preferentially in certain sites throughout the body — the kidney glomerulus, the joints, the lungs, and the skin. The reasons for this preference may vary from organ to organ. The deposit of immune complexes in the kidney may occur because the blood pressure in the glomerular capillaries is four times higher than in other capillaries. Also, the glomerulus is a filter through which body fluids have to pass and it may retain immune complexes by a simple filtering effect. For a similar reason, immune complexes may also accumulate on other body filters: the ciliary body of the eye, where aqueous humour forms, and the choroid plexus in the brain, where cerebrospinal fluid is produced. The characteristics of the disease which leads to immune-complex deposits may also determine the site for the deposit. Systemic lupus erythematosus, for example, is characterized by the appearance of DNA-specific antibodies (see Chapter 24) and since DNA has affinity for collagen in the basement membrane of the glomerulus, most of the DNA-anti-DNA complexes accumulate in this organ. Another example is rheumatoid arthritis, in which plasma cells produce Ig-specific antibodies in the synovium of the joint and the immune complexes thus initiate an inflammatory response at this site. Why the deposition of immune complexes only occurs in certain diseases is not known. Possible contributory factors include the affinity of the antibodies and the valency of the antigen (low-affinity antibodies combining with low-valency antigens may form complexes that the body has difficulty clearing); the participation of complement (binding of C3b and C3d to immune complexes solubilizes deposited complexes and the lack of appropriate complement involvement may have the opposite effect); and the nature of the antigen, as was pointed out earlier.

Immune complexes form frequently in autoimmune diseases such as systemic lupus erythematosus and rheumatoid arthritis. The other two situations in which immune complexes may be

involved in the pathogenesis of the disease are, first, low-grade persistent infections such as those characterizing leprosy, malaria, African trypanosomiasis, and viral hepatitis; and second, repeated exposure of body surfaces, such as the lungs, to antigenic material such as pigeon antigens (leading to *pigeon fancier's disease*), or fungi from mouldy hay (leading to *farmer's lung disease*). The experimental models of these two situations are the Arthus reaction and serum sickness.

### Arthus reaction

In 1903, N. Maurice Arthus and Maurice Breton described an experiment in which they repeatedly injected normal horse serum subcutaneously into rabbits, with an interval of several days between the individual injections. After the fifth or sixth injection, they observed a skin reaction characterized by firm induration, swelling, abscess formation, and eventual necrosis. It was not necessary that the site of the last injection coincided with that of previous injections; the reaction could be observed at any site where the last injection was made. The phenomenon, now referred to as the *Arthus reaction*, is not peculiar to rabbits; similar reactions were also observed in guinea-pigs, rats, dogs, and humans. The reaction is explained as follows (Fig. 21.17). The repeated injections induce

the formation of precipitating antibodies specific for horse proteins. As the antigen diffuses from the injection site through the tissue and into the regional blood vessels, it combines with the antibodies and insoluble antigen-antibody complexes form locally in the venules. The immune complexes are deposited between and beneath the endothelial cells, where they activate complement. The chemotactic factors liberated from the complement cascade begin to attract neutrophils and platelets to the reaction site. The neutrophils adhere to the tissue-bound immune complexes via their C3 receptors (CR1) and attempt to phagocytose them. Since, however, the complexes are attached to a nonphagocytosable substrate (the basement membrane), the phagocytosis is incomplete and the phagolysosome remains open to the exterior, releasing lysosomal enzymes into the surrounding medium. The released enzymes attack the basement membrane and the tissue surrounding it, collagenases disrupting collagen fibres, neutral proteases destroying the ground substance, and elastases degrading elastic fibres. The proteases also generate C5a from C5, which initiates degranulation of the neutrophils. The mediators released from the granules promote further neutrophil accumulation and degranulation. Some of the mediators act on mast cells and basophils causing their degranulation, thus further exacerbating the inflammatory reaction. Some of the

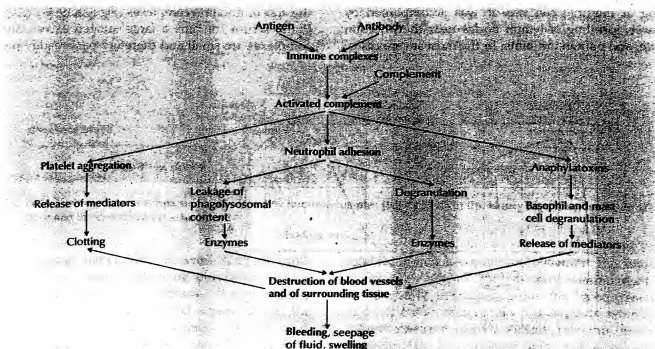


Fig. 21.17 Major mechanisms leading to the Arthus reaction.

# EXHIBIT N

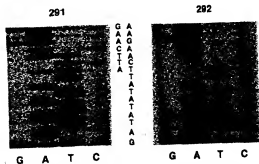


FIG. 3 Direct sequencing of the parents of the affected individual in family BOS22. PCR-amplified DNA was purified and asymmetrically amplified. The resulting single-stranded DNA was sequenced with the CF-17 primer. The sequence for the mother (no 291) matches that of the father (no. 292) and the published sequence up to the T residue (position 2566). Beyond this position, the sequence is a mixture of the two alleles owing to an AT insertion. METHODS. DNA amplified with primers CF-8 and CF-17 was electrophoresed on a nonfluorescent polyacrylamide gel. The product was excised from the gel and soaked in 100 µl water for 1 h at 65°C. Eluted DNA (5 µl) was reamplified with a 50:fold dilution of primer CF-17 for 40 cycles. The amplified DNA was purified with a Centrion 100 column (Amicon) and sequenced with Sequenase (USB) using dATP and <sup>32</sup>S-labelled dATP.

whereas the other carrier sibling had borderline values at 6-7 years of age (49-50 milliequivalents  $\text{Cl}^-$ ) that decreased to normal levels (38 milliequivalents  $\text{Cl}^-$ ) at 8 years of age. The mother had a normal sweat-test value. The difference in sweat-test values among these individuals could be due to environmental factors or inaccuracies in the sweat test, or reflect additional genetic control over ion transport in the sweat duct. In either case, a more detailed characterization of ion transport and regulation in these individuals should provide insight into these processes.

The CFTR 566 allele is due to the addition of an AT dinucleotide into a short segment (8 bp) of AT dinucleotides. Dinucleotide repeats are hotspots for mutations<sup>19,20</sup>. Although principally CA repeats have been examined, polymorphic AT repeats have also been characterized. A search of the prime sequences in the computerized database GenBank revealed >50 sequences containing AT repeats that were of 22 bp or more (M.D., data not shown). The mechanism for generating new alleles at these loci is not understood, but could involve unequal crossing-over or errors in replication. Examination of new alleles at other tandemly repeated loci, however, indicates that more complex mechanisms could be involved<sup>21</sup>.

The identification of all of the mutations that cause CF is essential for complete detection and diagnosis of the disease. Although the CFins2566 allele seems to be rare, the identification of this mutation provides some important insights. First, all of the CF mutations do not lie in the same exon, implying that complete detection will probably require examination of several regions of the gene. Second, frame-shift and other null mutations might not be uncommon. The most likely explanation for the failure so far to find such mutations in the CF gene is that individuals homozygous for such mutations are probably lethal, so that no selection against such alleles; these alleles would only be found in CF individuals, however, when balanced by a less severe allele. Frame-shift mutations could occur in virtually any region of the gene, making CF diagnosis difficult.

The continued identification of mutations in the CF locus is expected to help elucidate which regions of the CFTR are functionally important. Also, examination of the effects of these mutations in the allelic combinations in which they naturally occur should greatly increase our understanding of the function of the CFTR gene and its role in disease. □

Received 4 December 1989; accepted 6 February 1990.

10. Bost, F., Wehman, M. J. & Beusink, L. A. in *Mutagenesis Mechanisms of Inherited Disease* (Eds Smith, C. L., Beaudet, A. L., Sly, W. S. & Valle, D.) 2643-2680 (McGraw-Hill, New York, 1987).
11. Frazier, R. A. *Trends Microbiol.* **1**, 105-110 (1993).
12. Jettner, A. M., Yamashita, K., Stüttgen, M. J., Williams, R. J. & Boucher, R. C. *Science* **244**, 1472-1475 (1989).
13. Hwang, T.-C. et al. *Science* **244**, 1353-1353 (1989).
14. Li, M. et al. *Science* **244**, 1362-1366 (1989).
15. White, R. et al. *Nature* **334**, 385-388 (1991).
16. Dean, M. et al. *Nature* **353**, 356-360 (1993).
17. Tsai, L.-C. et al. *Science* **260**, 1054-1057 (1985).
18. Warrington, B. J. et al. *Nature* **334**, 364-365 (1991).
19. Lemory, G. M. et al. *Am. J. Hum. Genet.* **42**, 362-364 (1988).
20. Dean, M. *Genomics* **3**, 93-99 (1988).
21. Rondon, J. M. et al. *Science* **248**, 1069-1073 (1989).
22. Ronsmans, J. M. et al. *Science* **248**, 1050-1052 (1989).
23. Keen, B.-S. et al. *Science* **246**, 1073-1080 (1989).
24. Saki, R. et al. *Science* **238**, 487 (1988).
25. Rosenblatt, H. & Liebermann, T. S. in *Oxidative Inherited Disorders* (ed. Taussig, L. M.) 85-114 (Thieme-Stratton, New York, 1984).
26. Amos, J. A., Jones, S. R. & Eric, W. C. *Arch. Invest. Med.* **41**, 5-11 (1989).
27. de Sant'Anna, F. et al. *Am. J. Hum. Genet.* **43**, 555-559 (1982).
28. Litt, M. & Luty, J. *Am. J. Hum. Genet.* **44**, 397-401 (1989).
29. Weber, J. L. & May, P. E. *Am. J. Hum. Genet.* **44**, 308-310 (1989).
30. Powell, R. K., Nussbaum, R. L. & White, G. *Am. J. Hum. Genet.* **44**, 374-381 (1989).
31. Eschwald, E. Schmittke, J., Williams, R. J. & Warrington, B. *Hum. Genet.* **74**, 320-322 (1986).
32. Estévez, K. et al. *Am. J. Hum. Genet.* **44**, 70-73 (1989).
33. Januzzi, M. C. et al. *Am. J. Hum. Genet.* **44**, 696-702 (1989).
34. Barak, I., Gresserhous, K. H., Cooper, D. N. & Schmiede, J. *Am. J. Hum. Genet.* **38**, 290-297 (1986).
35. Samuels, T., Fritsch, E. P. & Sambrano, J. in *Molecular Cloning: A Laboratory Manual* (Cold Spring Harbor, New York, 1989).

**ACKNOWLEDGEMENTS:** We thank Janet Buchanan for discussions, and Dean Mann and Annette Perry for comments on the manuscript. This study was supported by the Department of Health and Human Services.

### Biological properties of a CD4 immunoadhesin

**Randal A. Byrn\*, Joyce Mordenti, Catherine Lucas,  
Douglas Smith, Scot A. Marsters,  
Jennifer S. Johnson\*, Paul Cossum,  
Steven M. Chamow, Florian M. Wurm,  
Timothy Gregory, Jerome E. Groopman\*  
& Daniel J. Capon**

Genentech Inc., 460 Point San Bruno Boulevard, South San Francisco,  
California 94080, USA

\* Division of Hematology-Oncology, Harvard Medical School, New England Deaconess Hospital, Boston, Massachusetts 02215, USA

**MOLECULAR fusions of CD4, the receptor for human immunodeficiency virus (HIV; refs 1-4), with immunoglobulin (termed CD4 immunoadhesins) possess both the gp120-binding and HIV-blocking properties of recombinant soluble CD4, and certain properties of IgG, notably long plasma half-life and Fc receptor binding<sup>5,6</sup>. Here we show that a CD4 immunoadhesin can mediate antibody-dependent cell-mediated cytotoxicity (ADCC) towards HIV-infected cells, although, unlike natural anti-gp120 antibodies, it does not allow ADCC against uninfected CD4-expressing cells. In addition, CD4 immunoadhesin, like natural IgG molecules, is efficiently transferred across the placenta of a primate. These observations have implications for the therapeutic application of CD4 immunoadhesins, particularly in the area of perinatal transmission of HIV infection.**

We have previously described CD4 immunoadhesins containing the first two immunoglobulin-like domains of CD4 joined to the entire constant region of human IgG1 heavy chain<sup>5</sup>. As the presence of light chain was found to be unnecessary for secretion of dimeric molecules<sup>5</sup>, we constructed additional derivatives lacking the CH1 domain of the IgG1 heavy chain (Fig. 1). The gp120-binding and Fc receptor-binding properties and the improved half-life characteristics of this molecule were comparable to the CD4 immunoadhesin containing the CH1 domain (not shown).

As CD4 immunoadhesin binds Fc receptors, we examined



TABLE 1 Placental transfer of rCD4 and CD4-IgG in pregnant rhesus monkeys

Rhesus monkey	Protein	Concentration (ng ml <sup>-1</sup> ) in maternal serum		Concentration (ng ml <sup>-1</sup> ) in newborn serum	Infant/maternal concentration ratio
		Mean	Range		
1	CD4-IgG	489	(276-673)	15.2	3.1%
2	CD4-IgG	217	(155-301)	7.6	3.5%
3	rCD4	682	(360-820)	1.1	0.16%
4	rCD4	437	(205-504)	<0.8	<0.18%

Four pregnant rhesus monkeys at 150-160 days gestation (normal gestation period 160-170 days) received a loading dose of CD4 immunoadhesin (CD4-IgG) or rCD4 by rapid intravenous injection followed by continuous infusion for 24 h; the infants were delivered by caesarian section. Blood was obtained from the mother after 1 min and after 4, 8, 12, 16, 20 and 24 h of infusion and from the infant and cord blood at the time of delivery. For maternal catheterization the animals were placed into jackets, and no additional anaesthesia was given. Animals received the loading dose of drug as an intravenous bolus into the femoral vein catheter over 5 s followed by saline flush to clear the catheter of drug. The infusion was started immediately thereafter. For CD4 immunoadhesin, a 0.135 mg kg<sup>-1</sup> loading dose was given, followed by 1.12 mg kg<sup>-1</sup> over 24 h; for rCD4, a 0.135 mg kg<sup>-1</sup> loading dose was given, followed by 28 mg kg<sup>-1</sup> over 24 h. Serum concentrations of each protein were determined by double antibody enzyme-linked immunosorbent assays (ELISA) each using monoclonal antibody Leu3a (Becton-Dickinson). As this antibody recognizes the gp120 binding domain of CD4, the assays thus detect CD4-containing molecules still capable of binding gp120. To measure rCD4 concentration, Leu3a in 0.05 M carbonate buffer, pH 9.6, was used to coat 96-well microtitre plates overnight at 4 °C. After three washes with PBS containing 0.05% Tween 20 (PBS-Tween), plates were blocked for 1 h at room temperature with ELISA diluent (PBS containing 0.5% BSA, 0.05% Tween 20 and 0.01% thimerosal). rCD4 standards and samples diluted in rhesus serum were incubated for 2 h, and plates were washed again with PBS-Tween. For detection of rCD4, monoclonal antibody OKT4 (Ortho) was conjugated to horseradish peroxidase (HRP, Boehringer Mannheim) by the periodate method<sup>14</sup>. After appropriate dilution in ELISA diluent, the conjugated antibody was incubated for 1 h at ambient temperature. Orthophenylene diamine dihydrochloride (Sigma), 2.2 mM in 0.05 M sodium phosphate/0.1 M citrate buffer, pH 5.0, containing 0.01% H<sub>2</sub>O<sub>2</sub>, was used as a substrate for 20-30 min at room temperature. Reactions were stopped with 4.5 N H<sub>2</sub>SO<sub>4</sub> and plates were read at 492 nm. Data were reduced using a four-parameter curve-fitting program<sup>20</sup>. The range for this assay was 0.8 to 25 ng ml<sup>-1</sup>. For the measurement of CD4 immunoadhesin, the same procedure was used, except that Leu3a was conjugated to HRP and used for detection; monoclonal antibody L104.5 (provided by B. Fendly, Genentech), which recognizes domain 2 of rCD4, was used for antigen capture. The range for this assay was 0.19 to 12.0 ng ml<sup>-1</sup>.

whether it could mediate ADCC towards HIV-infected cells by human peripheral blood mononuclear cells. Indeed, CD4 immunoadhesin mediates ADCC towards HIV-infected, but not uninfected, CEM human T-lymphoblastoid cells in a dose-dependent manner (Fig. 2a and b). Soluble recombinant (rCD4) does not mediate ADCC (not shown), but can inhibit cell lysis mediated by CD4 immunoadhesin (Fig. 2a), demonstrating that specific binding to gp120 by CD4 immunoadhesin is essential.

It has been suggested that ADCC in AIDS patients may be a mechanism of pathogenesis rather than protection<sup>21</sup>, as soluble gp120, by binding to healthy CD4-expressing 'bystander' cells, can make such cells targets for ADCC, mediated by the anti-gp120 antibodies found in HIV-infected individuals. In contrast to natural anti-gp120 antibodies, CD4 immunoadhesin does not

mediate killing of uninfected CEM cells preincubated with soluble gp120 (Fig. 2b). A likely explanation is that CD4 immunoadhesin, unlike natural anti-gp120 antibodies, cannot bind gp120 already bound to cell-surface CD4, because soluble gp120 is thought to have only one CD4-binding site.

An increasing number of paediatric AIDS patients are infected *in utero* by transmission from the mother<sup>2</sup>. As natural IgG molecules are selectively transported across the placenta of primates in an Fc receptor-dependent manner, we tested whether CD4 immunoadhesin shared this property. Pregnant rhesus monkeys near to term were given a bolus dose of either rCD4 or CD4 immunoadhesin, then were continuously infused to a relatively constant concentration for 24 h before delivery by caesarian section. Serum concentrations were determined by

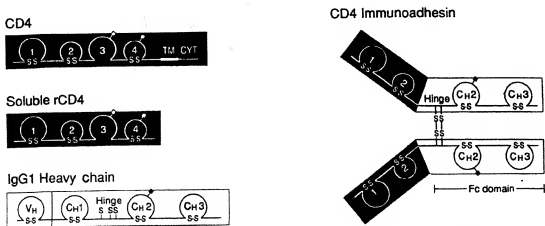


FIG. 1 Structure of CD4 immunoadhesin, soluble rCD4 and the parent human CD4 and IgG1 heavy chain molecules. CD4- and IgG1-derived sequences are indicated by shaded and unshaded regions, respectively. The immunoglobulin-like domains of CD4 are numbered 1-4; TM and CYT refer to the transmembrane and cytoplasmic domains. Soluble rCD4 is truncated after proline 368 of the mature CD4 polypeptide<sup>14</sup>. The variable (VH) and constant (CH1, hinge, CH2, and CH3) regions of IgG1 heavy chain are shown. Disulfide bonds are indicated by S-S. CD4 immunoadhesin consists of

residues 1-180 of the mature CD4 protein fused to IgG1 sequences beginning at aspartic acid 216 (taking amino acid 114 as the first residue of the heavy chain constant region<sup>19</sup>) which is the first residue in the IgG1 hinge after the cysteine residue involved in heavy-light chain bonding. The CD4 immunoadhesin shown, which lacks a CH1 domain, was derived from a CH1-containing CD4 immunoadhesin<sup>14</sup> by oligonucleotide-directed deletion mutagenesis<sup>22</sup>, expressed in Chinese hamster ovary cells and purified to >99% purity using protein A-Sepharose chromatography as described<sup>14</sup>.

immunoassay at various times in the mother and in the newborn within 5 min of birth. The concentration of CD4 immunoadhesin in fetal serum was  $\geq 3\%$  of the maternal level after 24 h (Table 1), indicating a significant rate of placental transfer. By contrast, rCD4 did not accumulate in the fetal serum to a significant extent. This is most probably due to lack of active transport across the placental barrier, although it is possible that transfer would not be detected owing to the shorter half-life of rCD4 (ref. 5).

Although the rate at which a protein appears in the fetal circulation cannot be directly translated into a rate of placental transfer, because the rate of degradation of the protein in the fetus is unknown, comparisons can be made with the appearance rate of human antibody in classical human experiments. Dancs *et al.*<sup>9</sup> gave radiolabelled human  $\gamma$ -globulin to women in their third month of pregnancy before abortion of the fetus, and observed a concentration in the fetus that was 2.8% of maternal levels after 18–24 h. Similarly, Gitlin *et al.*<sup>10</sup> gave women who were nearly to term a single intravenous injection of radiolabelled  $\gamma$ -globulin up to 4 weeks before birth and observed an increase in the infant plasma concentration of  $\sim 3\%$  of maternal level per day. Thus the rate of appearance of CD4 immunoadhesin in a primate fetus is close to that of normal human IgG in humans.

CD4-based strategies have an important theoretical advantage

over other AIDS therapeutics, as HIV must bind CD4 to be able to infect its cellular target (the T cell) specifically. Soluble CD4 derivatives have thus been developed with two objectives: to block gp120-mediated events such as the spread of viral infection, formation of syncytia and binding of gp120 to uninfected 'bystander' cells, and to use CD4 as a targeting agent to direct a cytotoxic agent to HIV-infected cells (for example, CD4-ricin<sup>11</sup>, CD4-pseudomonas exotoxin<sup>12</sup>). Here we have shown that CD4 immunoadhesin can direct the killing of HIV-infected cells, as well as blocking gp120-mediated events<sup>13</sup>. Significantly, CD4 immunoadhesin, unlike natural anti-gp120 antibodies, cannot kill CD4-expressing bystander cells coated with soluble gp120.

The fetal acquisition of passive immunity in humans is mediated by selective placental transfer of maternal IgG. As CD4 immunoadhesin shares this property, passive immunity to HIV could be established in the fetus by maternal administration, possibly preventing perinatal transmission of infection. The mechanism underlying selective transport of IgG involves binding to Fc receptors on the apical surface of the syncytiotrophoblast, resulting in protected endocytotic transport<sup>14</sup>. The fact that this, and so many other different properties of IgG, can be conferred on CD4 by the addition of an Fc region suggests that such functions could be acquired by any adhesion molecule capable of being linked to Fc in place of the Fab sequences

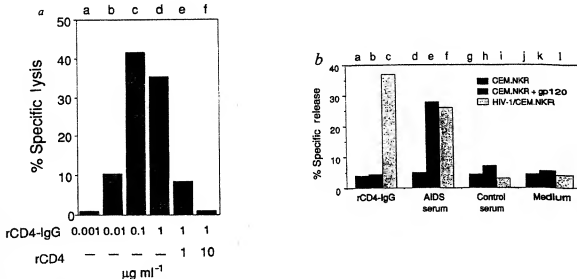


**FIG. 2** Antibody-dependent cell-mediated cytotoxicity (ADCC) shown by CD4 immunoadhesin. CEM T-lymphoblastoid target cells were labelled with  $^{51}\text{Cr}$ , incubated with CD4 immunoadhesin, rCD4, serum, or control media for 30 min, and mixed with peripheral blood mononuclear cells (PBMCs) as effector cells at an effector-to-target ratio of 50:1. The cell mixtures were incubated for 20 h at 37 °C, and the cell-free supernatant was collected and assayed for  $^{51}\text{Cr}$  released from target cells. A lysis of HIV-1-infected CEMNKR target cells by effector cells in the presence of CD4 immunoadhesin at 0.001  $\mu\text{g ml}^{-1}$  (lane a), 0.01  $\mu\text{g ml}^{-1}$  (lane b), 0.1  $\mu\text{g ml}^{-1}$  (lane c) and 1.0  $\mu\text{g ml}^{-1}$  (lanes d–f). Also shown is the lysis of rCD4 at 1.0  $\mu\text{g ml}^{-1}$  (lane e) and 10  $\mu\text{g ml}^{-1}$  (lane f) of target cell lysis mediated by 1.0  $\mu\text{g ml}^{-1}$  CD4 immunoadhesin. The level of cell lysis observed with CD4 immunoadhesin was comparable to that mediated by a control AIDS patient serum. rCD4 itself does not mediate target cell lysis at concentrations up to 10  $\mu\text{g ml}^{-1}$ . Uninfected CEMNKR targets were not lysed by effector cells in the presence of CD4 immunoadhesin, AIDS patient serum or normal human serum (see below), but could be lysed in the presence of a rabbit anti-CD4 serum (not shown). **a**, ADCC towards uninfected CEMNKR target cells (lanes a, b, c, d, e, f), uninfected CEMNKR cells incubated with soluble gp120 (ref. 17) (lanes b, c, e, h and i), and HIV-1-infected CEMNKR (lanes c, f, i and j) mediated by CD4 immunoadhesin (lanes a–c), AIDS patient serum at 1:1,000 final dilution (lanes d–f), serum from an uninfected individual at 1:1,000 final dilution (g–i) and complete medium (lanes j–l).

**METHODS.** The CEMNKR T-lymphoblastoid cell line, which is resistant to NK-mediated lysis<sup>18</sup>, was used for all experiments. HIV-1-infected CEMNKR cells were produced by inoculating  $10^5$  CEMNKR cells with  $10^5$  TCID<sub>50</sub> of HIV-1<sub>IIIB</sub>. The culture was monitored for infection using reverse transcriptase (RT) activity and HIV-1 specific antibodies for immunofluorescence. After  $\sim 2$  weeks the culture became stable, with  $> 70\%$  of cells

immunofluorescence-positive, and  $> 10^6$  c.p.m.  $\text{ml}^{-1}$  RT activity in the medium. Cells were maintained in RPM 1640 medium (Gibco) containing 20% fetal bovine serum (MA bioproducts), penicillin, streptomycin and L-glutamine (complete medium). Target cells were labelled by incubation of  $10^6$  cells with 100  $\mu\text{Ci}$   $^{51}\text{Cr}$  in 0.5 ml for 2 h at 37 °C. After two washes, cells were suspended at  $2 \times 10^6$  per ml in complete medium and 25- $\mu\text{l}$  aliquots (containing  $5 \times 10^5$  cells) were dispensed to wells of a 96-well plate. For the lysis assay, 25  $\mu\text{l}$  purified recombinant proteins or sera diluted in complete medium, or control medium, were added to each well and incubated for 30 min at room temperature. Assays were carried out in triplicate. Effector PBMCs were prepared from heparinized blood obtained from a healthy, HIV-seronegative donor by centrifugation through Ficoll-Paque (Pharmacia). After two washes in RPM 1640 the cells were suspended to  $5 \times 10^6$  cells per ml in complete medium and 50- $\mu\text{l}$  aliquots were added to appropriate wells. The total incubation volume was therefore 100  $\mu\text{l}$ . The concentrations indicated are final concentrations after effector cells were added. Plates were incubated for 16–18 h at 37 °C in 5% CO<sub>2</sub>. For analysis of cell lysis, 50- $\mu\text{l}$  samples of supernatant were pipetted from each well, mixed with detergent to inactivate HIV, then mixed with 0.5 ml Protosol (New England Nuclear) and 5 ml Betaluffer (National Diagnostics) and analysed by scintillation counting. Maximum lysis, spontaneous lysis and complete medium controls were included in each assay for each target cell, in triplicate. Maximum lysis was obtained by substituting 25  $\mu\text{l}$  of 2% Triton X-100 for the test sample. Spontaneous release wells received 70  $\mu\text{l}$  complete medium instead of effector cells. Complete medium controls received medium instead of the test sample. Percentage specific lysis was calculated using the formula, % specific lysis = (test sample – spontaneous release)/(maximum lysis – spontaneous release).

## LETTERS TO NATURE

normally constituting the antigen-binding site of IgG. Therefore, in principle, any such receptor can be given the functional characteristics of an antibody, with the ability to select desirable characteristics at will. □

Received 7 December 1989; accepted 19 February 1990.

1. Dingley, A. et al. *Nature* **332**, 763-767 (1984).
2. Hattmann, O. et al. *Nature* **332**, 767-768 (1984).
3. Macdon, P. et al. *Cell* **47**, 333-348 (1986).
4. Macdon, P. et al. *Science* **234**, 380-385 (1986).
5. Capon, D. et al. *Nature* **337**, 525-531 (1989).
6. Trautwein, A., Schneider, J., Kiefer, H. & Karsch, K. *Nature* **339**, 68-70 (1989).
7. Lively, H., Matthews, T., Langlois, A., Bolognesi, D. & Weisbach, K. *Proc. Natl. Acad. Sci. U.S.A.* **84**, 4602-4605 (1987).
8. Katz, S. & Willert, C. *New Engl. J. Med.* **320**, 1687-1688 (1989).
9. Dorek, J., Lind, J., Ortiz, M., Sridhara, J. & Viera, P. *Am. J. Otolaryngol.* **82**, 167-171 (1981).
10. Olin, O., Kurnas, J., Larrat, J. & Morera, C. *J. Clin. Invest.* **43**, 1938-1951 (1964).
11. Yli, M. et al. *Science* **242**, 1166-1168 (1988).
12. Chaudhary, A. et al. *Nature* **336**, 369-372 (1988).
13. Johnson, P. & Brown, P. *Pharmacol. Rev.* **3**, 259-269 (1981).
14. Smith, O. et al. *Science* **238**, 1704-1707 (1987).
15. Hake, E. et al. *Sequences of Proteins of Immunological Interest* 4th edn (1987).
16. Zeller, M. & Smith, M. *Nucleic Acids Res.* **10**, 6487-6500 (1982).
17. Lasky, L. et al. *Science* **233**, 209-212 (1986).
18. Howell, O., Anselotti, P., Domini, J. & Grossman, P. *J. Immunol.* **134**, 971 (1985).
19. Haines, P. & Parnes, G. *J. Cell Biol.* **33**, 307-318 (1987).
20. Marquet, D. *J. Soc. and appl. Math.* **34**, 431-441 (1983).

**ACKNOWLEDGMENTS.** We thank Steven Frie for performing enzyme-linked immunosorbent assays, Dr. Pam Frost and Natalia Gaylord (Pharmaceutical Research Institute, New Mexico State University) for assistance with animal studies, and Dr. Rebecca Ward for critical comments on the manuscript. This work was supported by Genentech, Inc. and the NIH (S.B. and J.G.).

## Calcium entry through stretch-inactivated ion channels in *mdx* myotubes

Alfredo Franco Jr & Jeffry B. Lansman\*

Department of Pharmacology, School of Medicine, University of California, San Francisco, California 94143-0450, USA

RECENT advances in understanding the molecular basis of human X-linked muscular dystrophies (for a review, see ref. 1) have come from the identification of dystrophin, a cytoskeletal protein associated with the surface membrane<sup>2-4</sup>. Although there is little or virtually no dystrophin in affected individuals<sup>5,6</sup>, it is not known how this causes muscle degeneration. One possibility is that the membrane of dystrophic muscle is weakened and becomes leaky to  $Ca^{2+}$  (refs 7-9). In muscle from *mdx* mice, an animal model of the human disease<sup>10</sup>, intracellular  $Ca^{2+}$  is elevated and associated with a high rate of protein degradation<sup>11</sup>. The possibility that a lack of dystrophin alters the resting permeability of skeletal muscle to  $Ca^{2+}$  prompted us to compare  $Ca^{2+}$ -permeable ionic channels in muscle cells from normal and *mdx* mice. We now show that recordings of single-channel activity from *mdx* myotubes are dominated by the presence of  $Ca^{2+}$ -permeable mechanotransducing ion channels. Like similar channels in normal skeletal muscle, they are rarely open at rest, but open when the membrane is stretched by applying suction to the electrode<sup>12-14</sup>. Other channels in *mdx* myotubes, however, are often open for extended periods of time at rest and close when suction is applied to the electrode. The results show a novel type of mechanotransducing ion channel in *mdx* myotubes that could provide a pathway for  $Ca^{2+}$  to leak into the cell.

We recorded single-channel activity from cell-attached patches on myotubes from normal and *mdx* mice with 110 mM  $BaCl_2$  in the patch electrode. Figure 1a shows a continuous record of single-channel activity recorded ~1 min after the patch electrode formed a seal on the surface of a myotube from normal mouse muscle. At a holding potential of -60 mV, the single-channel

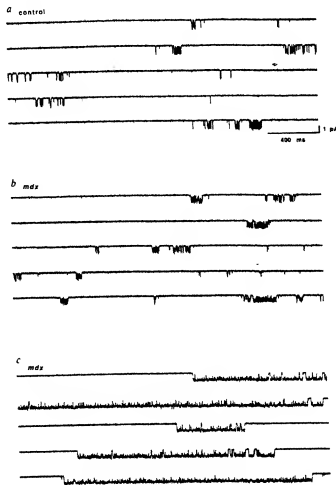


FIG. 1 Channel activity recorded from the surface of myotubes from normal and *mdx* mice with 110 mM  $BaCl_2$  in the patch electrode showing unitary  $Ba^{2+}$  currents at a constant holding potential of -60 mV. The traces are sequential and represent a segment of a continuous recording (~10 seconds channel activity). Currents were filtered at 1 kHz with an eight-pole Bessel filter and sampled at 5 kHz. a, Recording from a cell-attached patch on a normal myotube. b, Recording from a cell-attached patch on a *mdx* myotube showing low channel activity. c, Recording from a different *mdx* myotube in which channel activity was high.

**METHODS.** Myotubes were prepared by dissecting hind-limb or outcuneopectoral muscles from 7-day-old normal C57BL/6J mice or *mdx* mice (Jackson Laboratory) after killing by cervical dislocation. The muscle was minced and incubated for ~15 min at 37 °C in  $Ca^{2+}$ - and  $Mg^{2+}$ -free Hank's buffer containing 0.125% trypsin. Cells were dissociated by passing through a small-bore pipette and filtered through 100-µm gauze. The suspension was preplated for ~1 h to remove fibroblasts, after which the remaining cells in suspension were plated on gelatin-coated tissue culture dishes at a density of ~5,000 cells per cm<sup>2</sup> in DMEM medium supplemented with 20% FCS and chick embryo extract. Myoblasts began to fuse and form myotubes after ~4-5 days in culture. Recordings were made from myotubes 1-5 days after the first myotubes formed. Recordings of single-channel activity from cell-attached patches were made with a List EPC-7 amplifier as described previously<sup>15</sup>. Current signals were recorded on video tape and replayed onto the hard disk of a laboratory computer (PDP 11/73) for later analysis. Patch electrodes were made from borosilicate capillary pipettes (Rochester Scientific) and had resistances of 2-4 MΩ, when filled with 110 mM  $BaCl_2$  and immersed in the bath. The bathing solution contained 150 mM potassium aspartate, 5 mM  $MgCl_2$ , 5 mM EGTA, 10 mM glucose and 10 mM HEPES buffer. The pH was adjusted to 6.5 with KOH. An isotonic potassium bathing solution was used to zero the resting potential of the cell. Occasionally, voltage shifts were detected after patch excision which indicated a maximum voltage error of ~10 mV. The bathing solution produced no obvious signs of cell deterioration.

\* To whom correspondence should be addressed.

# EXHIBIT O



The successful approach relied on two observations. First, 1-2-Cx and 1-2-3-4-Cx were secreted, whereas 1-Cx and 1-2-3-Cx were not, suggesting to us that CD4 domains associate pairwise into two stable units consisting of 1-2 and 3-4 domains respectively. Second, the analysis of human heavy-chain disease proteins has shown that heavy chains of different subclasses can be secreted without light chains when the first constant region domain is deleted<sup>11</sup>. We therefore constructed plasmids in which the exons encoding the first two N-terminal domains of CD4 were linked to all but the  $V_H$  and  $C_H1$  domains of either the mouse  $\mu$  heavy chain (CD4-M $\mu$ ) or the mouse  $\gamma_2a$  heavy chain (CD4-M $\gamma_2a$ ) (see Fig. 1).

Both CD4-M $\mu$  and CD4-M $\gamma_2a$  were found in the culture supernatants at levels of  $1-5 \mu\text{g ml}^{-1}$  after the corresponding constructs were introduced into a myeloma cell line X63-0 (Fig. 2). Immunoprecipitations of the secreted proteins with relevant antibodies or protein A and subsequent western blot analyses showed that the molecules produced had the expected apparent molecular weights (Fig. 2). A similar analysis under non-reducing conditions indicated that CD4-M $\mu$  was most probably secreted as a pentamer, whereas CD4-M $\gamma_2a$  formed dimers, consistent with the fact that CD4-M $\gamma_2a$  bound to protein A (ref. 14) (Fig. 2b, c). Both CD4-M $\mu$  and CD4-M $\gamma_2a$ , as well as the previously produced CD4-M $\kappa$ , were able to bind to HIV gp120 (Fig. 2d). Because recombinant gp120 was not available, we used metabolically labelled preparations of gp120 derived from the supernatants of HIV-infected (H9) cell cultures in our co-immunoprecipitation tests.

Importantly, the effector functions of normal immunoglobulin molecules, such as binding to Fc $\gamma$  receptors and C1q were kept intact in the hybrid molecules (Fig. 3). This suggests that removal of the CH1 domain does not create major structural alterations

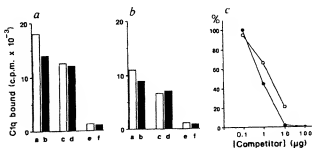


FIG. 3 Characterization of binding properties of CD4-immunoglobulin molecules. a, b, C1q binding assay. Microtiter plates were coated with purified CD4-immunoglobulin and natural control proteins of appropriate subclasses at the concentrations of  $10 \mu\text{g ml}^{-1}$  (a) and  $1 \mu\text{g ml}^{-1}$  (b). The direct binding of <sup>125</sup>I-labelled C1q was then measured. a, CD4-M $\gamma_2a$ ; b, OKT3 (IgG2a, K); c, CD4-M $\mu$ ; d, TEPC 183 (IgM, K); e, CD4-M $\kappa$ ; f, BSA. c, Binding of CD4-immunoglobulin molecules to Fc $\gamma$  receptors on the mouse macrophage cell line M29. Competition between <sup>125</sup>I-labelled CD4-M $\gamma_2a$  and the indicated amounts of CD4-M $\gamma_2a$  (○) and OKT3 (IgG2a) (●) proteins. METHODS. a, b, Polyvinyl chloride microtiteration plates were coated with <sup>125</sup>I-labelled C1q at concentrations of  $10 \mu\text{g ml}^{-1}$  (a) and  $1 \mu\text{g ml}^{-1}$  (b). After overnight incubation the plates were blocked with 1% BSA solution and binding of <sup>125</sup>I-labelled human C1q ( $\sim 2 \text{ ng}$ , 50,000 c.p.m.) was measured after incubation for 6 h at room temperature. Radiolabelling of C1q (a gift from Dr A. Erdel) was carried out by the iodogen method, according to the recommendations of the manufacturer (PIERCE). c, Fc $\gamma$  receptor binding was assayed by incubating  $2 \times 10^6$  M29 mouse macrophage cells (a gift from Dr G. Stockinger) with <sup>125</sup>I-labelled CD4-M $\gamma_2a$  (200 ng), plus competitor proteins in  $100 \mu\text{L}$  medium containing 5% fetal calf serum for 1 h at 4°C. After incubation the samples were centrifuged through a 200  $\mu\text{L}$  cushion of fetal calf serum and the radioactivity in the pellets was measured. The radioactivity obtained after adding 500-fold excess of unlabelled IgG2a (OKT3) was assumed to be due to nonspecific binding and was subtracted before calculating the percentage inhibitions shown. Radiolabelling was performed as described above.

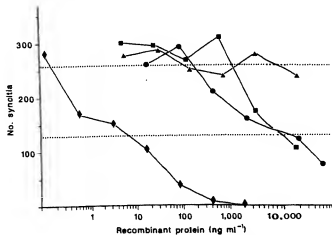


FIG. 4 Inhibition of syncytium formation by different recombinant proteins. The number of syncytia is plotted against the final concentrations of the recombinant proteins (●) CD4-M $\mu$ ; (■) CD4-M $\gamma_2a$ ; (▲) CD4-M $\kappa$ ; (△) L3T4-M $\kappa$  (ref. 9). The dotted lines indicate the number of syncytia in the absence of any inhibitory proteins and the number at 50% inhibition.

METHODS. A pretitrated amount of HIV-1-HAN was incubated at room temperature with serially diluted recombinant proteins for 30 min. Thereafter, 25  $\mu\text{L}$  of each mixture was transferred in triplicate into the wells of a 96-well plate which contained 25,000 MT-2 cells<sup>28</sup> per well in 50  $\mu\text{L}$  of medium. After 3 days culture, 100  $\mu\text{L}$  of fresh medium was added per well and after 5 days the syncytia were counted. The sums of syncytia of the triplicates were used for inhibition curves. HIV-1-HAN was isolated from the PBL of an AIDS patient. Partially determined nucleotide sequence of HIV-1-HAN shows about 90% sequence homology to HTLV-III<sub>g</sub> (U. Sauerbrenn and J. Mous, unpublished observation). Culture supernatants of MT-2 or Jurkat cells infected with HIV-1-HAN contained ten times more syncytium-forming capacity than similar culture supernatants of H9/HTLV-III<sub>g</sub> cells.

in the regions of the CH2 domain responsible for C1q and Fc $\gamma$  receptor binding.<sup>3,16</sup>

To assay the biological activity of these molecules, we tested them in the syncytium inhibition assay<sup>7,18</sup> (Fig. 4). CD4-M $\mu$  was by far the best inhibitor of syncytium formation: 50% inhibition was obtained at a concentration of  $10 \text{ ng ml}^{-1}$  which was about 1,000-fold less than the concentration ( $\sim 10 \mu\text{g ml}^{-1}$ ) of CD4-M $\gamma_2a$  and CD4-M $\kappa$  proteins needed for the same effect. Complete abolition of syncytia formation was possible with CD4-M $\mu$  at concentrations of about  $1-2 \mu\text{g ml}^{-1}$ . The CD4-M $\kappa$  protein exists as a noncovalently-associated dimer (data not shown), possibly due to the Cx portion of the molecules. Thus it seems that the effectiveness of these molecules increases as a function of their valence. Truly monovalent CD4, which we do not have, has not been compared directly with the dimeric forms of recombinant CD4 molecules (CD4-M $\gamma_2a$  and CD4-M $\kappa$ ) in this particular assay.

Soluble CD4 provides the optimal specificity for neutralization of the HIV-1 for many reasons. First, the strength of the interaction of the CD4 and gp120 is very high, of the order of  $10^{-9} \text{ M}$  (refs 5, 19). Second, the genetic variants of HIV-1 (refs 20-23) which emerge frequently during the infection must retain their CD4-binding properties to maintain their infectivity. Third, the immunity against gp120 acquired during the infection can have serious deleterious effects on the immune system: free gp120 which is shed from the virus<sup>24,25</sup> can be trapped specifically on the CD4-positive cells and in this way the non-infected cells can become targets of various forms of anti-gp120 immune attacks<sup>26-29</sup>. Passive immunity based on CD4 specificity would avoid this bystander destruction because it would discriminate between gp120 molecules which are already bound on cell-surface CD4 and those molecules which are produced by infected cells.

Although the human CD4-immunoglobulin chimera reported by Capon *et al.*<sup>10</sup> was secreted, they found that a similar hybrid protein, based on the mouse  $\gamma_1$  heavy chain, was retained intracellularly. We have also noticed that hybrid molecules containing the C<sub>H1</sub> domain, for example CD4-IgM chimeras, are not secreted (unpublished observation) and we suspect that in the absence of immunoglobulin light chains, the hydrophobic face of the C<sub>H1</sub> domain interacts strongly with the heavy chain

binding protein, thus preventing secretion<sup>10,31</sup>.

We believe that hybrid proteins which combine the specificity of CD4 with the multivalency and effector functions of different immunoglobulin subclasses could provide a realistic approach to AIDS therapy. We also think that our approach to designing hybrid immunoglobulin molecules could be applied more generally for building novel immunoglobulin molecules. □

Received 27 February; accepted 27 March 1989.

1. Dargatzis, A. *et al.* *Nature* **312**, 763-766 (1984).
2. Kistmann, D. *et al.* *J. Immunol.* **136**, 3151-3162 (1986).
3. McDougal, J. *et al.* *J. Immunol.* **136**, 3151-3162 (1986).
4. Madson, P. *et al.* *Cell* **47**, 333-346 (1986).
5. Smith, D. W. *et al.* *Science* **238**, 1704-1707 (1987).
6. Fischer, R. E. *et al.* *Nature* **331**, 78-81 (1988).
7. Deen, K. C. *et al.* *Nature* **331**, 82-84 (1988).
8. Trautwein, A., Lillie, W. & Karpman, K. *Nature* **331**, 84-86 (1988).
9. Capon, D. J. *et al.* *Nature* **337**, 525-531 (1989).
10. Seigrist, M., Milnes, L., Proulx, J., Capon, F. & Brouet, J. C. *Immunol. Rev.* **48**, 145-167 (1979).
11. Classon, J. B., Tsagaratos, J., McKenzie, I. F. & Walter, I. D. *Proc. natn. Acad. Sci. U.S.A.* **83**, 4499-4503 (1986).
12. Trautwein, A., Dolder, B., Oliveri, F. & Karpman, K. *Immun. Today* **10**, 29-32 (1989).
13. Duncan, A. R. & Winter, G. *Nature* **332**, 738-740 (1988).
14. Dargatzis, A., R. & Winter, G. *Nature* **332**, 563-569 (1988).
15. Duncan, A. R., Winter, G., M. & Winter, G. *Nature* **332**, 470-474 (1986).
16. Soderstrom, J., Goh, W. C., Rosen, C., Campbell, K. & Heston, W. A. *Nature* **332**, 725-728 (1986).
17. Lifson, J. D. *et al.* *Nature* **332**, 725-728 (1986).
18. Lasky, L. *et al.* *Cell* **80**, 975-985 (1987).
19. Hahn, B. H. *et al.* *Proc. natn. Acad. Sci. U.S.A.* **82**, 4813-4817 (1985).
20. Wong-Staal, F. *et al.* *Science* **229**, 759-762 (1985).
21. Alizon, M., Wain-Hobson, S., Montagnier, L. & Sonig, P. *Cell* **46**, 63-74 (1986).
22. Starach, B. R. *et al.* *Cell* **46**, 637-648 (1986).
23. Geleziou, H. R., Reuhs, H. & Paul, G. *Lancet* **ii**, 1015-1017 (1985).
24. Schneider, J., Kaden, O., Copeland, T. D., Grassl, S. & Hummels, G. J. *J. gen. Virol.* **67**, 2533-2539 (1986).
25. Lyster, H. K., Matthews, T. J., Langlois, A. J., Biopress, D. P. & Wehrhahn, K. J. *Proc. natn. Acad. Sci. U.S.A.* **84**, 4507-4515 (1987).
26. Wehrhahn, K. J. *et al.* *M. Lancet* **ii**, 902-905 (1988).
27. Lanzavecchia, A., Rosenk, E., Gregory, T., Bernan, P. & Abnigian, S. *Nature* **334**, 530-534 (1988).
28. Silvano, R. F. *et al.* *Cell* **54**, 551-575 (1988).
29. Host, L. G. & Wirth, M. *Nature* **306**, 387-389 (1984).
30. Bole, D. G., Henderson, L. M. & Kearney, J. F. *Cell* **50**, 1558-1566 (1986).
31. Trautwein, A., Dolder, B. & Karpman, K. *Eur. J. Immunol.* **18**, 853-854 (1988).
32. Popovic, M., Sengupta, M. G., Reid, E. & Galla, R. C. *Science* **224**, 447-450 (1984).
33. Schneider, J. *et al.* *Virology* **132**, 1-11 (1984).
34. Miyoshi, I. *et al.* *Nature* **284**, 770-771 (1981).

ACKNOWLEDGMENTS. We would like to thank Ludwine Ahnborn, Filippo Oliveri, John Hatten and Reinhard Schütz for technical assistance, Nicole Schöpf for preparing the manuscript, Hans Peter Steinberger for the graphic and Drs Alan Tuncall and Richard Schermer for critical reading. We would also like to thank Dr Ulrike Sauerwein, German Primate Center for providing HIV-1MAN and Dr Jan Mous for discussions. The Basel Institute for Immunology was founded and is supported by F. Hoffmann-La Roche Ltd Co., Basel, Switzerland.

## Activation of HIV gene expression during monocyte differentiation by induction of NF- $\kappa$ B

George E. Griffin<sup>†</sup>, Kwanyee Leung<sup>†</sup>,  
Thomas M. Folks<sup>‡</sup>, Steven Kunkel<sup>§</sup>  
& Gary J. Nabel<sup>¶</sup>

<sup>\*</sup> Howard Hughes Medical Institute, University of Michigan Medical Center, Departments of Internal Medicine and Biological Chemistry, Ann Arbor, Michigan 48109, USA  
<sup>†</sup> Retrovirus Diseases Branch, Centers for Disease Control, Atlanta, Georgia 30333, USA  
<sup>‡</sup> Department of Pathology, University of Michigan Medical School, Ann Arbor, Michigan 48109, USA

THE latent period of AIDS is influenced by factors which activate human immunodeficiency virus (HIV) replication in different cell types. Although monocyte cells may provide a reservoir for virus production *in vivo*<sup>1-4</sup>, their regulation of HIV transcription has not been defined. We now report that HIV gene expression in the monocyte lineage is regulated by NF- $\kappa$ B, the same transcription factor known to stimulate the HIV enhancer in activated T cells<sup>5</sup>; however, control of NF- $\kappa$ B and HIV in monocytes differs from that observed in T cells. NF- $\kappa$ B-binding activity appears during the transition from promonocyte to monocyte in U937 cells induced to differentiate *in vitro* and is present constitutively in mature monocytes and macrophages. In a chronically infected promonocytic cell, U1, differentiation is associated with HIV-1 replication as well as NF- $\kappa$ B binding activity. These findings suggest that NF- $\kappa$ B binding activity is developmentally regulated in the monocyte lineage, and that it provides one signal for HIV activation in these cells.

We transfected monocytic cell lines from progressive stages of differentiation with a plasmid containing the HIV enhancer linked to the chloramphenicol acetyltransferase (CAT) gene. Twenty-four hours after transfection, cells were incubated in medium alone or in the presence of 12-O-tetradecanoylphorbol-13-acetate (TPA). Expression of the HIV enhancer was induced by TPA in two immature monocyte leukaemia lines, a human granulocyte-macrophage leukaemia, HL-60, and the human promonocytic line, U937 (Fig. 1a). TPA treatment did not augment CAT expression in the mature macrophage leukaemic cells, THP-1, PUS-1.8, which showed higher basal activity (Fig. 1b; note scale changes).

Using a mutant HIV-CAT plasmid containing alterations in both  $\kappa$ B sites<sup>6</sup>, we showed that induction of HIV-CAT expression in the immature lines, HL-60 and U937 (Fig. 1a), and constitutive expression in the mature lines was dependent on the  $\kappa$ B sites (Fig. 1b). This suggested that NF- $\kappa$ B is present in the induced progenitors and in the mature cells, and we therefore looked for NF- $\kappa$ B binding activity in nuclear extracts from these cell lines. NF- $\kappa$ B binding activity in the immature lines, HL-60 and U937, was induced by TPA, whereas in the mature macrophage lines, THP-1, PUS-1.8, and P388D1, it was constitutively expressed (Fig. 2a). We then determined whether NF- $\kappa$ B binding activity is present in normal human monocytes and/or macrophages. Nuclear extracts were prepared from human peripheral blood monocytes or adherent mononuclear cells, and NF- $\kappa$ B binding activity was found in both cell types as well as in mouse peritoneal macrophages (Fig. 2b). NF- $\kappa$ B binding is therefore constitutively active in normal and neoplastic mature mononuclear phagocytes, including blood monocytes and adherent macrophages.

Treatment of immature monocytes with TPA, or the water-soluble phorbol-12, 13-dibutyrate<sup>10</sup> (PDB) (which is more easily removed from cells) causes differentiation into mature monocytes and macrophages, as judged by changes in cell growth, morphology, surface glycoproteins, and phagocytic function (Fig. 3, see also refs 11-15). HL-60 cells treated with PDB acquired characteristics of mature macrophages, displaying growth arrest, increased phagocytosis, adherence, FcR and Mo1 expression. At the same time, these cells began to express NF- $\kappa$ B binding activity which persisted even two days after

<sup>†</sup> Permanent address: Department of Communicable Diseases, St George's Hospital Medical School, London, UK  
<sup>‡</sup> To whom correspondence should be addressed.

# EXHIBIT P



40. Richmond, G. L. *Chem. Phys. Lett.* **110**, 571-575 (1984).
41. Richmond, G. L., Rejzhanalab, H. M., Robinson, J. M. & Shannon, V. L. *J. Opt. Soc. Am.* **64**, 228-236 (1987).
42. Corn, R. M., Romagnoli, M., Levenson, M. D. & Philpott, M. R. *J. Chem. Phys.* **81**, 4127-4132 (1984).
43. Furtak, T. E., Meraghiotis, J. & Korenowski, G. M. *Phys. Rev. B* **35**, 2596-2597 (1987).
44. Richmond, G. L., Koss, D. A., Robinson, J. M. & Shannon, V. L. *Bull. Am. Phys. Soc.* **33**, 1648 (1988).
45. Shannon, V. L., Koss, D. A. & Richmond, G. L. *J. Chem. Phys.* **87**, 1440-1441 (1987); *Appl. Opt.* **26**, 3579-3583 (1987).
46. Shannon, V. L., Koss, D. A. & Richmond, G. L. *J. Phys. Chem.* **91**, 5548-5555 (1987).
47. Shannon, V. L., Koss, D. A., Robinson, J. M. & Richmond, G. L. *Chem. Phys. Lett.* **142**, 323-328 (1987).
48. Mingos, J. & Furtak, T. E. *Phys. Rev. B* **37**, 1028-1030 (1988).
49. Rasing, Th., Kim, M. W., Shen, Y. R. & Grubb, S. *Phys. Rev. Lett.* **55**, 2903-2906 (1985).
50. Berkovic, G., Rasing, Th. & Shen, Y. R. *J. Chem. Phys.* **85**, 7374-7376 (1986).
51. Bhattacharyya, K., Sitzmann, E. V. & Eisenthal, K. B. *J. Chem. Phys.* **87**, 1442-1443 (1987).
52. Grubb, S. G., Kim, M. W., Rasing, Th. & Shen, Y. R. *Langmuir* **4**, 452-454 (1988).
53. Freund, I. & Oestrich, M. *Opt. Lett.* **11**, 94-96 (1986).
54. Heinz, T. F., Chen, C. K., Ricard, D. & Shen, Y. R. *Phys. Rev. Lett.* **48**, 478-481 (1983).
55. Zhu, X. Q., Suter, H. & Shen, Y. R. *Phys. Rev. B* **35**, 3047-3050 (1987).
56. Hunt, J. H., Guyot-Sionnest, P. & Shen, Y. R. *J. Chem. Phys. Lett.* **133**, 189-192 (1987).
57. Guyot-Sionnest, P., Hunt, J. H. & Shen, Y. R. *Phys. Rev. Lett.* **59**, 1597-1600 (1987).
58. Hunt, J. H., Guyot-Sionnest, P. & Shen, Y. R. in *Laser Spectroscopy VIII* (eds Persson, W. & Svanberg, S.) 253-266 (Springer, Berlin, 1987).
59. Guyot-Sionnest, P., Superfine, R. & Hunt, J. H. *J. Chem. Phys.* **144**, 1-5 (1988).
60. Harris, A. L., Chidley, C. E. O., Levinson, N. J. & Loiacono, O. N. *Chem. Phys. Lett.* **141**, 350-356 (1987).
61. Superfine, R., Guyot-Sionnest, P., Hunt, J. H., Kao, C. T. & Shen, Y. R. *Surf. Sci.* **200**, L445-L450 (1988).

## ARTICLES

# Designing CD4 immunoadhesins for AIDS therapy

Daniel J. Capon, Steven M. Chamow\*, Joyce Mordenti†, Scot A. Marsters, Timothy Gregory\*, Hiroaki Mitsuya\*, Randal A. Byrn†, Catherine Lucas†, Florian M. Wurm†, Jerome E. Groopman†, Samuel Broder† & Douglas H. Smith

Departments of Molecular Biology, \* Recovery Process Research and Development, † Pharmacological Sciences, ‡ Medicinal and Analytical Chemistry, § Cell Culture Research and Development, Genentech, Inc., 460 Point San Bruno Boulevard, South San Francisco, California, 94080, USA

† The Clinical Oncology Program, National Cancer Institute, National Institutes of Health, Bethesda, Maryland, 20892, USA  
§ Division of Hematology-Oncology, Harvard Medical School, New England Deaconess Hospital, Boston, Massachusetts, 02215, USA

**A newly-constructed antibody-like molecule containing the gp120-binding domain of the receptor for human immunodeficiency virus blocks HIV-1 infection of T cells and monocytes. Its long plasma half-life, other antibody-like properties, and potential to block all HIV isolates, make it a good candidate for therapeutic use.**

DESPITE the exquisite ability of the immune system to distinguish between self and non-self, and to put forth an impressive diversity in its antigen-recognizing repertoire, it can still be outflanked by a rapidly changing pathogen. Human immunodeficiency virus type 1 (HIV-1) is an example of such a pathogen, and, as a result, its consequences are devastating. Every individual infected with the virus is expected to develop a serious or life-threatening illness<sup>1</sup>; no protective state has been shown to be generated in natural infections. It has not yet been possible to generate a protective response by immunizing chimpanzees with gp120, the HIV-1 envelope glycoprotein<sup>2,3</sup>, or to confer passive immunity to chimpanzees using human IgG<sup>4</sup>. Even neutralizing antibodies made in experimental animals can block the infectivity of only a few HIV-1 isolates<sup>5,6</sup>. Thus, the prospects for eliciting protective immunity against HIV-1, or for using antibodies as therapeutic agents to control HIV-1 disease are bleak. Anti-retroviral chemotherapy using dideoxynucleosides such as AZT does help some patients, but the toxicity is such that new strategies are needed<sup>7</sup>.

We have therefore attempted to block HIV-1 infectivity with soluble derivatives of CD4, the receptor for HIV-1, with the rationale that the CD4-binding domain of gp120 is the only part of gp120 that the virus cannot afford to change<sup>8</sup>. CD4 is a cell-surface glycoprotein found mostly on a subset of mature peripheral T cells that recognize antigens presented by class II MHC molecules<sup>9,10</sup>. Antibodies to CD4 block HIV-1 infection of T cells<sup>11,12</sup> and human cells not susceptible to HIV-1 infection become so after transfection with a CD4 cDNA<sup>12</sup>. Gp120 binds CD4 with high affinity ( $K_D \sim 10^{-10}$  M), suggesting that it is this interaction which is crucial to the entry of virus into cells<sup>13</sup>. Indeed, we and others<sup>14-16</sup> have shown that soluble rCD4, lacking the transmembrane and cytoplasmic sequences of CD4, can block HIV-1 infectivity, syncytium formation, and cell killing by gp120 (ref. 19). rCD4 blocks the infectivity of diverse HIV-1 isolates (R.B., J.G., H.M. and S.B., unpublished results),

and in theory should block all. At best, however, soluble rCD4 offers only a passive defence against the virus.

Active immunity requires a molecule such as an antibody, which can specifically recognize a foreign antigen or pathogen and mobilize a defence mechanism. Antibodies comprise two functionally independent parts, a rather variable domain (Fab), which binds antigen, and an essentially constant domain (Fc), providing the link to effector functions such as complement or phagocytic cells. It is almost certainly the lack of an antigen-binding domain which can neutralize all varieties of virus that hampers the development of humoral immunity to HIV-1. We reasoned that the characteristics of CD4 would make it ideal as the binding site of an antibody against HIV-1. Such an antibody would bind and block all HIV-1 isolates, and no mutation the virus could make, without losing its capacity to infect CD4<sup>+</sup> cells specifically, would evade it. We therefore set out to construct such an antibody by fusing CD4 sequences to antibody domains.

We had two major aims for our hybrid molecules: first, as pharmacokinetic studies in several species predict that the half-life of soluble CD4 will be short in humans (30-120 min; J.M., unpublished results) we wished to construct a molecule with a longer half-life; second, we wanted to incorporate functions such as Fc receptor binding, protein A binding, complement fixation and placental transfer, all of which reside in the Fc portion of IgG. The Fc portion of immunoglobulin has a long plasma half-life, like the whole molecule, whereas that of Fab is short, and we therefore expected to be able to fuse our short-lived CD4 molecule to Fc and generate a longer-lived CD4 analogue. Because CD4 is itself part of the immunoglobulin gene superfamily, we expected that it would probably fold in a way that is compatible with the folding of Fc. We have therefore produced a number of CD4-immunoglobulin hybrid molecules, using both the light and the heavy chains of immunoglobulin, and investigated their properties. We have named one

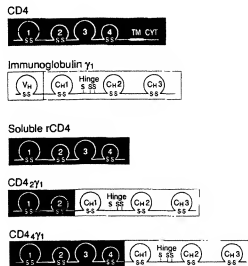


**Fig. 1** Structure of cell surface CD4, human IgG1 ( $\gamma 1$ ), soluble rCD4, and CD4 immunoadhesins (2 $\gamma 1$  and 4 $\gamma 1$ ). The immunoglobulin-like domains of CD4 are numbered 1 to 4; TM and CYT refer to the transmembrane and cytoplasmic domains. Soluble rCD4 is truncated after proline 368 of the mature CD4 polypeptide. This results in a secreted, soluble polypeptide with an affinity for gp120 similar to that of cell surface CD4 (ref. 7). The vertical division within IgG1 indicates the junction of the variable (VH) and constant (CH1, hinge, CH2, and CH3) regions. Disulphide bonds formed within IgG1 domains and the immunoglobulin-like domains of CD4 are indicated by (S-S). The positions of cysteine residues that form intermolecular disulphide bridges connecting the IgG1 heavy-chain hinge to light and heavy chains are indicated by (S). CD4-derived and IgG1-derived domains of 2 $\gamma 1$  and 4 $\gamma 1$  are indicated by shaded and unshaded regions, respectively. The 2 $\gamma 1$  and 4 $\gamma 1$  immunoadhesins consist of residues 1 to 180 and residues 1 to 366 of the mature CD4 polypeptide, respectively, fused to the first residue (serine 114) of the human IgG1 heavy-chain constant region.

**Methods.** For the expression of CD4 immunoadhesins, the sequences of CD4 and human IgG1 were fused by oligonucleotide-directed deletion mutagenesis after their insertion into a mammalian expression vector used for soluble rCD4 expression<sup>7</sup>. A human IgG1 heavy-chain cDNA, obtained from a human spleen cDNA library using probes based on the published sequence<sup>47</sup>, was inserted at a unique *Xba*I site found immediately 3' of the CD4 coding region in the same reading orientation as CD4. Synthetic 48-mer oligodeoxynucleotides, complementary to the 24 nucleotides at the borders of the desired CD4 and IgG1 fusion sites, were used as primers in the mutagenesis reactions using the plasmid described above as the template<sup>48</sup>.

particularly interesting class of these CD4-immunoglobulin hybrids 'immunoadhesins', because they contain part of an adhesive molecule<sup>20</sup> linked to the immunoglobulin Fc effector domain.

### Synthesis of CD4 immunoadhesins

CD4 is an integral membrane protein with an extracellular region comprising four domains with homology to immunoglobulin variable domains<sup>1,22</sup> (Fig. 1). Soluble CD4 derivatives consisting of this extracellular region bind gp120 with the same affinity as cell-surface CD4 (ref. 7). CD4 variants containing only domains 1 and 2 also bind gp120<sup>17,18</sup>, but the affinity of this interaction is not known. We constructed a series of hybrid molecules consisting of the first two or all four immunoglobulin-like domains of CD4 fused to the constant region of antibody heavy and light chains (Fig. 1).

We investigated the synthesis and secretion of these hybrids using transient expression in a human embryonic kidney-derived cell line. As shown in Fig. 2, immunoglobulin light and heavy

chains are efficiently expressed in these cells, and light chain is efficiently secreted, but heavy chain is not unless a light chain is coexpressed. Thus the rules governing immunoglobulin chain secretion in these cells are the same as those for plasma or other lymphoid cells<sup>23</sup>. We first constructed hybrids that fused CD4 with the constant regions of murine  $\kappa$ - or  $\gamma 1$ -chains. These hybrids contained either the first two or all four immunoglobulin-like domains of CD4, linked at a position chosen to mimic the spacing between disulphide-linked cysteines seen in immunoglobulins (Fig. 1). As expected, the CD4- $\kappa$  hybrids were secreted well, whereas hybrids between CD4 and mouse  $\gamma 1$ -chain were expressed but not secreted unless a  $\kappa$ -chain or a CD4- $\kappa$  hybrid was present.

A different and unexpected picture emerged when analogous CD4-heavy-chain hybrids were constructed using the constant region of human IgG1 heavy chain instead of mouse heavy chain. Such hybrids, containing either the first two or all four immunoglobulin-like domains of CD4 (named 2 $\gamma 1$  and 4 $\gamma 1$  respectively), were secreted in the absence of wild-type or hybrid light chains (Fig. 2a). Both 2 $\gamma 1$  and 4 $\gamma 1$  could be directly immunoprecipitated using *Staphylococcus aureus* protein A, which binds the Fc portion of IgG1, indicating that the protein A-binding sites of these constructs are fully functional. Indeed, both molecules can be purified to near homogeneity on protein A columns (Fig. 2b).

### Structure of CD4 immunoadhesins

We examined the subunit structure of these immunoadhesin molecules using SDS-polyacrylamide gels (Fig. 2b). Without any reducing agent, the apparent relative molecular mass ( $M_r$ ) of each construct doubled, demonstrating that both immunoadhesins are disulphide-linked dimers. The hinge region of each immunoadhesin contains three cysteine residues, one normally involved in disulphide bonding to light chain, the other two in the intermolecular disulphide bonds between the two heavy chains in IgG. As the molecules are dimers at least one, and perhaps all three, of these cysteine residues are involved in intermolecular disulphide bonds. We examined the capacity of 2 $\gamma 1$  and 4 $\gamma 1$  to form disulphide links with light chains. When an immunoadhesin construct was cotransfected with a light chain, the light chain produced could be precipitated by protein A. Mutagenic substitution of the first hinge-region cysteine with alanine abolished light-chain bonding, but did not affect dimerization (data not shown), indicating that this cysteine bonds the light chain in these hybrids, as in normal IgG. Thus the disulphide bond structure of these immunoadhesins seems to be analogous to that of immunoglobulins.

### gp120 binding

To determine whether our immunoadhesins retain the ability to bind gp120 with high affinity, and whether the first two immunoglobulin-like domains are sufficient, we carried out saturation binding analyses with radiolabelled gp120. Binding is saturable, showing a simple mass action curve (Fig. 3a). The dissociation constant ( $K_d$ ) for the interaction of each immunoadhesin with gp120, calculated by Scatchard analysis (Fig. 3a, inset), was indistinguishable from that of soluble rCD4 ( $\sim 10^{-9}$  M) (Table 1). Thus, the N-terminal 170 amino acids of CD4 are sufficient for high-affinity binding. As these immunoadhesins are homodimeric, they should each have two gp120-binding sites. We examined this possibility by coating plastic microtitre wells with gp120, then adding soluble CD4 or immunoadhesins. Both immunoadhesins could bind added labelled gp120, whereas soluble rCD4, with only one gp120 binding site, could not (J. Porter and S. C., unpublished results). To confirm the bivalent nature of 2 $\gamma 1$  and 4 $\gamma 1$ , we examined their ability to agglutinate sheep red blood cells coated with gp120. Again, both CD4 immunoadhesins, but not soluble rCD4, agglutinated the cells, showing that binding to gp120 molecules on different cells is not sterically hindered.

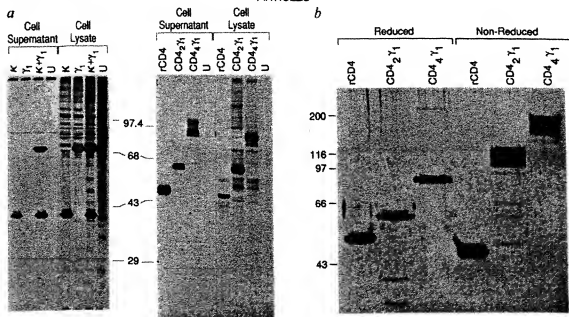


**Fig. 2** Expression, secretion and subunit structure of CD4 immunoadhesins and soluble rCD4. **a**, Expression and secretion of mouse immunoglobulins, soluble rCD4 and CD4 immunoadhesins expressed in mammalian cells. Cells were transfected with vectors directing the expression of murine  $\kappa$ -light chain (lanes  $\kappa$ ) or  $\gamma$ 1-heavy chain (lanes  $\gamma$ 1) individually or together (lanes  $\kappa + \gamma$ 1), vectors encoding soluble rCD4 (lanes rCD4), and the CD4 immunoadhesins 2y1 (lanes CD4<sub>2</sub> $\gamma$ 1) or 4y1 (lanes CD4<sub>4</sub> $\gamma$ 1). After metabolic labelling with [<sup>35</sup>S]methionine, cell supernatants and cell lysates were analysed by immunoprecipitation. Lanes U, untransfected cells. **b**, Subunit structure of secreted CD4 immunoadhesins and soluble rCD4. Soluble rCD4, 2y1 and 4y1 were purified from culture supernatants of transfected cells and analysed by electrophoresis on a 7.5% SDS-polyacrylamide gel. Samples were prepared in buffer with 10 mM dithiothreitol (DTT) (reducing conditions) or without DTT (non-reducing conditions). The positions of relative molecular mass standards are indicated (in thousands). Both immunoadhesins behaved as disulphide-linked dimers; in contrast, soluble rCD4 which is monomeric, displayed only a minor change in mobility upon reduction of its intra-molecular disulphide bonds.

**Methods.** **a**, Cells were transfected by a modification of the calcium phosphate procedure, labelled with [<sup>35</sup>S]methionine, and cell lysates prepared as described<sup>24</sup>. Immunoprecipitation analysis was carried out as previously described<sup>24</sup>, with the exception that no preadsorption with Pansorbin (Calbiochem) was done, and the precipitating antibodies used were 2  $\mu$ l of rabbit anti-mouse IgG serum (Cappel) for mouse IgG heavy and light chains, 0.25  $\mu$ g of OKT4A (Ortho) for soluble rCD4, and no added antibody (Pansorbin only) for the CD4 immunoadhesins. Immunoprecipitated proteins were resolved on 10% SDS-PAGE gels, and visualized by autoradiography. **b**, CD4 immunoadhesins were purified from transfected cell supernatants by protein A affinity chromatography followed by ammonium sulphate precipitation. Purified proteins were subjected to SDS-PAGE under both reducing and non-reducing conditions and visualized by silver staining.

### *In vivo* plasma half-life

We examined whether the immunoadhesins share the long *in vivo* half-life of antibodies. Studies of rCD4 in rabbits provide clearance data that extrapolate well to other species, including humans (J.M., unpublished results). The change in plasma concentration with time for each of the three CD4 analogues in rabbits is shown in Fig. 4. Analysis of these data reveals that soluble rCD4 has a terminal half-life in rabbits of ~15 min, whereas 4y1 and 2y1 have terminal half-lives of ~7 and 48 h, respectively (Table 1). Thus the half-life of 2y1 in rabbits is nearly 200 times longer than that of rCD4 and comparable to that of human IgG in rabbits (4.7 days)<sup>24</sup>. The half-life of 2y1 in humans is expected to be longer than that in rabbits, because of the decreased proportional blood flow to eliminating organs

as species increase in size<sup>25</sup>, and should be comparable with that of human IgG1 (21 days).

Our results confirm our initial hypothesis that, as in the case of immunoglobulin itself, one can increase the stability of a rapidly cleared molecule (Fab or rCD4) by fusing it to a long-lived molecule, Fc. The swift clearance of rCD4 is probably largely due to its size,  $M_r$  55,000, which means it is just small enough to be cleared efficiently by renal filtration. One component in the increased half-lives of these molecules is therefore probably their larger size; but this cannot be the whole story as 4y1, although larger than 2y1, has a shorter half-life. Both 4y1 and rCD4, but not 2y1, contain two CD4-derived Asn-linked carbohydrate sites which are glycosylated in rCD4 (R. Harris and M. Spellman, unpublished results); these sugar moieties

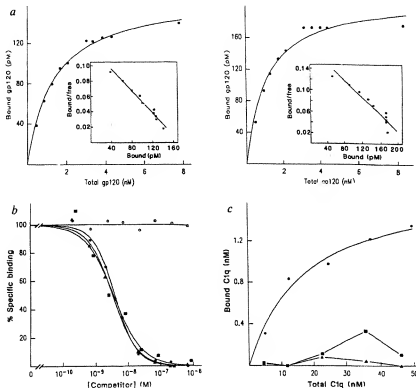
**Table 1** Properties of CD4 immunoadhesins and soluble rCD4

	Calculated $M_r$	Subunit structure	gp120 binding (nM)*	Blocks infectivity T cells M0	Plasma half-life in rabbits (hours)†	Fc binding (nM)*	Complement binding	Protein A binding
rCD4	41,000	monomer	2.3 $\pm$ 0.4	Yes	Yes	0.25 $\pm$ 0.01	No	No
4y1	154,000	dimer	1.2 $\pm$ 0.1	Yes	Yes	6.7 $\pm$ 1.1	No	Yes
2y1	112,000	dimer	1.4 $\pm$ 0.1	Yes	Yes	48.0 $\pm$ 8.6	No	Yes
IgG1	146,000	tetramer (H <sub>2</sub> L <sub>2</sub> )	—	—	—	113†	Yes	Yes

\* Standard error of the mean was determined using the Inplot and Scatplot programs (see Fig. 3 legend). † Standard deviation indicated in hours.

† Determined in ref. 24 (IgG1 has a half-life of 21 days in humans).

**Fig. 3** Binding properties of CD4 immuno-adhesins. **a**, Cpl120 saturation binding analysis of CD4 immuno-adhesins. Immuno-adhesin proteins 4y1 (left) or 2y1 (right) in transfected cell supernatants were incubated with increasing concentrations of purified soluble rgp120 (ref. 50) radioiodinated with lactoperoxidase. The lines drawn for the binding curves and for the Scatchard plots of the data (shown in the insets) represent the best fit as determined by unweighted least-squares linear regression analysis. Dissociation constants calculated from these results and from binding studies of gp120 to soluble rCD4 performed in parallel are given in Table 1. **b**, Binding of CD4 immuno-adhesins to Fc receptors on U937 cells. Competition binding analysis was carried out by mixing  $0.1 \mu\text{g ml}^{-1}$  of  $^{125}\text{I}$ -labelled human IgG1 (Calbiochem) with increasing concentrations of purified human IgG1 (solid circle), 2y1 (solid square), 4y1 (solid triangle), or soluble rCD4 (open circle) proteins. Curves drawn represent the best fit as determined by unweighted least-squares nonlinear (IgG1, 2y1 and 4y1) or linear (rCD4) regression analysis. Dissociation constants calculated from these results are shown in Table 1. **c**, C1q saturation binding analysis of CD4 immuno-adhesins. Purified anti-gp120 IgG2a mouse monoclonal antibody (solid circle), 2y1 (solid square), or 4y1 (solid triangle) proteins were aggregated by binding to gp120-coupled Sepharose, and incubated with increasing concentrations of purified human C1q (Calbiochem) radioiodinated with lactoperoxidase. The curve drawn for the anti-gp120 monoclonal antibody (mAb) represents the best fit as determined by least-squares nonlinear regression analysis; the dissociation constant for C1q binding to this gp120-aggregated anti-gp120 mAb was  $\sim 1.8 \times 10^{-8} \text{ M}$ . **Methods.** **a**, Cpl120 saturation binding analysis was carried out as described<sup>27</sup> except that gp120-CD4 immuno-adhesin complexes were collected directly onto Panisorbin: binding was comparable to that observed when complexes were collected with OKT4A as for soluble rCD4. Specifically bound  $^{125}\text{I}$ -labelled gp120 was determined from the difference in binding in the presence or absence of a 1,000-fold excess of unlabelled rgp120 and is plotted against the total  $^{125}\text{I}$ -labelled gp120 concentration. **b**, FcR binding analysis was done essentially as described<sup>27</sup> except that after centrifugation free IgG1 was removed by aspiration of the aqueous and oil layers. Mixtures of  $^{125}\text{I}$ -labelled human IgG1 and IgG1, CD4 immuno-adhesins or soluble rCD4 were incubated with U937 cells ( $2 \times 10^6$  cells per tube) for 60 min at  $4^\circ\text{C}$ . Specific binding was calculated by subtracting residual nonspecific binding (<25% of specific binding) which could not be competed out by a 1,000-fold excess of unlabelled human IgG1. **c**, C1q binding analysis was done essentially as described<sup>25</sup>, except that gp120 coupled to CNBr-activated Sepharose 6B (Pharmacia) was used as the solid support to aggregate CD4 immuno-adhesins or the anti-gp120 mouse mAb. Proteins were adsorbed to gp120 coupled-beads, incubated with varying concentrations of  $^{125}\text{I}$ -labelled C1q, and bound and free C1q were then separated by centrifugation through 20% sucrose. Specific binding was determined from the difference in binding in the presence or absence of added antibody or immuno-adhesin. All data analysis was carried out using the Inplot and Scatplot programs (R. Vandlen, Genentech). Scatplot was modified from the Ligand program (P. Muncy, NIH).



may facilitate clearance by receptors in the liver. The charge of the molecule may also be important, as the CD4 portion of 4y1 contributes a net excess of eleven positively charged amino acids on 4y1, but only three on 2y1. This may increase uptake of rCD4 and 4y1 onto anionic surfaces, accelerating their clearance from the circulation.

### Fc receptor and complement binding

Two major mechanisms for the elimination of pathogens are mediated by the Fc portion of specific antibodies. Fc activates the classical pathway of complement, ultimately resulting in lysis of the pathogen, whereas binding to cell Fc receptors can lead to ingestion of the pathogen by phagocytes or lysis by killer cells. The binding sites for Fc cell receptors and for the initiating factor of the classical complement pathway, C1q, are found in the constant region of heavy chain<sup>26</sup> (the CH2 domain for C1q<sup>27</sup> and the region linking the hinge to CH2 for Fc cell receptors<sup>28</sup>). We aimed to incorporate both of these functions into the immuno-adhesins. We chose the IgG1 subtype to supply the Fc domain because IgG1 is the best compromise between Fc binding, C1q binding, and long half-life. We show below that the immuno-adhesins bind FcR well, but do not bind C1q.

Three types of Fc cell receptors are known to be expressed on a variety of leukocytes. Of these FcR1, principally expressed

on mononuclear phagocytes, is the only one which binds monomeric human IgG1 with high affinity<sup>26</sup>. We used competition binding analysis with FcR1 receptors on the U937 monocyte/macrophage cell line to characterize the Fc receptor binding of 2y1 and 4y1. Direct saturation binding analysis with human IgG1 gave a  $K_d$  of  $\sim 3 \times 10^{-8} \text{ M}$ . In competition binding analyses, the two CD4 immuno-adhesins, but not rCD4, bound to Fc receptors on U937 cells to the same extent and with an affinity indistinguishable from human IgG1 (Fig. 3b, Table 1).

We examined the ability of the immuno-adhesins to bind to the first component of the classical pathway of complement, C1q, by saturation binding analysis. Because binding of C1q increases with the aggregation state of the antibody, with an affinity of  $\sim 10^{-4}$  for monomers and  $\sim 10^{-8}$  for tetramers of IgG<sup>26</sup>, we first aggregated the immuno-adhesin using gp120 linked to Sepharose. As a positive control, we measured C1q binding to an anti-gp120 mouse IgG2a monoclonal antibody, (which like human IgG1 binds C1q with high affinity<sup>29</sup>) aggregated by the same gp120-Sepharose. The affinity of the mouse antibody for C1q determined by Scatchard analysis was  $1.8 \times 10^{-8} \text{ M}$  (Fig. 3c), comparable to that observed for other mouse IgG2a and for human IgG1 antibodies. In contrast, neither immuno-adhesin bound C1q to any detectable extent (Fig. 3c),

**Fig. 4** Pharmacokinetics of CD4 immunoadhesins and soluble rCD4. Shown are the mean plasma concentrations ( $\text{ng ml}^{-1}$ ) for 2y1 (triangles), 4y1 (squares), and rCD4 (circles) following a single intravenous administration in rabbits. *a*, Time course of plasma clearance over the first 120 minutes; *b*, time course over 8 days after injection of the CD4 analogues.

**Methods.** Ten female New Zealand white rabbits (Rabbitek, Modesto, California) were injected intravenously (via an ear vein catheter) with a single bolus dose ( $40 \mu\text{g kg}^{-1}$  in a volume of 1 ml) of either rCD4 ( $n=3$ ), 4y1 ( $n=4$ ), or 2y1 ( $n=3$ ). Blood samples were obtained from an arterial catheter in the opposite ear; after 24 hours, blood samples were obtained by venipuncture. Plasma concentrations of each protein were determined by an enzyme-linked immunosorbent assay. This capture assay used two antibodies, including an anti-CD4 monoclonal directed against the gp120-binding site (and capable of blocking gp120 binding), and thus provided a sensitive assay for CD4-containing molecules that are still capable of binding gp120. Exponential equations were fitted to the data of individual rabbits using a nonlinear least squares regression program NONLIN84<sup>®</sup> (Statistical Consultants, Lexington, Kentucky). The concentration ( $C$ ,  $\text{ng ml}^{-1}$ ) versus time ( $t$ ) data for rCD4 were best described by a biexponential equation  $C = 541 e^{-2.1t} + 620 e^{-0.47t}$ , where time is in minutes; the average terminal half-life was 14.7 min, and the average clearance was  $3 \text{ ml min}^{-1} \text{ kg}^{-1}$ . The 4y1 data were best described by a triexponential equation,  $C = 546 e^{-2.11t} + 193 e^{-20.31t} + 46.8 e^{-2.54t}$ , where time is in hours. The average terminal half-life was 6.7 hours, and the average clearance was  $0.91 \text{ ml min}^{-1} \text{ kg}^{-1}$ . The 2y1 data were best described by a triexponential equation,  $C = 153 e^{-53.2t} + 342 e^{-2.19t} + 183 e^{-0.35t}$ , where time is in hours. The average terminal half-life was 48 hours, and the average clearance was  $0.039 \text{ ml min}^{-1} \text{ kg}^{-1}$ .

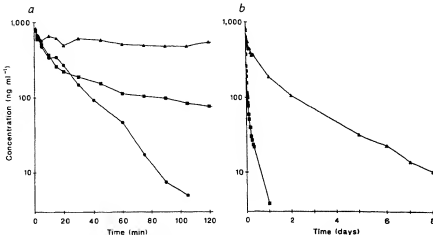
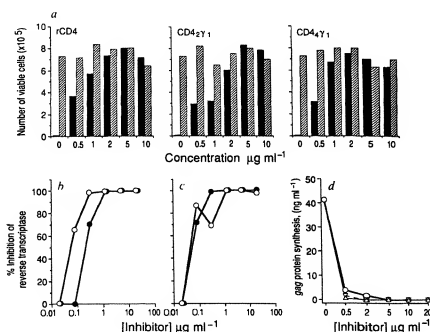


**Fig. 5** Inhibition of HIV-1 infectivity by CD4 immunoadhesins and soluble rCD4. *a*, Inhibition of the cytopathic effects on ATH8 cells by HIV-1 was examined as described<sup>32</sup> with the HTLV-IIIB isolate<sup>31</sup>. The number of viable cells at day 10 after infection is shown for varying concentrations of each molecule in the presence (solid bars) or absence (shaded bars) of added virus. The absence of an effect of each CD4 analogue on cell number in the absence of virus indicates that none of these molecules inhibited cell growth. *b*, Inhibition of infection of H9 cells by HIV-1 was carried out as described<sup>7</sup> with the HTLV-IIIB isolate. Reverse transcriptase activity was determined 7 days after infection and is given as the percentage of the level seen in the absence of inhibitor. Solid and open circles represent 2y1 and 4y1, respectively. *c*, Inhibition of infection of U937 cells by HIV-1 (HTLV-IIIB isolate) was carried out as described above for H9 cells. *d*, Inhibition of infection of fresh human monocytes by the monocytotropic HIV-1 isolate Ba-L (ref. 35). HIV-1 replication was determined by measuring the level of p24 gag antigen synthesis 10 days after infection using a commercial assay kit (Dupont). Circles, inverted triangles and triangles represent inhibition of p24 synthesis by soluble rCD4, 2y1 and 4y1, respectively.



although both did bind the gp120-Sepharose matrix in amounts comparable to the control antibody.

Thus, our immunoadhesins bind well to Fc receptors. It is perhaps surprising that they do not bind C1q. As far as is known, all the critical contact residues for C1q binding reside in the CH2 domain of the heavy chain<sup>26</sup> and are conserved among all the human IgG isotypes. However, these have varying abilities to mediate complement fixation. Thus steric hindrance or other aspects of protein conformation (for example, the segmental flexibility of antibodies<sup>30</sup>) may be important.

### Infectivity studies

Two systems were used to study the *in vitro* ability of CD4 immunoadhesins to block infection of CD4-bearing T cells by

the HIV-1 T-lymphotrophic isolate HTLV-IIIB (ref. 31). Infection with HIV-1 exerts a profound cytopathic effect on the human T-cell clone ATH8, with more than 98% of the cells being killed by day 10 after infection<sup>32</sup> (Fig. 5a). Both CD4 immunoadhesins blocked cell killing with the same potency as soluble rCD4, without inhibiting cell proliferation; each CD4 analogue completely abolished cell killing at a concentration of  $\sim 0.05 \mu\text{M}$  (Fig. 5a). Complete protection was also observed at comparable concentrations with a different HIV-1 isolate, HTLV-III RF, which is not neutralized by sera from animals immunized with rgp120 from the IIIB isolate<sup>5</sup>. We also examined the production of HIV-1 reverse transcriptase activity after infection of the H9 human T-cell line. Again, both immunoadhesins completely blocked virus production by day 7 (Fig. 5b), at

concentrations comparable to rCD4 (data not shown); moreover the potency of each CD4 analogue was markedly higher (~fivefold) than that observed in the ATH8 assay.

### Monocyte infection

Because it has been suggested that antibodies present in sera from HIV-1 infected individuals may enhance the infectivity of HIV-1 in Fc receptor (FcR)-bearing cells such as primary blood monocytes<sup>33</sup>, and monocyte cell lines<sup>34</sup>, we examined the effect of rCD4 and CD4 immunoadhesins on HIV-1 infection of FcR-expressing cells of monocyte/macrophage origin. Both CD4 immunoadhesins completely blocked HIV-1 IIIB virus production in U937 cells at similar concentrations to those found to be effective on H9 cells (Fig. 5c), with a potency comparable to that of soluble rCD4 (data not shown). In another system, the replication of a monocytotropic HIV-1 isolate, Ba-L<sup>35</sup>, in fresh monocytes was monitored by the production of p24 antigen. Soluble rCD4 completely blocked infection, indicating that infection of monocytes by the Ba-L isolate does involve CD4. Both CD4 immunoadhesins also completely blocked p24 production, at concentrations equal to or lower than rCD4 (Fig. 5d). Thus the CD4 immunoadhesins are at least comparable to soluble rCD4 in their ability to prevent infection of monocyte/macrophages by HIV; no evidence was found for enhancement of infection by immunoadhesins (or by soluble rCD4) in cells which express high affinity Fc receptors.

### Implications for treatment of HIV-1 disease

Because the hallmark of HIV-1 disease is the specific destruction of CD4<sup>+</sup> T cells, and the progression of infected individuals to AIDS closely parallels their decline in CD4<sup>+</sup> T-cell number<sup>36</sup>, it is reasonable to believe that the interaction of gp120 with CD4, either by direct HIV-1 infection of CD4<sup>+</sup> cells or otherwise, underlies the killing of CD4<sup>+</sup> cells. Therefore, if this interaction can be stopped it may be possible to prevent disease progression. But despite the logic of this hypothesis, the observation that only a very few lymphocytes are actively infected with HIV-1 *in vivo*<sup>37</sup> has posed a problem to those attempting to explain the causative role of HIV-1 in the aetiology of AIDS<sup>38</sup>. Two observations may explain the 'catalytic' ability of HIV-1 to deplete CD4<sup>+</sup> lymphocytes: first, a single infected cell can fuse many uninfected CD4<sup>+</sup> cells to itself, creating an inviable mass<sup>39,40</sup>; and second, gp120 is shed from the surface of HIV-1-infected cells and virions<sup>41</sup>, as its link to gp41, its anchor protein partner, is probably non-covalent. This shed gp120 binds to surface CD4 on uninfected cells with high affinity, and can result in their functional alteration<sup>42,43</sup> or death by one of two pathways shown to operate *in vitro*. Bystander cells coated with gp120 bound to their CD4 surface molecules become targets for anti-gp120 antibodies produced by HIV-1 infected individuals and can be killed via antibody-dependent cell-mediated cytotoxicity<sup>44</sup>. Also, MHC class II-positive CD4<sup>+</sup> T cells can internalize gp120 bound tightly to CD4 on their surface, process it, and present peptides derived from it on their class II molecules, thus becoming sensitive, even at low gp120 concentrations, to lysis by gp120-specific cytotoxic T cells<sup>45,46</sup>. The important common factor in all these proposed mechanisms of cell destruction is that gp120 must bind specifically to cell-surface CD4. If these mechanisms are important *in vivo*, this would imply that soluble rCD4 could intervene.

But to affect the disease noticeably, one would expect to need to maintain a high concentration of rCD4, which is hampered by its rapid clearance. Our approach to this problem was to fuse the CD4-binding domain of CD4 to a molecule well designed to avoid the clearance mechanisms of the body. Indeed, the Fc domain and CD4 sequences are structurally compatible, as the hybrid molecules have important properties of both parents. Thus, they bind gp120 and block infection of T cells by T-lymphotropic HIV-1 and of monocytes by monocytotropic HIV-1. They are also comparable to antibodies in

their long plasma half-life and their ability to bind Fc receptors and protein A. This combination of properties allows both a better passive defence, due to the higher plasma concentrations attainable even with infrequent injection, and the possibility of actively attacking HIV-1 and infected cells. A high steady-state level also makes it more likely that effective concentrations will be attained in lymph and lymphatic organs, where HIV may be most active.

The high-affinity binding of the immunoadhesins to Fc receptors implies that mechanisms of pathogen elimination, such as phagocytic engulfment and killing by antibody-dependent cell-mediated cytotoxicity, may be recruited by these immunoadhesins to kill HIV-1 infected cells and virus. As it is possible that antibody-dependent cell-mediated cytotoxicity in an infected individual may be more a mechanism of pathology in HIV-1 infection than a protective response<sup>44</sup>, it is important to note a difference between CD4 immunoadhesins and the patients' own anti-gp120 antibodies: the immunoadhesin, in contrast to antibody, cannot recognize gp120 bound to an uninfected CD4<sup>+</sup> bystander cell, as gp120 has only a single binding site for CD4. Because placental transfer of antibody, unique to the IgG subclass, also proceeds through an FcR-dependent mechanism, CD4 immunoadhesins may also be transferred *in utero*. This may have implications for the prevention of perinatally transmitted HIV-1 infection.

Although it is not yet clear which of the functions of immunoglobulins will be advantageous when applied to HIV infection, we have taken the approach of trying to add all possible functions to our immunoadhesins. Once the structural requirements for the optimal molecule are established, functions can be tailored at will, as the parent antibody molecule is so well understood.

We thank Drs Paula Jardiue, Avi Ashkenazi and Stephen Sherwin for advice and helpful discussions, Dr Rebecca Ward for helpful discussions and critical reading of the manuscript, Steven Frie for performing CD4 enzyme-linked immunosorbent assays, Vivek Bajaj and Wally Tanaka for large scale cell culture, Drs R. Harris, M. Spellman and J. Porter for allowing us to cite unpublished data, Steve Williams for murine immunoglobulin cDNAs, Mark Vasser, Parkash Jhurani and Peter Ng for synthetic DNA, Dr Brian Fendly and Kim Rosenthal for anti-gp120 monoclonals, and Carol Morita and Kerrie Andow for preparation of the figures. R.B. and J.G. are supported by grants from the NIH and the US Defense Department.

Received 3 November; accepted 16 December 1988.

- Curran, J. *et al. Science* **229**, 610-616 (1985).
- Hu, S.-L. *et al. Nature* **328**, 721-723 (1987).
- Berman, P. *et al. Proc. natn. Acad. Sci. U.S.A.* **85**, 5200-5204 (1988).
- Prince, A. *et al. Proc. natn. Acad. Sci. U.S.A.* **85**, 6944-6948 (1988).
- Weiss, R. *et al. Nature* **324**, 572-575 (1986).
- Mitsuya, H. & Broder, S. *Nature* **325**, 773-778 (1987).
- Smith, O. *et al. Science* **238**, 1704-1707 (1987).
- Santelmo, C. & Weiss, R. *Cell* **52**, 631-633 (1988).
- Jaenzy, C. *Nature* **335**, 286-290 (1988).
- Ostergaard, E. *et al. Nature* **331**, 763-767 (1984).
- Kleinmann, D. *et al. Nature* **331**, 767-768 (1984).
- Maddon, P. *et al. Cell* **47**, 333-348 (1986).
- McDougal, J. *et al. Science* **231**, 382-385 (1986).
- Fisher, R. *et al. Nature* **331**, 76-78 (1988).
- Hussey, R. *et al. Nature* **331**, 78-81 (1988).
- Hussey, R. *et al. Nature* **331**, 82-84 (1988).
- Dern, K. *et al. Nature* **331**, 84-86 (1988).
- Truncker, A., Luke, W. & Karjalainen, K. *Nature* **331**, 84-86 (1988).
- Berger, E., Fucini, T. & Moss, B. *Proc. natn. Acad. Sci. U.S.A.* **85**, 2357-2361 (1988).
- Siliciano, R. *et al. Cell* **54**, 561-575 (1988).
- Doyle, C. & Strominger, J. *Nature* **330**, 256-259 (1987).
- Maddon, P. *et al. Cell* **47**, 93-104 (1985).
- Clark, S., Jefferys, W., Barclay, A., Cragg, J. & Williams, A. *Proc. natn. Acad. Sci. U.S.A.* **84**, 1649-1653 (1987).
- Dorai, H. & Moore, G. J. *Immun.* **139**, 4232-4241 (1987).
- Nakamura, R., Spiegelberg, H., Lee, S. & Wiegman, W. J. *Immun.* **100**, 376-383 (1983).
- Mordant, J. J. *Pharmacol. Sci.* **75**, 1028-1040 (1986).
- Burton, A. *Molec. Immun.* **23**, 161-206 (1985).
- Duncan, A. & Winter, G. *Nature* **332**, 738-740 (1988).
- Oncescu, L., Wood, J., Partridge, L., Burrows, C. & Winter, G. *Nature* **332**, 563-564 (1988).
- Leatherbarrow, R. & O'Keefe, R. *Molec. Immun.* **21**, 321-327 (1984).
- Feinstein, A., Richardson, N. & Taussig, M. J. *Immun. Today* **7**, 169-174 (1986).
- Gallo, R. C. *et al. Science* **224**, 500-505 (1984).
- Mitsuya, H. & Broder, S. *Proc. natn. Acad. Sci. U.S.A.* **83**, 1911-1915 (1986).

33. Homy, J., Tateno, M. & Levy, J. *Lancet* **i**, 1285-1286 (1988).
34. Takeda, A., Tuzson, C. & Ennis, F. *Science* **242**, 580-583 (1988).
35. Gantner, S. *et al. Science* **233**, 215-219 (1986).
36. Lang, H. & Faudi, A. *Rev. Immun.* **3**, 477-500 (1985).
37. Harper, M., Marselle, L., Gallo, R. & Wong-Staal, F. *Proc. natn. Acad. Sci. U.S.A.* **83**, 772-776 (1986).
38. Duenberg, P. *Science* **241**, 514 (1988).
39. Lifson, J., Reyes, G., McGrath, M., Stein, B. & Engelman, E. *Science* **232**, 1123-1127 (1986).
40. Soderstrom, J., Goh, W., Rosen, C., Campbell, K. & Haeftling, W. *Nature* **370**, 474-476 (1986).
41. Schneider, I., Kaaden, O., Copeland, T. D., Orosian, S. & Hunsman, G. *J. gen. Virol.* **67**, 2533-2539 (1986).
42. Lynette, G., Hartzman, R., Ledbetter, J. & June, C. *Science* **241**, 573-576 (1988).
43. Kornfeld, H., Cruikshank, W., Pyle, S., Berman, J. & Center, D. *Nature* **335**, 445-448 (1988).
44. Lyle, H., Matthews, T., Langdon, A., Bolognesi, D. & Weinhold, K. *Proc. natn. Acad. Sci. U.S.A.* **86**, 4001-4005 (1987).
45. Lanzavecchia, A., Roonbeck, E., Gregory, T., Berman, P. & Abrignani, S. *Nature* **334**, 530-532 (1988).
46. Seth, N., Naher, H. & Stroehmann, I. *Nature* **335**, 178-181 (1988).
47. Ellison, J. P., Berson, B. J. & Hood, L. E. *Nucleic Acids Res.* **10**, 4071-4079 (1982).
48. Zoller, M. & Smith, M. *Nucleic Acids Res.* **10**, 6487-6500 (1982).
49. Murnag, M., Smith, D. & Capon, D. *Cell* **48**, 691-701 (1987).
50. Lasky, L. *et al. Cell* **50**, 975-985 (1987).

## LETTERS TO NATURE

## A 110-ms pulsar, with negative period derivative, in the globular cluster M15

A. Wolszczan\*, S. R. Kulkarni†, J. Middleton‡, D. C. Backer§, A. S. Fruchter|| &amp; R. J. Dewey¶

\* Arecibo Observatory, Arecibo, Puerto Rico 00613

† Department of Astronomy, California Institute of Technology, Pasadena, California 91125, USA

‡ Computing and Communications Division, Los Alamos National Laboratory, New Mexico 87545, USA

§ Astronomy Department, University of California, Berkeley, California 94720, USA

|| Joseph Henry Laboratories and Physics Department, Princeton University, Princeton, New Jersey 08544, USA

¶ Center for Radiophysics and Space Research, Cornell University, Ithaca, New York, 14853, USA

We report the discovery of a 110-ms pulsar, PSR2127+11, in the globular cluster M15 (NGC7078)<sup>1</sup>. The results of nine months of timing measurements place the new pulsar about 2" from the centre of the cluster, and indicate that it is not a member of a close binary system. The measured negative value of the period derivative,  $\dot{P} \approx -2 \times 10^{-17} \text{ s s}^{-1}$ , is probably the result of the pulsar being bodily accelerated in our direction by the gravitational field of the collapsed core of M15. This apparently overwhelms a positive contribution to  $\dot{P}$  due to magnetic braking. Although PSR2127+11 has an unexpectedly long period, we argue that it belongs to the class of 'recycled' pulsars, which have been spun up by accretion in a binary system. The subsequent loss of the pulsar's companion is probably due to disruption of the system by close encounters with other stars<sup>2,3</sup>.

The discoveries of millisecond pulsars in globular clusters M28 (ref. 4) and M4 (ref. 5) led us to survey all clusters accessible to the 305-m Arecibo radio telescope ( $0^\circ \leq \delta \leq 38^\circ$ ). A dual-polarization, 40-MHz-bandwidth signal at 1415 MHz was passed through the Arecibo digital correlator, sampled with 128 lags every 506.6  $\mu\text{s}$ , and recorded on tape. The relatively high central radio frequency ensured an almost interference free signal and minimized the effects of interstellar dispersion and scattering, which can be significant for distant, low-galactic-latitude clusters. M15 was observed on 28 December 1987 for 90 minutes, which corresponds to  $\sim 11$  million samples.

The data were analysed at both the Cornell National Super-computer Facility (IBM 3090-600E) and the Los Alamos National Laboratory (Cray X-MP). Both analyses involved preliminary dispersion of the multichannel data at 128 or 64 trial dispersion measures, followed first by one-dimensional Fourier transformation of the dispersed time series and then by a search for harmonically related spikes in the resultant power spectra. The Cray X-MP analysis used the full, 11-million-sample data arrays to obtain maximum sensitivity with regard to isolated pulsars. The data analysed with the IBM supercom-

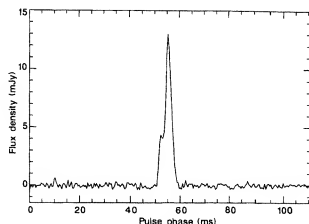


Fig. 1 The average pulse profile of PSR2127+11 at 1415 MHz. The effective resolution is  $\sim 800 \mu\text{s}$  and the integration time is 7 hours.

puter were divided into five 2-million-sample blocks, which were treated separately to maintain high sensitivity to binary pulsars with short orbital periods. The nominal  $6\sigma$  sensitivities of these two analysis schemes were 0.05 mJy and 0.1 mJy respectively, for the periods down to  $\sim 2.5$  ms.

The data analysis at Cornell revealed the presence of a 110-ms, high- $Q$  periodicity in the received signal with dispersion measure  $DM \approx 60 \text{ pc cm}^{-2}$ . This detection was subsequently confirmed at Los Alamos. Further observations made at Arecibo on 20 and 21 February 1988 confirmed the discovery of a 110-ms pulsar. The average pulse profile of PSR2127+11 observed at 1415 MHz is shown in Fig. 1. The pulsar parameters, derived from our twice-weekly timing observations over nine months, are summarized in Table 1. Errors quoted are the standard  $3\sigma$  errors of a model fit to the observed pulse arrival times.

Although the precise timing and Very Large Array (VLA) positions of PSR2127+11 will become known soon, the present positional accuracy is sufficient to conclude that the pulsar is located well within the  $6''$  core radius of the cluster,  $2.0''$  west and  $0.6''$  north of the centre<sup>6</sup>. The dispersion measure of PSR2127+11,  $DM = 67.25 \text{ pc cm}^{-2}$ , agrees well with that expected from a simple model of the galactic electron density distribution<sup>7</sup>, given the distance,  $D = 9.7 \text{ kpc}$ , and galactic coordinates,

Table 1 Measured parameters of the pulsar PSR2127+11

Pulsar period	$0.11066470954 \pm 0.0000000001 \text{ s}$
Period derivative	$(-20 \pm 1) \times 10^{-18} \text{ s s}^{-1}$
Epoch	JD 2447213.15
Dispersion measure	$67.25 \pm 0.05 \text{ pc cm}^{-2}$
Flux density (430 MHz)	$1.7 \pm 0.4 \text{ mJy}$
Flux density (1400 MHz)	$0.2 \pm 0.05 \text{ mJy}$
Right Ascension (B1950.0)	$21^{\text{h}}27^{\text{m}}33.22^{\text{s}} \pm 0.01$
Declination (B1950.0)	$11^{\circ}56'49.4'' \pm 0.3$
Distance	9.7 kpc

\* Present address: Jet Propulsion Laboratory, California Institute of Technology, Pasadena, California 91125, USA

# EXHIBIT Q



OVID

Full Text

[Results Display](#) | [Main Search Page](#) | [Ask the Amgen Library](#) | [Help](#) | [LOGOFF](#)

Arthritis and Rheumatism

© 1999, American College of Rheumatology Volume 42(9) SUPPLEMENT, September 1999, p S90

[About this Journal](#)[Browse Search Results](#)[Find Citing Articles](#) | [Save Article Text](#) | [Email Article Text](#) |[Print Preview](#)**COMPARATIVE ANALYSIS OF THE ABILITY OF ETANERCEPT AND INFLIXIMAB TO LYSE TNF-EXPRESSING CELLS IN A COMPLEMENT DEPENDENT FASHION.**

[Abstract Supplement; 1999 Annual Scientific Meeting:  
November 13 - 17, 1999; Boston, Massachusetts:  
ACR/ARHP Scientific Abstracts: Poster Sessions]

Barone, Dauphine; Krantz, Carol; Lambert, Dina; Maggiora,  
Kathy; Mohler, Kendall

Seattle, WA

Abstract 116

Published reports 2 have demonstrated that infliximab (REMICADE®), a mouse-human chimeric antibody to TNF, is able to kill some TNF-expressing cells *in vitro* in the presence of complement (C'). Those experiments utilized cells that were unable to shed TNF and thus expressed high levels of cell-surface TNF. We have examined the ability of etanercept (ENBREL®), a soluble fusion protein consisting of two human p75 TNF receptors linked to the Fc region of human IgG1, to kill TNF-expressing cells in the presence of C'. To directly assess the ability of etanercept to kill TNF-expressing cells, cDNAs containing the sequence for a mutated human TNF gene were obtained. The mutated genes encoded a sequence that greatly reduced the amount of TNF shed from the cell surface. These genes were transfected into CHO cells, and cell lines expressing high levels of cell surface TNF were generated following four sequential rounds of FACS staining and sorting with an anti-TNF monoclonal antibody. Etanercept and infliximab were equivalent in their ability to bind and neutralize the cell surface TNF as measured by FACS analysis and bioassay, respectively. As previously reported, infliximab was able to mediate complement-dependent killing of the TNF-expressing cells (60% lysis at 0.5 mg/mL). In contrast, etanercept was not able to mediate complement-dependent killing of the TNF-expressing cells (0% lysis at 1.0 mg/mL). The data highlight a unique difference between these TNF antagonists and suggests that etanercept and infliximab may have different mechanisms of action *in vivo*.

**Links**[Complete Reference](#)**Outline**

- Section Description

**Recent History**[COMPARATIVE ANALYSIS OF T...](#)

**Disclosure: work reported in this abstract was supported by:** Immunex Corporation, Seattle, Washington, supported work reported in this abstract.

1. Reference not provided.
2. Scallion et al. Cytokine 7:251-259, 1995. [Context Link]

## **Section Description**

Hall C Abstracts # 115 - 210

ACR Poster Session A

Health Services and Outcomes I

Sunday, November 14, 1999, 8:00 AM-9:30 AM

ACR Poster Session A

Cytokines and Mediators I

Sunday, November 14, 1999, 8:00 AM-9:30 AM

**Accession Number:** 00000889-199909001-00197

Copyright (c) 2000-2006 Ovid Technologies, Inc.  
Version: rel10.2.2, SourceID 1.11354.1.251

# EXHIBIT R

# Mechanisms of Cell Death Induced by Tumor Necrosis Factor Antagonists

Taruna Arora Khare, Seth R. Stevens, Jim S. Louie, Aaron Ellison, Ling Liu, Takahiko Kohno  
Angen Inc., Thousand Oaks, CA

## INTRODUCTION

### TNF Antagonists

- Tumor necrosis factor (TNF) antagonists have been shown to be efficacious in the treatment of several autoimmune diseases, including rheumatoid arthritis, psoriatic arthritis, ankylosing spondylitis, and psoriasis.
- There are currently 2 classes of biologic drugs that target TNF bioactivity: soluble TNF receptors (etanercept) and anti-TNF monoclonal antibodies (adalimumab and infliximab).
- At 3 currently approved agents bear the Fc portion of complement-activating human IgG1, the Fc region is a native component of the TNF antagonists and, whereas it is genetically fused to the soluble receptor

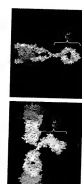
### Fc Components of TNF Antagonists

- Fc regions bind to Fc receptors (FcR), which are a family of immunoglobulin-binding molecules expressed on immune cells, including macrophages, granulocytes, natural killer cells, B cells, and platelets.
- Antibody-dependent cellular cytotoxicity (ADCC) is mediated by cross-linking of FcR.
- Complement-dependent cytotoxicity (CDC) may be enhanced by the cross-linking of Fc, which increases affinity for the complement component C1q.

## OBJECTIVE

To assess the ability of rituximab, adalimumab, and etanercept to bind to membrane-bound (mTNF) and the soluble (sTNF) TNF and to determine if rituximab, adalimumab, and etanercept to induce ADCC and CDC.

### Figure 1. Mechanisms of TNF Antagonists



TNF antagonists are shown in white, and TNF molecules are shown in green and red. The TNF-binding site of the anti-TNF antibody is shown in cyan.

## METHODS

- Construction of mTNF-expressing Chinese Hamster Ovary (CHO) cells.
- A mutant TNF that failed to induce membrane-bound TNF receptor (mTNF-R) binding was constructed by site-directed mutagenesis of the wild-type TNF DNA sequence to remove amino acids 77 through 81.
- Recombinant mTNF DNA sequence was cloned into a pCMV vector, which was used to transduce CHO cells.
- CHO cells expressing mTNF were treated with a fluorescent-activated cell sorter, using a fluorescence-activated cell sorter, using a fluorescence-activated cell sorter, using a fluorescence-activated cell sorter.
- Fluorescence-activated cell sorter (FACS) analysis of mTNF-expressing cells.
- Binding of TNF antagonists to mTNF.
- Fluorescein isothiocyanate-conjugated drug (FITC-anti-TNF) was incubated with mTNF cells alone or in the presence of 300-fold excess soluble TNF (0.3 µg/ml) for 4 hours.
- Flow cytometry.
- Cells were incubated with flow buffer (phosphate-buffered saline with 1% bovine serum albumin) to remove unbound drugs.
- Binding of TNF antagonists to cells was analyzed using FACSscan.
- ADCC assays (performed in triplicate).
- Cells were detached from tissue culture flasks with trypsin and washed with PBS.
- Cells were labeled with a membrane-impermeable fluorescent dye (CFSE) and incubated with varying concentrations of anti-TNF molecules at 4°C for 30 minutes.
- Cells were washed with PBS and resuspended in PBS.
- Cells were incubated with rituximab at 10:1 or 40:1 ratios for 4 hours.
- Propidium iodide (binds to the chromatin of dead or dying cells) was added to each well.
- The degree of cell death was measured by flow cytometry.
- Cells were incubated with rituximab and etanercept for 4 hours.
- ADCC assays (performed in triplicate).
- Cells were detached from tissue culture plates using cell dissociation buffer to form a single-cell suspension.
- MT-3 cells (0.5 × 10<sup>6</sup> cells) were incubated in the presence of mTNF and rituximab at the indicated concentrations for 1 hour at 4°C to allow binding to mTNF.
- Heat-inactivated fetal bovine serum (negative control), complement component C5-depleted serum (negative control), or human complement (positive control) was added at a final concentration of 10%.
- Cells and TNF antagonists were incubated in the presence of complement for 3 hours at 37°C.
- The degree of cell death was determined by flow cytometry.
- Cells were incubated with rituximab and etanercept for 4 hours.
- Cells were washed with PBS and resuspended in PBS.
- Cells were incubated with rituximab at 10:1 or 40:1 ratios for 4 hours.
- Propidium iodide (binds to the chromatin of dead or dying cells) was added to each well.
- The degree of cell death was measured by flow cytometry.
- Cells were incubated with rituximab and etanercept for 4 hours.
- ADCC assays (performed in triplicate).
- Cells were detached from tissue culture plates using cell dissociation buffer to form a single-cell suspension.
- MT-3 cells (0.5 × 10<sup>6</sup> cells) were incubated in the presence of mTNF and rituximab at the indicated concentrations for 1 hour at 4°C to allow binding to mTNF.
- Heat-inactivated fetal bovine serum (negative control), complement component C5-depleted serum (negative control), or human complement (positive control) was added at a final concentration of 10%.
- Cells and TNF antagonists were incubated in the presence of complement for 3 hours at 37°C.
- The degree of cell death was determined by flow cytometry.
- Cells were incubated with rituximab and etanercept for 4 hours.
- Cells were washed with PBS and resuspended in PBS.
- Cells were incubated with rituximab at 10:1 or 40:1 ratios for 4 hours.
- Propidium iodide (binds to the chromatin of dead or dying cells) was added to each well.
- The degree of cell death was measured by flow cytometry.
- Cells were incubated with rituximab and etanercept for 4 hours.
- ADCC assays (performed in triplicate).
- Cells were detached from tissue culture plates using cell dissociation buffer to form a single-cell suspension.
- MT-3 cells (0.5 × 10<sup>6</sup> cells) were incubated in the presence of mTNF and rituximab at the indicated concentrations for 1 hour at 4°C to allow binding to mTNF.
- Heat-inactivated fetal bovine serum (negative control), complement component C5-depleted serum (negative control), or human complement (positive control) was added at a final concentration of 10%.
- Cells and TNF antagonists were incubated in the presence of complement for 3 hours at 37°C.
- The degree of cell death was determined by flow cytometry.
- Cells were incubated with rituximab and etanercept for 4 hours.
- Cells were washed with PBS and resuspended in PBS.
- Cells were incubated with rituximab at 10:1 or 40:1 ratios for 4 hours.
- Propidium iodide (binds to the chromatin of dead or dying cells) was added to each well.
- The degree of cell death was measured by flow cytometry.
- Cells were incubated with rituximab and etanercept for 4 hours.
- ADCC assays (performed in triplicate).
- Cells were detached from tissue culture plates using cell dissociation buffer to form a single-cell suspension.
- MT-3 cells (0.5 × 10<sup>6</sup> cells) were incubated in the presence of mTNF and rituximab at the indicated concentrations for 1 hour at 4°C to allow binding to mTNF.
- Heat-inactivated fetal bovine serum (negative control), complement component C5-depleted serum (negative control), or human complement (positive control) was added at a final concentration of 10%.
- Cells and TNF antagonists were incubated in the presence of complement for 3 hours at 37°C.
- The degree of cell death was determined by flow cytometry.
- Cells were incubated with rituximab and etanercept for 4 hours.
- Cells were washed with PBS and resuspended in PBS.
- Cells were incubated with rituximab at 10:1 or 40:1 ratios for 4 hours.
- Propidium iodide (binds to the chromatin of dead or dying cells) was added to each well.
- The degree of cell death was measured by flow cytometry.
- Cells were incubated with rituximab and etanercept for 4 hours.
- ADCC assays (performed in triplicate).
- Cells were detached from tissue culture plates using cell dissociation buffer to form a single-cell suspension.
- MT-3 cells (0.5 × 10<sup>6</sup> cells) were incubated in the presence of mTNF and rituximab at the indicated concentrations for 1 hour at 4°C to allow binding to mTNF.
- Heat-inactivated fetal bovine serum (negative control), complement component C5-depleted serum (negative control), or human complement (positive control) was added at a final concentration of 10%.
- Cells and TNF antagonists were incubated in the presence of complement for 3 hours at 37°C.
- The degree of cell death was determined by flow cytometry.
- Cells were incubated with rituximab and etanercept for 4 hours.
- Cells were washed with PBS and resuspended in PBS.
- Cells were incubated with rituximab at 10:1 or 40:1 ratios for 4 hours.
- Propidium iodide (binds to the chromatin of dead or dying cells) was added to each well.
- The degree of cell death was measured by flow cytometry.
- Cells were incubated with rituximab and etanercept for 4 hours.
- ADCC assays (performed in triplicate).
- Cells were detached from tissue culture plates using cell dissociation buffer to form a single-cell suspension.
- MT-3 cells (0.5 × 10<sup>6</sup> cells) were incubated in the presence of mTNF and rituximab at the indicated concentrations for 1 hour at 4°C to allow binding to mTNF.
- Heat-inactivated fetal bovine serum (negative control), complement component C5-depleted serum (negative control), or human complement (positive control) was added at a final concentration of 10%.
- Cells and TNF antagonists were incubated in the presence of complement for 3 hours at 37°C.
- The degree of cell death was determined by flow cytometry.

## RESULTS

Figure 2. Binding of Etanercept, Adalimumab, and Infliximab to mTNF

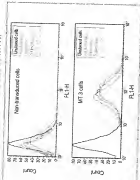


Figure 3. ADCC by Etanercept and Infliximab

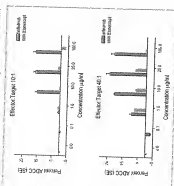
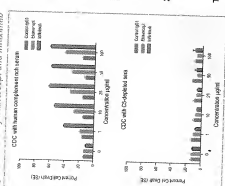


Figure 4. CDC by Etanercept and Infliximab



## DISCUSSION

- Soluble receptors and monoclonal antibodies that target TNF decrease levels of circulating TNF.
- Both classes of drugs demonstrate efficacy in the treatment of several autoimmune diseases.
- In prior studies, we found that both classes of TNF antagonists bound poorly to FcR and C1q on cells. In the presence of TNF, anti-TNF monoclonal antibodies, but not the soluble TNF receptor, increased binding to FcR and C1q.
- Current experiments showed that the anti-TNF monoclonal antibodies were more effective at inducing ADCC than the soluble TNF receptor.
- ADCC pathways in the spleen involve binding of FcR and C1q.
- These differences in the ability to induce ADCC and CDC pathways may explain the differing spectrum of disease states for which these agents are effective treatments.
- Furthermore, these differences may contribute to the higher rates of fungal and granulomatous infections, such as tuberculosis, observed with infliximab compared with etanercept.<sup>2,3</sup>

## CONCLUSIONS

- Both of the TNF antagonists tested, the soluble TNF receptor etanercept and the anti-TNF monoclonal antibody infliximab, bound to mTNF on CHO cells.
- Infliximab induced ADCC at lower effector:target ratios than etanercept.
- Infliximab was more effective than etanercept at inducing CDC in mTNF-expressing cells.

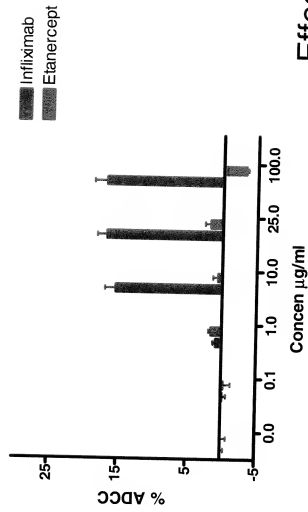
## REFERENCES

- Wells RS, Broder MS, Wong JY, Hovav AE, Benishviller DO. Granulomatous infectious diseases associated with anti-TNF receptor antagonists. *Clin Infect Dis*. 2004;38:1201-1204.
- Wells RS, Broder MS, Wong JY, Benishviller DO. Granulomatous infections due to tumor necrosis factor receptor antagonists. *Clin Infect Dis*. 2004;39:1254-1256.

Thanks to Randa Kachem for molecular imaging studies.  
Received for review: September 1, 2004; accepted: January 1, 2005.  
Copyright © 2005 by Lippincott Williams & Wilkins

Figure 3A

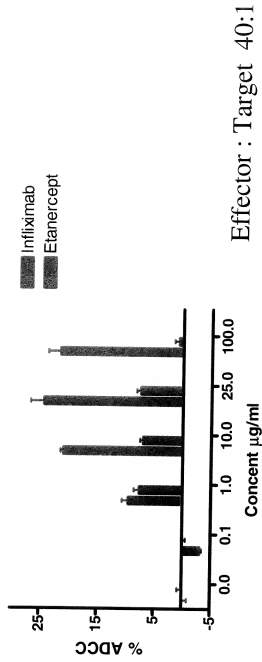
## ADCC by Etanercept and Infliximab



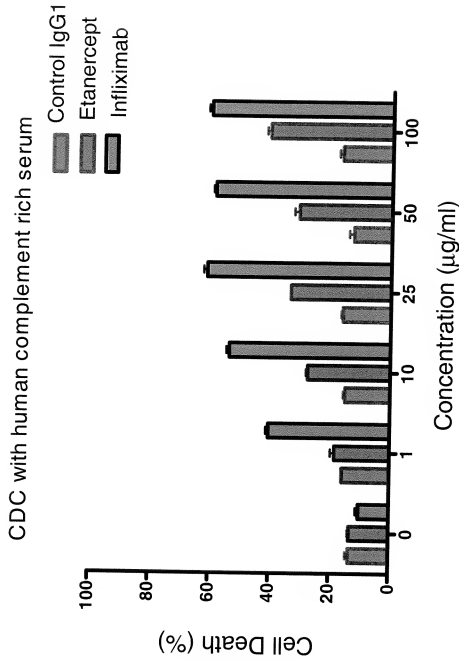
Effector : Target 10:1

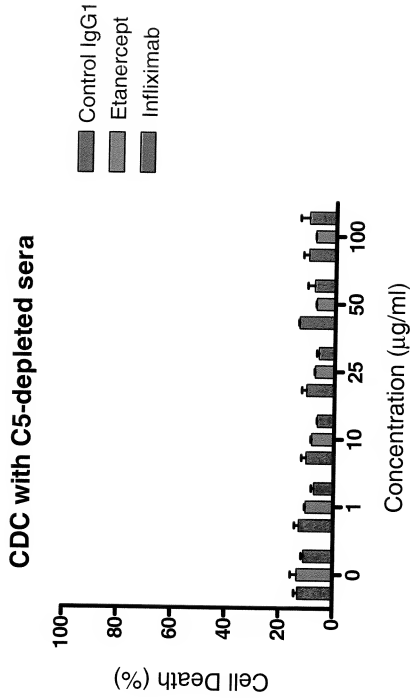
Figure 3B

## ADCC by Etanercept and Infliximab



# *CDC by Etanercept and Infliximab*



*CDC by Etanercept and Infliximab (Cont)*



# EXHIBIT S



NCBI

# results of BLAST

BLASTP 2.2.14 [May-07-2006]

**Reference:**

Altschul, Stephen F., Thomas L. Madden, Alejandro A. Schäffer, Jinghui Zhang, Zheng Zhang, Webb Miller, and David J. Lipman (1997), "Gapped BLAST and PSI-BLAST: a new generation of protein database search programs", *Nucleic Acids Res.* 25:3389-3402.

RID: 1150326844-7029-23201072992.BLASTQ4

**Database:** All non-redundant GenBank CDS

translations+PDB+SwissProt+PIR+PRF excluding environmental samples  
3,695,564 sequences; 1,269,795,892 total letters

If you have any problems or questions with the results of this search  
please refer to the [BLAST FAQs](#)

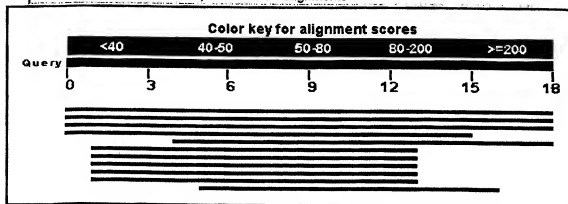
[Taxonomy reports](#)

**Query=**

Length=18

## Distribution of 11 Blast Hits on the Query Sequence

Mouse over to see the define, click to show alignments



[Tree view](#) NEW

Sequences producing significant alignments:

Score  
(Bits)    E  
Value

<a href="#">gi 54696716 gb AAV38730.1 </a>	tumor necrosis factor receptor sup...	<a href="#">56.2</a>	1e-07	
<a href="#">gi 339758 gb AAA36755.1 </a>	tumor necrosis factor receptor	<a href="#">56.2</a>	1e-07	
<a href="#">gi 37359212 gb AAN72434.1 </a>	soluble tumor necrosis factor rece...	<a href="#">56.2</a>	1e-07	
<a href="#">gi 825701 emb CAA56324.1 </a>	p75 TNF receptor [Homo sapiens]	<a href="#">46.4</a>	1e-04	
<a href="#">gi 6683130 dbj BAA89052.1 </a>	tumor necrosis factor receptor 2 [Hom	<a href="#">43.9</a>	8e-04	
<a href="#">gi 15030259 gb AAH11399.1 </a>	SYK protein [Homo sapiens] >gi 559...	<a href="#">28.6</a>	30	
<a href="#">gi 515871 emb CAA51970.1 </a>	protein tyrosin kinase [Homo sapiens]	<a href="#">28.6</a>	30	

<a href="#">gi 12804475 gb AAH01645.1</a>	Spleen tyrosine kinase [Homo sapie...	28.6	30	
<a href="#">gi 448916 prf 1918215A</a>	protein Tyr kinase	28.6	30	
<a href="#">gi 1092813 prf 2101280A</a>	p72syk protein	28.6	30	
<a href="#">gi 89061682 ref XP_944591.1</a>	PREDICTED: similar to dynein, ax...	26.1	174	

# Alignments

> ☐ [gi|54696716|gb|AAV38730.1](#) tumor necrosis factor receptor superfamily, member  
[gi|31419790|gb|AAH52977.1](#) Tumor necrosis factor receptor 2, precursor [Homo sap  
[gi|32891819|gb|AAP88939.1](#) tumor necrosis factor receptor superfamily, member 1B  
[gi|55663791|emb|CAH73721.1](#) tumor necrosis factor receptor superfamily, member 1  
[gi|56202703|emb|CAI19225.1](#) tumor necrosis factor receptor superfamily, member 1  
[gi|4507577|ref|NP\\_001057.1](#) tumor necrosis factor receptor 2 precursor [Homo sap  
[gi|29725900|gb|AAO89076.1](#) tumor necrosis factor receptor superfamily, member 1B  
[gi|61356471|gb|AAK41249.1](#) tumor necrosis factor receptor superfamily member 1B [s  
construct]  
[gi|21264534|sp|P20333|TNFR1B\\_HUMAN](#) Tumor necrosis factor receptor superfamily mem  
(Tumor necrosis factor receptor 2) (TNF-R2) (Tumor necrosis  
factor receptor type II) (p75) (p80 TNF-alpha receptor) (CD120b  
antigen) (Etanercept) [Contains: Tumor necrosis factor  
receptor superfamily member 1b, membrane form; Tumor necrosis  
factor-binding protein 2 (TBP2) (TBP-2)]  
[gi|1469541|gb|AAC50622.1](#) tumor necrosis factor receptor  
[gi|189186|gb|AAA59929.1](#) tumor necrosis factor receptor  
Length=461

Score = 56.2 bits (125), Expect = 1e-07  
Identities = 17/18 (94%), Positives = 17/18 (94%), Gaps = 0/18 (0%)

Query 1 LPAQVAFBPPYAEPGSTC 18  
LPAQVAF PYAEPGSTC  
Sbjct 23 LPAQVAFTPYAEPGSTC 40

> ☐ [gi|339758|gb|AAA36755.1](#) tumor necrosis factor receptor  
Length=461

Score = 56.2 bits (125), Expect = 1e-07  
Identities = 17/18 (94%), Positives = 17/18 (94%), Gaps = 0/18 (0%)

Query 1 LPAQVAFBPPYAEPGSTC 18  
LPAQVAF PYAEPGSTC  
Sbjct 23 LPAQVAFTPYAEPGSTC 40

> ☐ [gi|37359212|gb|AAN72434.1](#) soluble tumor necrosis factor receptor superfamily  
[Homo sapiens]  
Length=268

Score = 56.2 bits (125), Expect = 1e-07  
Identities = 17/18 (94%), Positives = 17/18 (94%), Gaps = 0/18 (0%)

Query 1 LPAQVAFBPPYAEPGSTC 18  
LPAQVAF PYAEPGSTC

Sbjct 23 LPAQVAFBPPYAPEPGSTC 40

> [gi|825701|emb|CAA56324.1](#) [p75 TNF receptor \[Homo sapiens\]](#)  
Length=37

Score = 46.4 bits (102), Expect = 1e-04  
Identities = 14/15 (93%), Positives = 14/15 (93%), Gaps = 0/15 (0%)

Query 1 LPAQVAFBPPYAPEPG 15  
LPAQVAF PYAPEPG  
Sbjct 23 LPAQVAFBPPYAPEPG 37

> [gi|6683130|dbj|BAA89052.1](#) [tumor necrosis factor receptor 2 \[Homo sapiens\]](#)  
Length=33

Score = 43.9 bits (96), Expect = 8e-04  
Identities = 13/14 (92%), Positives = 13/14 (92%), Gaps = 0/14 (0%)

Query 5 VAFBPPYAPEPGSTC 18  
VAF PYAPEPGSTC  
Sbjct 1 VAFBPPYAPEPGSTC 14

> [gi|15030259|gb|AAH11399.1](#) [SYK protein \[Homo sapiens\]](#)  
[gi|55958427|emb|CAI16875.1](#) [spleen tyrosine kinase \[Homo sapiens\]](#)  
[gi|496900|emb|CAA82737.1](#) [protein-tyrosine kinase \[Homo sapiens\]](#)  
Length=612

Score = 28.6 bits (60), Expect = 30  
Identities = 9/19 (47%), Positives = 11/19 (57%), Gaps = 7/19 (36%)

Query 2 PAQ-----VAFBPPYAPE 13  
PAQ V+F+PY PE  
Sbjct 285 PAQGNRQESTVSPNPEPE 303

> [gi|515871|emb|CAA51970.1](#) [protein tyrosin kinase \[Homo sapiens\]](#)  
Length=630

Score = 28.6 bits (60), Expect = 30  
Identities = 9/19 (47%), Positives = 11/19 (57%), Gaps = 7/19 (36%)

Query 2 PAQ-----VAFBPPYAPE 13  
PAQ V+F+PY PE  
Sbjct 303 PAQGNRQESTVSPNPEPE 321

> [gi|12804475|gb|AAH01645.1](#) [Spleen tyrosine kinase \[Homo sapiens\]](#)  
[gi|55958428|emb|CAI16876.1](#) [spleen tyrosine kinase \[Homo sapiens\]](#)  
[gi|1174527|sp|P43405|KSYK\\_HUMAN](#) [Tyrosine-protein kinase SYK \(Spleen tyrosine kin](#)  
[gi|12804209|gb|AAH02962.1](#) [Spleen tyrosine kinase \[Homo sapiens\]](#)  
[gi|21361553|ref|NP\\_003168.2](#) [spleen tyrosine kinase \[Homo sapiens\]](#)  
[gi|479013|gb|AAA36526.1](#) [protein tyrosine kinase](#)  
Length=635

Score = 28.6 bits (60), Expect = 30  
Identities = 9/19 (47%), Positives = 11/19 (57%), Gaps = 7/19 (36%)

Query 2 PAQ-----VAFBPHYAPE 13  
 PAQ V+F+PY PE  
 Sbjct 308 PAQGNRQESTVVSFNPVEPE 326

> [gi|448916|prf||1918215A](#) protein Tyr kinase  
 Length=630


Score = 28.6 bits (60), Expect = 30  
 Identities = 9/19 (47%), Positives = 11/19 (57%), Gaps = 7/19 (36%)

Query 2 PAQ-----VAFBPHYAPE 13  
 PAQ V+F+PY PE  
 Sbjct 303 PAQGNRQESTVVSFNPVEPE 321

> [gi|1092813|prf||2101280A](#) p72syk protein  
 Length=365

Score = 28.6 bits (60), Expect = 30  
 Identities = 9/19 (47%), Positives = 11/19 (57%), Gaps = 7/19 (36%)

Query 2 PAQ-----VAFBPHYAPE 13  
 PAQ V+F+PY PE  
 Sbjct 303 PAQGNRQESTVVSFNPVEPE 321

> [gi|89061682|ref|XP\\_944591.1|](#)  PREDICTED: similar to dynein, axonemal, heavy po-  
 sapiens]  
 Length=4107

Score = 26.1 bits (54), Expect = 174  
 Identities = 9/15 (60%), Positives = 9/15 (60%), Gaps = 4/15 (26%)

Query 6 AFBP----YAPEPGS 16  
 AF P Y PEPGS  
 Sbjct 3866 AFSPSGLYYTPEPGS 3880

Get selected sequences

Select all

Deselect all

Tree View

Database: All non-redundant GenBank CDS translations+PDB+SwissProt+PTR+PRF excludi  
 environmental samples

Posted date: Jun 10, 2006 4:09 AM

Number of letters in database: 1,269,795,892

Number of sequences in database: 3,695,564

Lambda K H  
 0.346 0.288 1.79

Gapped  
 Lambda K H  
 0.294 0.110 0.610

Matrix: PAM30

Gap Penalties: Existence: 9, Extension: 1

Number of Sequences: 3695564

Number of Hits to DB: 15358398

Number of extensions: 349668

Number of successful extensions: 1740

Number of sequences better than 20000: 1713

Number of HSP's better than 20000 without gapping: 0  
Number of HSP's gapped: 1740  
Number of HSP's successfully gapped: 1740  
Length of query: 18  
Length of database: 1269795892  
Length adjustment: 8  
Effective length of query: 10  
Effective length of database: 1240231380  
Effective search space: 12402313800  
Effective search space used: 12402313800  
T: 11  
A: 40  
X1: 15 (7.5 bits)  
X2: 35 (14.8 bits)  
X3: 58 (24.6 bits)  
S1: 38 (19.3 bits)  
S2: 38 (19.3 bits)